

ACTA MYOLOGICA

(Myopathies, Cardiomyopathies and Neuromyopathies)

Vol. XXXVI - September 2017

Official Journal of
Mediterranean Society of Myology
and
Associazione Italiana di Miologia

Founders: Giovanni Nigro and Lucia Ines Comi

Three-monthly

EDITOR-IN-CHIEF

Giovanni Nigro

ASSISTANT EDITOR

Vincenzo Nigro

MANAGING EDITOR

Luisa Politano

CO-EDITORS

Valerie Askanas

Giuseppe Novelli

Lefkos Middleton

Reinhardt Rüdel

HISTORICAL STUDIES EDITOR

Georges Serratrice



Established in 1982 as Cardiomyology

ACTA MYOLOGICA

(Myopathies, Cardiomyopathies and Neuromyopathies)

**Official Journal of
Mediterranean Society of Myology
and
Associazione Italiana di Miologia**

Founders: Giovanni Nigro and Lucia Ines Comi

Three-monthly

EDITORIAL BOARD

Ekrum Abdel-Salam, Cairo
Corrado Angelini, Padova
Enrico Bertini, Roma
Serge Braun, Paris
Kate Bushby, Newcastle upon Tyne
Kevin P. Campbell, Iowa City
Marinos Dalakas, Athens
Feza Deymeer, Istanbul
Salvatore Di Mauro, New York
Denis Duboc, Paris
Victor Dubowitz, London
King W. Engel, Los Angeles
Michel Fardeau, Paris
Fayçal Hentati, Tunis
Byron A. Kakulas, Perth
Frank Lehmann-Horn, Ulm
Carlo Minetti, Genova
Clemens Müller, Würzburg

Francesco Muntoni, Londra
Carmen Navarro, Vigo
Gerardo Nigro, Napoli
Anders Oldfors, Göteborg
Eijiro Ozawa, Tokyo
Heinz Reichmann, Dresden
Serenella Servidei, Roma
Piraye Serdaroglu, Istanbul
Yeuda Shapira, Jerusalem
Osman I. Sinanovic, Tuzla
Michael Sinnreich, Montreal
Andoni J. Urtizberea, Hendaye
Gert-Jan van Ommen, Leiden
Lord John Walton of Detchant, Oxford
Steve Wilton, Perth
Klaus Zerres, Aachen
Janez Zidar, Ljubljana



© 1981 Gaetano Conte Academy. All rights reserved

This journal and the individual contributions contained in it are protected by the copyright of Gaetano Conte Academy and the following terms and conditions apply to their use:

Photocopying

Single photocopies of single articles may be made for personal use as allowed by national copyright laws. Permission of the publisher and payment of a fee is required for all other photocopying, including multiple or systematic copying, copying for advertising or promotional purposes, resale, and all forms of document delivery. Special rates are available for educational institutions that wish to make photocopies for non-profit educational classroom use.

EDITOR-IN-CHIEF

Giovanni Nigro, Napoli

ASSISTANT EDITOR

Vincenzo Nigro, Napoli

MANAGING EDITOR

Luisa Politano, Napoli

CO-EDITORS

Valerie Askanas, Los Angeles

Lefkos Middleton, Nicosia

Giuseppe Novelli, Roma

Reinhardt Rüdell, Ulm

HISTORICAL STUDIES EDITOR

Georges Serratrice, Marseille

BOARD OF THE MEDITERRANEAN SOCIETY OF MYOLOGY

G. Nigro, *President*; H. Topaloglu, *President Elected*

L.T. Middleton, G. Siciliano, *Vice-presidents*

K. Christodoulou, *Secretary*

L. Politano, *Treasurer*

E. Abdel-Salam, M. Dalakas, F. Deymeer, F. Hentati, G. Meola, Y. Shapira, E. Tizzano, A. Toscano,

J. Zidar

Co-opted Members: V. Askanas, S. Di Mauro, K. Engel, R. Rüdell

Acta Myologica is cited in Index Medicus/MEDLINE, Medicine, Excerpta Medica Database (EMBASE), Index Copernicus and monitored for coverage in Chemical Abstracts Service. The Journal is available on PubMed Central (<http://www.ncbi.nlm.nih.gov/pmc/journals/1221/>).

Acta Myologica publishes 4 issues per year in March, June, September, December.

Acta Myologica will be sent free of charge to the members of the Gaetano Conte Academy and of the Mediterranean Society of Myology.

All correspondence should be addressed to Gaetano Conte Academy, Viale dei Pini 101 - 80131 Napoli - Italy.

Tel./Fax: +39-081-5874438

E-mail: giovanni.nigro@unina2.it

Editor in Chief: Giovanni Nigro

Tribunal Authorization, Napoli N. 3827, January 10, 1989 - Journal registered at "Registro pubblico degli Operatori della Comunicazione" (Pacini Editore srl registration n. 6269 - 29/8/2001).

The editor remains at the complete disposal of those with rights whom it was impossible to contact, and for any omissions.

Photocopies, for personal use, are permitted within the limits of 15% of each publication by following payment to SIAE of the charge due, article 68, paragraphs 4 and 5 of the Law April 22, 1941, No 633.

Reproductions for professional or commercial use or for any other other purpose other than personal use can be made following a written request and specific authorization in writing from AIDRO, Corso di Porta Romana, 108, 20122 Milan, Italy, E-mail: segreteria@aidro.org and web site: www.aidro.org.

Publisher

Pacini
Editore

Via A. Gherardesca - 56121 Pisa, Italy

Published by Pacini Editore Srl - Pisa, Italy, September 2017

CONTENTS

ORIGINAL ARTICLES

- Myotonia permanens with Nav1.4-G1306E displays varied phenotypes during course of life*
Frank Lehmann-Horn, Adele D'Amico, Enrico Bertini, Mauro LoMonaco, Luciano Merlini, Kevin R. Nelson,
Heike Philippi, Gabriele Siciliano, Frank Spaans and Karin Jurkat-Rott 125
- Arrhythmogenic right ventricular cardiomyopathy in Boxer dogs: the diagnosis as a link to the human disease*
Annina S. Vischer, David J. Connolly, Caroline J. Coats, Virginia Luis Fuentes, William J. McKenna,
Silvia Castelletti and Antonios A. Pantazis 135
- Multi-slice MRI reveals heterogeneity in disease distribution along the length of muscle in Duchenne muscular dystrophy*
Stephen M. Chrzanowski, Celine Baligand, Rebecca J. Willcocks, Jasjit Deol, Ilona Schmalfuss, Donovan J. Lott,
Michael J. Daniels, Claudia Senesac, Glenn A. Walter and Krista Vandenborne. 151
- Leber's hereditary optic neuropathy (LHON) in an Apulian cohort of subjects*
Angelica Bianco, Luigi Bisceglia, Paolo Trerotoli, Luciana Russo, Leonardo D'Agruma,
Silvana Guerriero and Vittoria Petruzzella 163

CASE REPORT

- Bethlem myopathy in a Portuguese patient – case report*
Ana Inês Martins, Cristina Marques, Jorge Pinto-Basto and Luis Negrão. 178

- ERRATA CORRIGE** 182

NEWS FROM AROUND THE WORLD

- AIM 184
- GCA 184
- MSM 184
- WMS 184

- FORTHCOMING MEETINGS** 185

- Instructions for Authors 189

ORIGINAL ARTICLES

Myotonia permanens with Nav1.4-G1306E displays varied phenotypes during course of life

FRANK LEHMANN-HORN¹, ADELE D'AMICO², ENRICO BERTINI², MAURO LOMONACO³, LUCIANO MERLINI⁴, KEVIN R. NELSON⁵, HEIKE PHILIPPI⁶, GABRIELE SICILIANO⁷, FRANK SPAANS⁸ AND KARIN JURKAT-ROTT⁹

¹ Division of Neurophysiology, Ulm University, Ulm, Germany; ² Unit of Neuromuscular and Neurodegenerative Disorders, Laboratory of Molecular Medicine, Bambino Gesù Children's Hospital, Rome, Italy; ³ Department of Neurosciences, Catholic University, Rome, Italy; ⁴ Laboratory of Musculoskeletal Cell Biology, Istituto Ortopedico Rizzoli, Bologna, Italy; ⁵ Medical Affairs, University of Kentucky, Lexington, KY, USA; ⁶ Frankfurt University, Sozialpädiatrisches Zentrum, Epilepsieambulanz, Frankfurt, Germany; ⁷ Department of Clinical and Experimental Medicine, Neurological Unit, University of Pisa, Italy; ⁸ Clinical Neurophysiology, Maastricht University, Maastricht, The Netherlands; ⁹ Department of Neurosurgery, Ulm University, Ulm, Germany

Introduction. Myotonia permanens due to Nav1.4-G1306E is a rare sodium channelopathy with potentially life-threatening respiratory complications. Our goal was to study phenotypic variability throughout life.

Methods. Clinical neurophysiology and genetic analysis were performed. Using existing functional expression data we determined the sodium window by integration.

Results. In 10 unrelated patients who were believed to have epilepsy, respiratory disease or Schwartz-Jampel syndrome, we made the same *prima facie* diagnosis and detected the same heterologous Nav1.4-G1306E channel mutation as for our first myotonia permanens patient published in 1993. Eight mutations were *de-novo*, two were inherited from the affected parent each. Seven patients improved with age, one had a benign phenotype from birth, and two died of respiratory complications. The clinical features age-dependently varied with severe neonatal episodic laryngospasm in childhood and myotonia throughout life. Weakness of varying degrees was present. The responses to cold, exercise and warm-up were different for lower than for upper extremities. Spontaneous membrane depolarization increased frequency and decreased size of action potentials; self-generated repolarization did the opposite. The overlapping of steady-state activation and inactivation curves generated a 3.1-fold window area for G1306E vs. normal channels. **Discussion.** Residue G1306 Neonatal laryngospasm and unusual distribution of myotonia, muscle hypertrophy, and weakness encourage direct search for the G1306E mutation, a hotspot for *de-novo* mutations. Successful therapy with the sodium channel blocker flecainide is due to stabilization of the inactivated state and special effectiveness for enlarged window currents. Our G1306E collection is the first genetically clarified case series from newborn period to adulthood and therefore helpful for counselling.

Key words: muscular and respiratory tract diseases, neonate, stridor

Introduction

Myotonia is defined as slowed muscle relaxation after voluntary contraction. It is experienced by patients as muscle stiffness. Symptoms are caused by recessive or dominant mutations in the *CLC1* chloride channel or by dominant mutations in the Nav1.4 sodium channel of skeletal muscle. Typically, myotonia lessens with muscle usage, the so-called warm-up phenomenon. However, not all forms of myotonia have a warm-up phenomenon. For example, there is a rare form of myotonia whose severity never varies and is therefore termed myotonia permanens. This phenotype was originally acknowledged by (1) as new entity in a patient (Table 1, patient 4) previously published elsewhere (2). The phenotype is characterized by severe, continuous myotonia associated with a unique EMG pattern of persistent myotonic activity. Additionally, stiffness and hypertrophy of facial, bulbar, neck and shoulder muscles and episodes of respiratory distress are predominant features. The underlying *SCN4A* mutation encodes p.G1306E, a glycine-to-glutamate substitution. G1306 is highly conserved in all voltage-gated sodium channels and situated in the fast inactivation gate of the sodium channel Nav1.4 i.e., the intracellular loop connecting domains III and IV of the channel protein. The main pathogenetic mechanism is thought to be a slowed and incomplete channel inactivation (2).

Alongside epilepsy and respiratory diseases, the disorder has been diagnosed as myogenic type of Schwartz-

Table 1. Life course of myotonia permanens patients with the *SCN4A*-p.G1306E mutation. Abbreviations: CMZ, carbamazepine; DPH, diphenylhydantoin. * DPH reduced apnoeic episodes but not the myotonia; SNEL, severe neonatal episodic laryngospasm; R, added to the patient number, means a relative. Symbols: + present; - absent; (+) mild; 0 mother and 5 siblings healthy and G1306E excluded, father with no history of myotonia; · parents deceased with no history of myotonia; 2 siblings, both healthy.

Patient number	Current age	Gender	Neonatal onset	De-novo G1306E	Age of examination	Inspiratory stridor	Laryngospasms	Loss of consciousness	Hypertrophy & myotonia	Painful muscle cramps	Persistent EMG activity	Weakness	Factors which provoke myotonia and respiratory distress throughout life	Medication response to	Remarks	Course during life
1	22	m	+	+	Birth 2 y 3.5 y 7 y 13 y 22 y	+	+	+	+	+	+	-	Heat exercise	See text	Disease misinterpreted as laryngomalacia, epilepsy; bent posture; failure to thrive	SNEL reduction, constant myotonia
2	8	f	+	+	Birth 5 y	-	+	-	-	+	+	-	K-rich food; frequent suffocation after oral liquid intake	Mexiletine	Large tongue, failure to thrive; if falling unable to get up for 2min	SNEL reduction, constant myotonia
3	2	f	+	+	1 mo 1 y 2 y	+	+	-	+	+		-	Infections, K-rich food, coldness	CMZ, mexiletine effective. Not effective: acetazolamide aggravation by penicilline	Disease misinterpreted as epilepsy, tracheomalacia; bent posture, rotated arms, swallowing of liquids impaired, clenched hand	SNEL reduction, constant myotonia
4	50	f	+	+°	Birth 6 y 26 y 36 y	+	+	+	+	+	+	-	Cortico-steroid, stress, infection, exercise, pregnancy	Barbiturate, flecainide superior to mexiletine, CMZ, tocainide, quinidine	Disease misinterpreted as epilepsy, SJS Lerche et al. 1993 Desaphy et al. 2013	SNEL reduction, constant myotonia
4R	12	m	+	-	Birth 5 y	+	+	-	+	+	+	-		Flecainide superior to mexiletine	Rotated arms, Desaphy et al. 2013; severe orbicularis, eyelid, tongue m.	SNEL reduction, constant myotonia
5	17	m	+	+	Birth 3 mo 1.5 y 10 y 17 y	+	+	+	-	-		-	Sleep, coldness	Mexiletine superior to CMZ, DPH*	Disease misinterpreted as epilepsy, SJS; no painful cramps	SNEL reduction, constant myotonia
6	63	f	+	+‘	Infant 42-63 y	+	+	-	+	+	+	(+)	Exercise, coldness, K-rich food	Effective are flecainide, to-cainide. not effective are: mexiletine, lamotrigine		SNEL reduction, constant myotonia
7	50	m	+	+	3 mo 6 mo 41-46 y	+	+	+	+	+		-	Exercise	Mexiletine	Disease misinterpreted as epilepsy, stomach hiatus, painful rectus cramping, bent posture	SNEL reduction, constant myotonia
8	67	m	-	+	9 mo Adult	-	-	-	+	+	?	-	Exercise	Mexiletine	Mild phenotype	Constant myotonia
9	-	m	+	+	1 mo 3 mo 11 y	+	+	+	+	+	+		Coldness, exercise	Heat, dilantin, desipramine	Died at age 11 y of cardiorespiratory insufficiency due to severe myotonic reaction	Lethal
9R1	22	m	-	-	Birth 4 mo 1 y 22 y	-	-	-	-	+	+		Coldness, elevated K+	Dilantin, desipramine	Weakness neck, shoulder girdle, upper arms	SNEL reduction, constant myotonia
9R2	43	f	+	+	5 day 14 mo	+	+	-	+	+	+		Pain, cold, exercise	Dilantin, desipramine	Succinylcholine-induced event	SNEL reduction, constant myotonia
10	-	m	+	+	Birth 9 mo 20 mo 4 y 21 y	-	-	-	+	+		-	Excitement	Mexiletine	Bent posture, failure to thrive, died at age 22 y	Lethal

Jampel syndrome (3, 4). Next to severe cases with potentially lethal laryngospasm, a very mild case of myotonia permanens has been reported (1). The questions on severity and prognosis are still a matter of debate. Although myotonia permanens is a rare entity, it is important that a pediatrician is familiar with this sodium channelopathy because it is life-threatening but treatable and, usually, misdiagnosed. Only limited clinical information is available in pediatric handbooks. This led us to pool 10 unrelated cases to evaluate the spectrum and phenotypic changes during the course of life (Table 1).

Patients and methods

Patients

The study was approved by the Ethics Committee of Ulm University. Written informed consent was taken from patients or their parents for publishing their pictures, clinical and genetic examination, and study of their history.

Genetics

Whole EDTA blood was drawn for extraction of genomic DNA. Using primers specific for exon 22 and the corresponding exon-intron boundaries (2), DNA was amplified by PCR and products bi-directionally sequenced with Applied Biosystems BigDye terminator v3.1 as per the manufacturer's instructions. The resulting sequencing reactions were resolved on an ABI3730 genetic analyzer (Applied Biosystems, Foster City, CA).

Excised muscle experiments

Previously unpublished experiments of excised quadriceps fiber segments obtained from patient 4 in 1993 were performed using capacity-compensated microelectrodes of 3–5 MOhm. Twitch force was analyzed for 3; 5; and 7 mM potassium (2, 4). The force of the muscle bundles, which were mounted in a sylgard-bottomed chamber, superfused at 37°C and stimulated supramaximally with single pulses of 0.2 ms duration, were measured with a strain gauge. The standard solution contained (in mM): NaCl 107.7; KCl 3.48; CaCl₂ 1.53; MgSO₄ 0.69; NaHCO₃ 26.2; NaH₂PO₄ 1.67; Na gluconate 9.64; glucose 5.5; sucrose 7.6 (315 mosm/l). The pH was adjusted to 7.4 by 95% O₂ and 5% CO₂.

Re-evaluation of published results

Our previously published data on heterologously expressed G1306E and wildtype (WT) Nav1.4 channels in HEK cells from 1995 (5) were re-evaluated, particu-

larly, to demonstrate the presence of a sodium window current in the mutant and to compare the percentage of sodium channels which can be activated at near-threshold potentials. Data points for steady-state activation (g/V) and steady-state inactivation were fitted by applying the Boltzmann function for the distribution of two-states (closed and open channels). The fits were used to determine the sodium window by integration.

Results

Genetics

All ten patients harbored a heterozygous *SCN4A* mutation c.3917G>A encoding G1306E in the major voltage-gated Nav1.4 sodium channel of skeletal muscle. In eight independent cases, the mutation occurred de-novo; in two families, affected relatives inherited the mutation in an autosomal dominant fashion (4R, 9R1, 9R2, Table 1). None of the unaffected parents or healthy siblings carried the mutation.

Clinical features over time

In the neonatal period, patients experienced episodes of severe laryngospasms, resulting in acute hypoventilation and cyanosis and, in five patients, unconsciousness (Table 1). For example, these episodes occurred up to several times per day and demanded mask ventilation or an oxygen supply in patient 1 (Fig. 1). Such cyanotic spells were life-threatening and required recurrent hospitalization of up to six months each. Several spells led to apnoea (SO₂=30%), opisthotonus, and unconsciousness and responded to barbiturate. In half of the patients, cyanotic episodes associated with apnoea and falls were interpreted as epileptic seizures even though the EEG was normal. This view was supported by the beneficial response to the administration of carbamazepine and barbiturates, drugs which block sodium channels and exert antimyotonic effects. Startling and sucking elicited the laryngospasm which was initially mistaken for laryngomalacia or gastroesophageal reflux. Chewing and swallowing was also impaired, leading to a transient failure to thrive in three patients.

In infancy and early childhood, an inspiratory stridor occurred in 80% of the patients. An example for an inspiratory stridor is shown in Figure 2 (patient 3) and the video (stridor.avi). Stridor EEG readings during awake, drowsy, and asleep states were normal. These patients developed episodes of shortness of breath when startled or during mental stress later in life, i.e. in adolescence and adulthood. These symptoms responded to anti-myotonic treatment. It is important to note that respiratory difficulties



Fig. 1. Patient 1 with neonatal respiratory distress as infant. In infancy and childhood, laryngospasm and myotonic stiffness of the ventilatory muscles resulted in cyanosis and demanded oxygen supply.



Fig. 2. Still image of the inspiratory stridor of patient 3 in the first month of life. The image is associated by a video (stridor.avi).

can worsen during anesthesia with muscle relaxants: at 11 years of age, patient 9 experienced increasing respiratory distress during general anesthesia and died of cardiorespiratory insufficiency due to a severe myotonic reaction, which was associated with initial jaw clenching and late occurrence of hyperkalemia and increased body temperature resembling a malignant-hyperthermia-like event.

In pre-school childhood, the habitus showed slow movements, excessive sweating and open mouth with drooling. In four patients, shoulder girdle and arms were typically rotated inwardly, with elevated shoulders, antero-flexion of the trunk (patient 1, Fig. 3A), and a bell-shaped thorax (patient 2, Fig. 3B). One patient, originally diagnosed with Schwartz-Jampel syndrome (SJS) (3) had laryngeal stridor, high-pitched voice, mask-like facies, myotonic and hypertrophic shoulder, neck and upper arm muscles (patient 10, Fig. 4A-C). Movements were scarce and slow. During locomotion there was toe-walking and the arms were held in semi-flexion.

Myotonia was present at all ages. Continuous muscle activity superimposed by myotonic bursts could be recorded in the EMG of the affected muscles, even during sleep. If a patient was startled, the EMG activity transiently increased further. Myotonia worsened with potassium-rich food in all three patients. Unexpectedly, the clinical responses of some muscle groups differed considerably. In facial and bulbar muscles, the myoto-

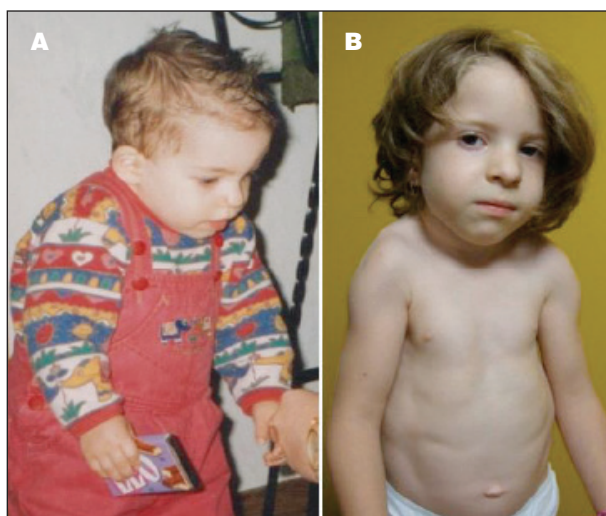


Fig. 3. A: Patient 1 with bent posture in childhood. **B:** Patient 2 with bell-shaped thorax and inwardly rotated shoulder girdle and pectoralis muscles. Note the hypertrophy of neck muscles and the mentalis.

nia worsened during repetitive exercise and cooling. Lid muscles were especially sensitive to cold and presented with paradoxical lid myotonia, even more extreme than in paramyotonia. In contrast, the myotonia disappeared in cooled forearm muscles. Trunk and upper extremities did



Fig. 4. Boy (patient 10) with postnatal laryngospasm and myotonia at age of 4.5 (A, B) and 11 years (C). **A:** Toe walking associated with involuntary closing the fists; **B:** The boy was asked to close his eyes whereby he also activated his mouth and other facial muscles; due to the myotonic stiffness of the hypertrophic muscles, the patient often fell following a sudden movement and injured himself. **C:** Short neck and hypertrophic neck and shoulder girdle muscles. Prior to detection of a G1306E sodium channel mutation causing myotonia permanens, the patient was thought to have a myogenic form of Schwartz-Jampel syndrome.

not show warm-up phenomenon so that patients were unable to arise from floor for minutes after falling, however, the lower extremities showed a warm-up phenomenon much like that in recessive, chloride channel myotonia. A milder phenotype with interrupted EMG activity was observed in one patient who originally had the clinical diagnosis of Becker myotonia and no respiratory episodes in childhood (patient 8).

Muscle hypertrophy was also present at all ages (Table 1). It was most pronounced in neck, face (particular the mentalis muscle), bulbar, shoulder and proximal arm muscles as shown for patient 3 (Fig. 5A), patient 4R (Fig. 5B), patient 5 (Fig. 5C), and patient 4 (Fig. 5D), the mother of the boy 4R. She enabled us to coin the term myotonia permanens as new entity. The hypertrophy corresponded well with myotonia and with painful cramps of working muscles, outlasting subsequent rest from which 90% of patients suffered. Motor development was delayed when without treatment.

Surprisingly, we found several instances of muscle weakness in the patients. One patient presented with hypotonia at birth and 40% of all patients presented with episodic or mild continuous weakness (Table). The epi-

sodes ranged from relatively sudden events of lower limbs for a few days with consequent falling (patient 7) up to mild but fixed proximal leg weakness (patient 6). Patient 10 had a weak such as an infant.

Generally, myotonic symptoms responded to antiepileptic and antiarrhythmic drugs. Since carbamazepine caused adverse effects at higher dosages, mexiletine and flecainide were most frequently used. Our patients generally preferred flecainide since, for example, flecainide was able to suppress the continuous activity completely when muscles were at rest (patient 6).

Excised muscle experiments

Muscle fiber segments obtained from patient 4 showed spontaneous membrane depolarizations similar to those previously published for patient 10 (4). The depolarizations were followed by intracellular myotonic bursts consisting of waxing action potential frequency and waning amplitude with subsequent self-generated repolarization characterized by an inverse pattern (Fig. 6). Pathological spontaneous muscle activity and twitch forces revealed an approximately 4-fold higher amplitude after elevation of potassium from 3 to 7 mM.

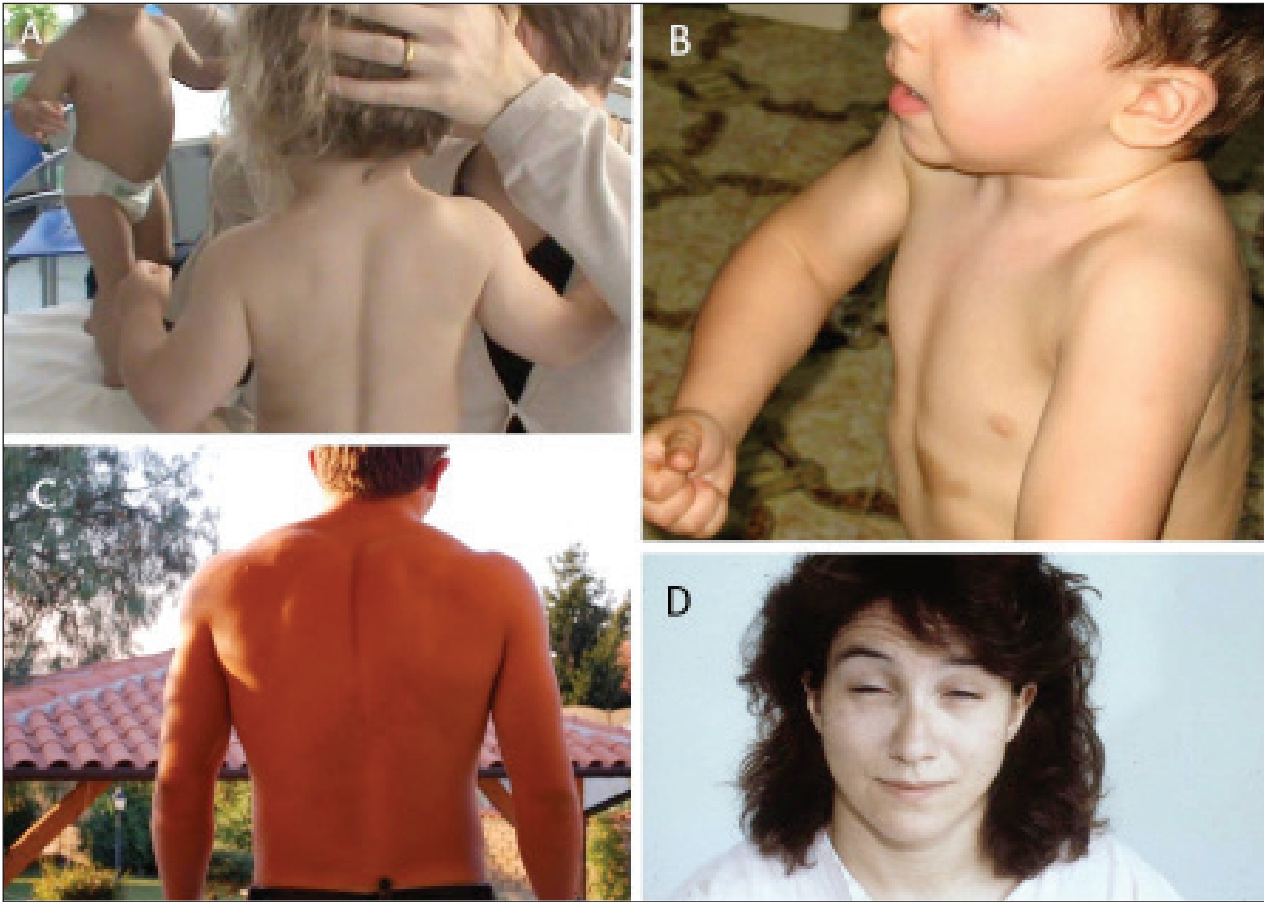


Fig. 5. Myotonic stiffness and muscle hypertrophy in 4 patients at different ages. Note the short neck and the hypertrophic shoulder, back and upper arm muscles. **A:** infancy (patient 3), **B:** childhood (patient 4R), **C:** adolescence (patient 5), **D:** Adulthood (patient 4); the picture shows the face of the first patient world-wide who was reported by Lerche et al. 1993 under the diagnosis of myotonia permanens. Note the blepharospasm.

Forearms cooled in water of 15°C for 30 min had the same effect, however, rewarming completely abolished myotonia.

Evaluation of fit parameters using the current dots published in our G1306E/V/A paper (5)

Using Boltzmann distribution $I/I_{\max} = A/(1 + \exp((V - V_{0.5})/k)) + I_0$, the best current fits of the dots of the steady-state curves were achieved for the following parameters: for inactivation of WT channels: $A = 0.98$, $V_{0.5} = -56 \pm 1$ mV, $k = 9.1$ mV; and for inactivation of G1306E channels $A = 0.95$, $V_{0.5} = -41 \pm 1$ mV, $k = 8.3$ mV ($N = 8-12$). The amplitude factors A and the slopes k did not differ significantly between WT and G1306E, only the 15 mV right-shift of the inactivation curve was significant ($p < 5\%$) (Fig. 7 A). The fit parameters for activation of WT channels were: $A = 0.95$, $V_{0.5} = -11.5 \pm 1$ mV, $k = -7.2$ mV and for activation of G1306E channels

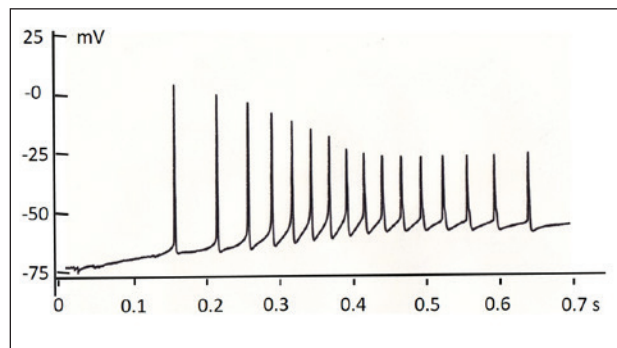


Fig. 6. Intracellular recording of a so far unpublished myotonic burst from a freshly excised muscle fiber of patient 4 when she was biopsied in 1993.

$A = 0.95$, $V_{0.5} = -17 \pm 1$ mV, $k = -7.1$ mV ($N = 8-12$). While A were the same, k did not substantially differ and I_0 was zero, the midpoint of G1306E channel activation

was shifted significantly to the left by 5.5 mV ($p < 5\%$) (Fig. 7B). This left-shift led to a decreased electrical threshold that increases muscle excitability. Additionally, we determined the percentage of channels, which could be opened near the electrical threshold of approximately -65 mV: 89% of G1306E and 72% of WT channels (Fig. 7A).

Window currents and their integration

The superimposition of the steady-state curves for inactivation and activation showed an overlap which corresponded to the window currents for WT and G1306E (Fig. 7C). For the integration of the window currents, the above mentioned Boltzmann distribution for the two channel states (open = activated and closed = inactivated) was used. The increased window current was caused by the left-shift of activation and the right-shift of inactivation. These shifts produced an approximately 3-fold G1306E window current at -30 mV and a 3.1-fold window area for G1306E vs. normal channels. The increased computed areas i.e., the integral sodium influx may generate weakness by depolarizing the membrane close to the threshold and inactivating co-existing wildtype channels *in vivo*. Due to kinetic and steady-state properties that depend on each other, the right-shift of the inactivation curve increases the number of „activatable“ channels at physiologically relevant test voltages. This peculiar property of the G1306E channel may further contribute to the severe and permanent myotonia.

Discussion

Clinical features

Our study is the first to examine a G1306E cohort from the neonatal period to adulthood. It expands knowledge of the phenotype presented in previous single case reports and enables early *prima facie* diagnosis which changes the patient's life. The presence of postnatal respiratory symptoms such as laryngospasm and stridor has been described for several Nav1.4 mutations including G1306E, I693T, A799S, N1297K, and T1313M (2, 6-13). Also for the milder myotonia fluctuans caused by G1306A, severe postnatal cyanosis has been reported (14). A milder G1306E phenotype we found in one patient is similar to (1) who reported father and son with severe myotonia aggravated by exercise and potassium, but only moderate impairment by the condition, even without treatment. In contrast, the presence of various degrees of weakness and the different reactions to exercise (exacerbation or warm-up) and cold (exacerbation or disappearance of myotonia) have

not yet been reported. This could be due to the physical examinations focusing on muscle especially affected by myotonia (eyelid and hand) for diagnosis whilst ignoring the lower extremities.

Differential diagnoses

Paroxysmal motor phenomena, obstructive sleep apnoea, opisthotonus, and unconsciousness may have led to the frequent suspicion of the diagnosis *epilepsy* in newborns. However these paroxysmal motor phenomena in euglycemic neonates are most likely brain stem release signs (15). Epileptic activity was finally excluded by several conventional and special EEGs such as video-EEG. Another differential diagnosis, the very rare Schwartz-Jampel syndrome (SJS), requires more extensive clinical, radiological, and EMG investigation. SJS is characterized by delayed onset after birth, blepharospasms and mask-like face, reduced tendon reflexes, and short stature (16). Lack of osteochondrodysplasia in the x-ray is an exclusion criterion. The atypical myotonia in SJS can be confirmed by EMG because the discharges are neurogenic and characterized by high frequency and low voltage. Since the existence of a myogenic SJS has long been disproven, we encourage to drop this term in the future.

Pathogenesis and treatment

Until now, mainly the degree of the slowing of kinetics of inactivation with destabilization of the inactivated state was held responsible for the clinical severities of the Nav1.4 mutations G1306A, G1306V, and G1306E (5,17). Our evaluation suggests that i) lowering of the G1306E threshold, ii) increased window currents, and iii) increased mutant channel availability at near-threshold potentials may contribute decisively to the phenotype. Additionally, the window current may explain the increased effectivity of flecainide as shown for the homologous heart Nav1.5 channel (18, 19). Flecainide can be started in the neonatal period and will permit a life-long treatment of symptoms (7, 20).

Conclusions

Myotonia permanens is a very rare disease. Our collection of 10 unrelated patients is a genetically clarified case series from newborn period to adulthood and is relevant for parent counselling and early *prima facie* diagnosis. Unusual distribution of myotonia, muscle hypertrophy, and weakness should not exclude a genetic test for the G1306E mutation – especially if laryngospasm or respiratory difficulties are present – because therapy is available: flecainide.

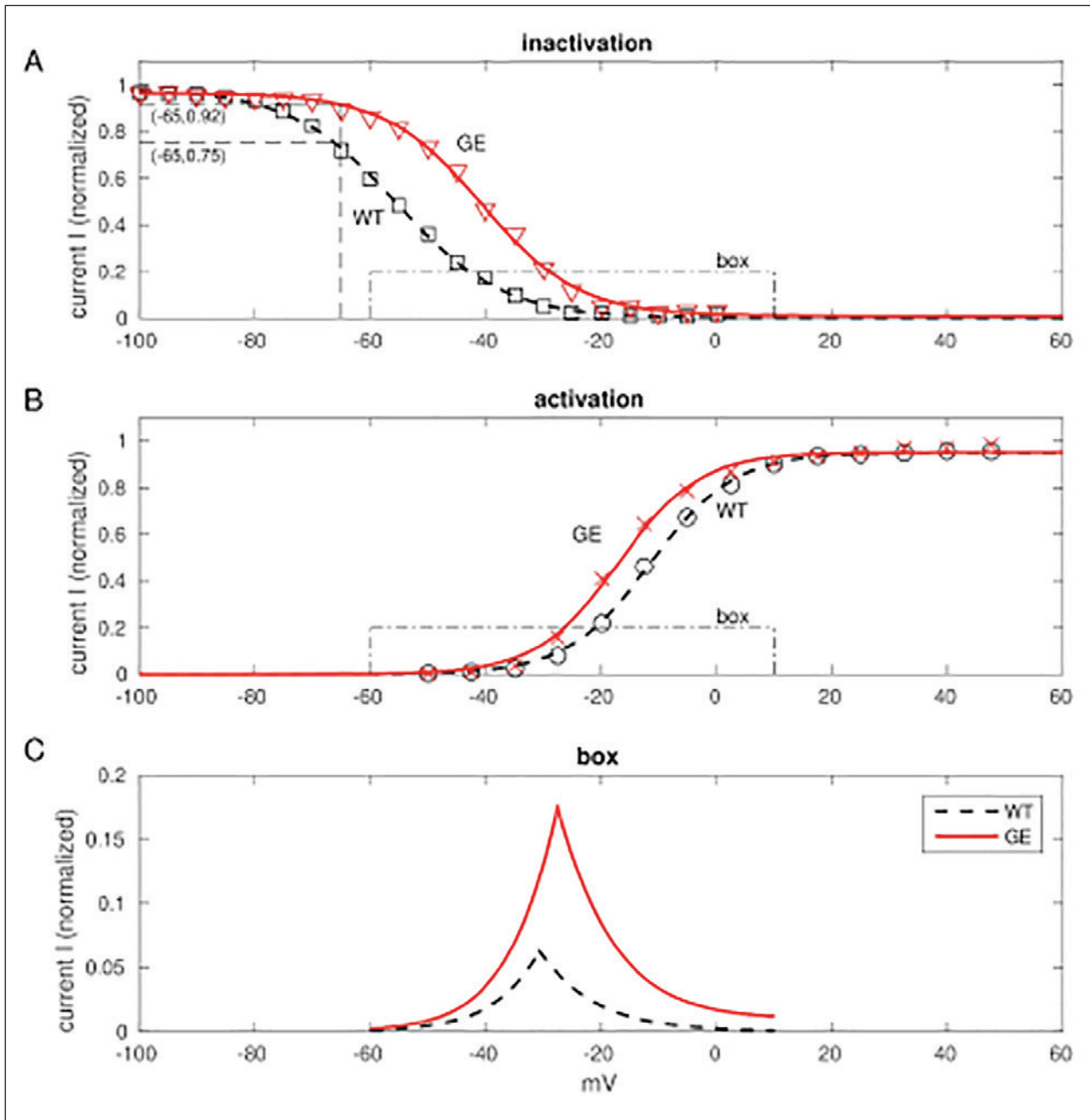


Fig. 7. A-C: Measured values (spots) and Boltzmann fits (lines) of steady-state inactivation (**A**) and steady-state activation (**B**) for normal (WT) and G1306E (GE) mutant channels. The currents were normalized to the maximum sodium current. The deviation between spots (dashedlines) and fits (continuous lines) is minimal for WT and neglectable for physiologically relevant voltages of the mutant channel. The percentage of channels which are not inactivated at an electrical threshold of -65 mV is higher for G1306E (92%) than for WT (75%). As steady-state inactivation at 0 mV was induced by a relatively short 35-ms pulse to the indicated test voltage, we also applied 500-ms prepulses and found no change in the size of the shift. C: The overlapping area (box) of the fits in A and B shows the current size and the voltage range of the window current. The two triangles were used for integration.

Acknowledgements

We thank Drs H. Lerche and P.A. Iaizzo for fruitful discussions and Drs C. Gill and B. Reitter for help to recruit patients for the study and the families for their collaboration. This work is dedicated to Dr. K. Ricker. This study was supported by the IonNeurOnet of the German BMBF Ministry of Research, the German DGM Muscle Disease Society, and the non-profit Hertie-Foundation.

References

1. Colding-Jørgensen E, Duno M, Vissing J. Autosomal dominant monosymptomatic myotonia permanens. *Neurology* 2006;67:153-5.
2. Lerche H, Heine R, Pika U, et al. Human sodium channel myotonia: Slowed channel inactivation due to substitutions for a glycine within the III/IV linker. *J Physiol (Lond)* 1993;470:13-22.
3. Spaans F, Theunissen P, Reekers A, et al. Schwartz-Jampel syndrome: Part I. Clinical, electromyographic, and histologic studies. *Muscle Nerve* 1990;13:516-27.
4. Lehmann-Horn F, Iaizzo PA, Franke Ch, et al. Schwartz-Jampel syndrome. Part II: Na⁺ channel defect causes myotonia. *Muscle Nerve* 1990;13:528-35.
5. Mitrovic N, George AL Jr, Lerche H, et al. Different effects on gating of three myotonia-causing mutations in the inactivation gate of the human muscle sodium channel. *J Physiol* 1995;487:107-14.
6. Caietta E, Milh M, Sternberg D, et al. Diagnosis and outcome of SCN4A-related severe neonatal episodic laryngospasm (SNEL): 2 new cases. *Pediatrics* 2013;132:e784-7.
7. Desaphy JF, Modoni A, Lomonaco M, et al. Dramatic improvement of myotonia permanens with flecainide: a two-case report of a possible bench-to-bedside pharmacogenetics strategy. *Eur J Clin Pharmacol* 2013;69:1037-9.
8. Singh RR, Tan SV, Hanna MG, et al. Mutations in SCN4A: a rare but treatable cause of recurrent life-threatening laryngospasm. *Pediatrics* 2014;134(5):e1447-50.
9. Gay S, Dupuis D, Faivre L, et al. Severe neonatal non-dystrophic myotonia secondary to a novel mutation of the voltage-gated sodium channel (SCN4A) gene. *Am J Med Genet A* 2008;146:380-3.
10. Matthews E, Guet A, Mayer M, et al. Neonatal hypotonia can be a sodium channelopathy: recognition of a new phenotype. *Neurology* 2008;71:1740-2.
11. Lion-Francois L, Mignot C, Vicart S, et al. Severe neonatal episodic laryngospasm due to de novo SCN4A mutations: a new treatable disorder. *Neurology* 2010;75:641-5.
12. Simkin D, Léna I, Landrieu P, et al. Mechanisms underlying a life-threatening skeletal muscle Na⁺ channel disorder. *J Physiol (Lond)* 2011;589:3115-24.
13. Matthews E, Manzur AY, Sud R, et al. Stridor as a neonatal presentation of skeletal muscle sodium channelopathy. *Arch Neurol* 2011;68:127-9.
14. Torbergesen T, Jurkat-Rott K, Stalberg EV, et al. Painful cramps and giant myotonic discharges in a family with the Nav1.4-G1306A mutation. *Muscle Nerve* 2015;52:680-3.
15. Orivoli S, Facini C, Pisani F. Paroxysmal nonepileptic motor phenomena in newborn. *Brain Dev* 2015;37:833-9.
16. Nicole S, Topaloglu H, Fontaine B. 102nd ENMC International Workshop on Schwartz-Jampel syndrome, 14-16 December, 2001, Naarden, The Netherlands. *Neuromuscul Disord* 2003;13:347-51.
17. Groome JR, Fujimoto E, Ruben PC. K-aggravated myotonia mutations at residue G1306 differentially alter deactivation gating of human skeletal muscle sodium channels. *Cell Mol Neurobiol* 2005;25:1075-92.
18. Desaphy JF, De Luca A, Didonna MP, George AL Jr, Camerino Conte D. Different flecainide sensitivity of hNav1.4 channels and myotonic mutants explained by state-dependent block. *J Physiol* 2004;554(Pt 2):321-34.
19. Amarouch MY, Swan H, Leinonen J, et al. Antiarrhythmic action of flecainide in polymorphic ventricular arrhythmias caused by a gain-of-function mutation in the Nav 1.5 Sodium channel. *Ann Noninvasive Electrocardiol* 2016;21:343-51.
20. Portaro S, Rodolico C, Sinicropi S, et al. Flecainide-responsive myotonia permanens with snel onset: a new case and literature review. *Pediatrics*. pii: peds 2015:3289.

Arrhythmogenic right ventricular cardiomyopathy in Boxer dogs: the diagnosis as a link to the human disease

ANNINA S. VISCHER^{1,2}, DAVID J. CONNOLLY³, CAROLINE J. COATS¹, VIRGINIA LUIS FUENTES³,
WILLIAM J. MCKENNA⁴, SILVIA CASTELLETTI^{1,5} AND ANTONIOS A. PANTAZIS^{1,6}

¹ Inherited Cardiovascular Disease Unit, St Bartholomew's Hospital, London, UK; ² Medizinische Poliklinik, Universitätsspital Basel, Switzerland; ³ Royal Veterinary College, London, UK; ⁴ Institute of Cardiovascular Science, University College of London, London, UK; ⁵ Centre for Cardiac Arrhythmia of Genetic Origin, Istituto Auxologico Italiano, Milan, Italy; ⁶ Cardiomyopathy Service, Royal Brompton Hospital, London, UK

Background. Arrhythmogenic right ventricular cardiomyopathy (ARVC) is a myocardial disease with an increased risk for ventricular arrhythmias. The condition, which occurs in Boxer dogs, shares phenotypic features with the human disease arrhythmogenic cardiomyopathy (ACM) suggesting its potential as a natural animal model. However, there are currently no universally accepted clinical criteria to diagnose ARVC in Boxer dogs. We aimed to identify diagnostic criteria for ARVC in Boxer dogs defining a more uniform and consistent phenotype. **Methods and Results.** Clinical records from 264 Boxer dogs from a referral veterinary hospital were retrospectively analysed. ARVC was initially diagnosed according to the number of ventricular premature complexes (VPCs) in the 24-hour-Holter-ECG in the absence of another obvious cause. Dogs diagnosed this way had more VPCs, polymorphic VPCs, couplets, triplets, VTs and R-on-T-phenomenon and syncope, decreased right ventricular function and dilatation in comparison to a control group of all other Boxer dogs seen by the Cardiology Service over the same period. Presence of couplets and R-on-T-phenomenon on a 24h-ECG were identified as independent predictors of the diagnosis. A diagnosis based on ≥ 100 VPCs in 24 hours, presence of couplets and R-on-T phenomenon on a 24h-ECG was able to select Boxer dogs with a phenotype most similar to human ACM.

Conclusion. We suggest the diagnosis of ARVC in Boxer dogs requires two out of the three following criteria: presence of ≥ 100 VPCs, presence of couplets or R-on-T-phenomenon on a 24 h-ECG. This results in a uniform phenotype similar to that described in human ACM and may result in the adoption of the term ACM for this analogous condition in Boxer dogs.

Key words: arrhythmogenic right ventricular dysplasia/cardiomyopathy, ventricular tachycardia, Holter electrocardiography

Introduction

Humans

Arrhythmogenic cardiomyopathy (ACM) is a genetically determined myocardial disorder defined histologically by progressive replacement of the right ventricular (RV) myocardium with adipose and fibrous tissue (1, 2). Although these abnormalities predominantly occur in the RV they may also involve the left ventricle (LV) producing a dilated phenotype (3). The fibrofatty replacement affects intercellular electrical conduction increasing the risk of life-threatening ventricular arrhythmias (4). Dilatation and regional wall motion abnormalities of the RV are frequently seen (5) and may occur at any time during the disease (6).

The clinical diagnosis is based on criteria defined by the European Society of Cardiology Task Force in 1994 (7), revised in 2010 (8). The criteria include structural changes identified by cardiac MRI, echocardiography or RV angiography, histopathology, as well as characteristic ECG-changes, documentation of arrhythmias, and family history (8).

ACM can lead to recurrent sustained or non-sustained ventricular tachyarrhythmia and/or myocardial failure and possible death. However, a significant percentage of patients experiences little or no symptoms (9). ACM in humans can imitate dilated cardiomyopathy (DCM), however it usually presents with a severity of ventricular arrhythmia disproportionate to the extent of LV dilatation (10).

Performed at the Royal Veterinary College, London, United Kingdom

Address for correspondence: Dr Antonios Pantazis, Royal Brompton Hospital, Sydney Street, London SW3 6NP, United Kingdom.
E-mail a.pantazis@nhs.net

Boxer dogs

Arrhythmogenic right ventricular cardiomyopathy (ARVC), a disease similar to ACM in humans, was first described in Boxer dogs in 1983, which unlike cardiomyopathies in other dogs, lacked ventricular dilation and atrial fibrillation but was distinguished by extensive histological alterations including fibrofatty replacement of cardiomyocytes, ventricular premature complexes (VPCs) and frequent ventricular tachycardia (VT) (11) and can concern both RV and LV (12, 13).

Subsequent research focused on arrhythmogenic risk and the genetic causes of the disease (Supplemental Material, Table 1) and it was suggested that Boxer dogs might serve as a naturally occurring model for the human disease, based on the close clinical and pathological resemblances of the two conditions (12). However, there is no consensus on diagnostic criteria for ARVC in Boxer dogs resulting in a discrepancy of diagnostic criteria between different studies, which prevents direct comparison between them. Previously used diagnostic criteria are shown in the Supplemental Material, Table 1.

Purpose

Our objective was to develop diagnostic criteria for ARVC in Boxer dogs, which can be easily applied to

clinical practice and do not rely solely on the number of VPCs in a single 24h-ECG, in order to standardise disease classification. We anticipate that a more uniform and consistent clinical definition of the canine phenotype will allow direct comparison with the human phenotype and enhance the utility of this naturally occurring model.

Methods

Data collection

All Boxer dogs admitted to the cardiology service of The Royal Veterinary College between 2001 and 2013 were included. The reason for referral, clinical signs, and medications were obtained from clinical records. 24h-ECGs and echocardiograms were analysed retrospectively.

24h-ECGs were analysed for the number of VPCs, couplets, triplets, and episodes of VT. The morphology of VPCs, couplets, triplets and VTs were evaluated and defined as monomorphic or polymorphic. Monomorphic VPCs had the same visual vector, polymorphic VPCs had > 1 vector. The most commonly appearing morphology was used to describe the overall vector. The duration and rate of supraventricular and ventricular arrhythmias was recorded. Couplets, triplets and VTs were defined as poly-

Table 1. Significant clinical data characteristics between affected and control dogs, when 2 of 3 criteria were (≥ 100 VPCs, couplets, R-on-T in 24h-ECG) fulfilled.

	ARVC (n=61)	Controls (n=70)	p-value
Age	7.21 \pm 3.07	4.63 \pm 3.14	0.000
24h-ECG	61 (100%)	70 (100%)	NA
VPCs present	61 (100%)	64 (91.4%)	0.030
Number VPCs	2240 \pm 3066	446 \pm 1858	0.000
Polymorphic VPCs	55 (91.7%)	39 (60.9%)	0.000
Couplets present	54 (88.5%)	14 (20.0%)	0.000
Number Couplets	565 \pm 1913	2 \pm 8	0.015
Polymorphic couplets	26 (49.1%)	1 (7.7%)	0.010
Triplets present	34 (55.7%)	5 (7.1%)	0.000
Number Triplets	144 \pm 481	0 \pm 0.5	0.013
VT present	30 (49.2%)	7 (10.0%)	0.000
R-on-T	46 (76.7%)	9 (13.6%)	0.000
RA dilatation	4 (6.6%)	0 (0.0%)	0.045
LA diameter (mm)	36.4 \pm 9.39	28.2 \pm 4.5	0.000
LVEF (%)	42.0 \pm 16.5	53.0 \pm 10.1	0.001
LVIDd (mm)	43.3 \pm 8.7	37.8 \pm 4.8	0.000
LVIDs (mm)	33.5 \pm 10.2	26.4 \pm 4.7	0.000
FS (%)	24 \pm 11	30 \pm 8	0.001
AV Vmax (m/s)	2.03 \pm 0.86	2.55 \pm 1.28	0.023

ARVC: Arrhythmogenic right ventricular cardiomyopathy, ECG: electrocardiogram, VPCs: ventricular premature complexes, VT: ventricular tachycardia, RA: right atrial, LA: left atrial, LVEF: left ventricular ejection fraction, LVIDd: enddiastolic left ventricular internal diameter, FS: fractional shortening, AV Vmax: aortic valve maximal velocity

morphic if they displayed different morphologies within their single beats. R-on-T phenomenon was defined as a VPC superimposed on the T wave from other sinus beats as postulated (14). 24h-ECGs were excluded if the print-out quality was sub-optimal for analysis.

Left ventricular end-diastolic (LVIDd) and end systolic (LVIDS) diameter were measured in echocardiograms in the parasternal long-axis view using 2D images. Ejection fraction was calculated using the Simpson's method of disks (15).

DCM was defined by LVIDd > 5.18 cm, LVIDS > 3.63 cm and FS $< 23\%$ which are the 95th and 5th percentiles in normal boxers, respectively (16). The presence of aortic stenosis (AS) was determined using standard Doppler assessment of AV flow. AS was defined by a AV max velocity ≥ 2.25 m/s (17). Diastolic function was assessed by mitral inflow pattern using PW-Doppler (18). RVOT size was measured at end-diastole in the parasternal short axis, from the anterior RV wall to the aortic valve when echocardiographic loops of appropriate quality and the correct plane were available (15). RV function, dilatation and wall motion abnormalities were estimated visually by one investigator, blinded to the number of VPCs, and categorised as mild, moderate and severe.

Traditional diagnosis

The diagnosis of ARVC was made if ≥ 100 VPCs were present on the 24h-ECG (19, 20). Dogs with DCM and AS were excluded from this group and added to the control group. All other Boxer dogs were used as controls. The control group therefore consisted of normal Boxer dogs as well as dogs with AS and DCM. In order to test the diagnostic accuracy of a cut-off of 100 VPCs, we repeated all calculations after the cut-off for the diagnosis of ARVC was altered to ≥ 50 VPCs and ≥ 200 VPCs, using the same exclusion criteria. This diagnostic method is henceforth referred to as "traditional diagnosis".

Novel diagnostic criteria

Independent variables were identified based on the p-values obtained from Chi-Square and independent sample T-tests and then added manually in a forward fashion to the multivariable logistic regression model, starting from the lowest p-value. Independent variables were kept in the model, when Odds Ratio was significant, or removed, when Odds Ratio was non-significant, respectively.

A novel diagnostic score was developed using all significant parameters from the logistic regression model. Additionally, the criterion ≥ 100 VPCs was kept, as it was used in the traditional diagnosis. Each parameter was assigned with one point, therefore giving a maximal number of 3 points for each dog.

Chi-square and independent sample T-tests were repeated to compare the phenotypes when the diagnosis was based entirely on the novel diagnostic score independent of any echocardiographic exclusion. Sensitivity, specificity, positive predictive value and negative predictive value were calculated based on the traditional definitions.

Statistical methods

Statistical analyses were performed using SPSS Version 22 for Mac. A p-value of ≤ 0.05 was considered statistically significant. Univariable analysis consisted of Chi-square and independent sample T-tests. Receiver operating characteristic (ROC) curves and area under the curve (AUC) were utilized to find the ideal cut-off for continuous parameters. Multivariable logistic regression was used to find predictors for the disease.

Results

Data from 264 Boxer dogs were analysed. The dogs were referred for a variety of reasons including syncope, heart failure, incidentally discovered signs such as murmurs or VPCs and for breeding examinations.

Information on presenting signs was available in 213 dogs (80.7%). 24h-ECGs were available in 131 dogs (49.6%). Echocardiograms were available in 261 dogs (98.9%).

Traditional diagnosis

Utilising 24h-ECGs, the dogs were diagnosed on the number of VPCs, using a cut-off of ≥ 50 VPCs, ≥ 100 VPCs and ≥ 200 VPCs. This resulted in an ARVC group of 66, 63 and 57 Boxer dogs, respectively. From all groups, 8 dogs were moved to the control group due to a dilated LV; 12 dogs were moved from the ≥ 50 and ≥ 100 VPCs group and 9 from the ≥ 200 VPCs group to the control group due to AS, leaving 46, 43 and 40 dogs, respectively, that fulfilled the inclusion criteria for ARVC and 218, 221 and 224 dogs, respectively, in the control group. There was no significant difference in sex between the groups, but ARVC dogs were significantly older than dogs in the control group for all cut-offs (Supplemental Material Table 2).

Syncope or pre-syncope (collapse without loss of consciousness) was a common presenting sign in ARVC dogs and significantly less so in the control group using all three cut-offs.

No 24h-ECGs needed to be excluded due to an insufficient recording time; the mean recording time was 24.4 ± 1.0 hrs. As expected, the number of VPCs was higher in all ARVC groups, as this was part of our inclusion criteria. The frequency of polymorphic VPCs, cou-

plets, triplets, VTs (Fig. 1) and R-on-T-phenomenon was significantly greater in dogs with ARVC with all cut-off criteria than in the control group. VTs in the ARVC group were also more prolonged than in control dogs (Supplemental Material Table 3).

Decreased visual RV function, visual RV dilatation and RV wall motion abnormalities, although uncommon, occurred more frequently in ARVC dogs than in the controls (Supplemental Material Table 4), however, there were no significant differences between dogs with and without ARVC regarding measured LV or RV internal diameters or LV ejection fraction (Supplemental Material Table 4).

Novel diagnostic criteria

ROC analysis identified the best cut-off for the number of couplets or triplets on 24-h-ECG to predict the di-

agnosis at 1.5 couplets or 0.5 triplets (Supplemental Material Fig. 1). These numbers were rounded to 1 couplet and 1 triplet in 24 hours for convenience and logic.

Simple binary logistic regression analysis showed that both the presence of couplets and R-on-T-phenomenon were significant predictors of the diagnosis. This remained unchanged with all the different traditional cut-off criteria (Supplemental Material Table 5).

As a result of this, the criteria to diagnose ARVC were refined to include ≥ 100 VPCs, presence of ≥ 1 couplet and R-on-T phenomenon on a 24h-ECG. Henceforth this is referred to as novel criteria.

If only one of the novel criteria was fulfilled without consideration of previously applied echocardiographic exclusion parameters, patients with RV dilatation were correctly placed in the ARVC group (Supplemental Material, Tables 6-9). Affected dogs were older, had a significantly higher prevalence of polymorphic VPCs and VTs

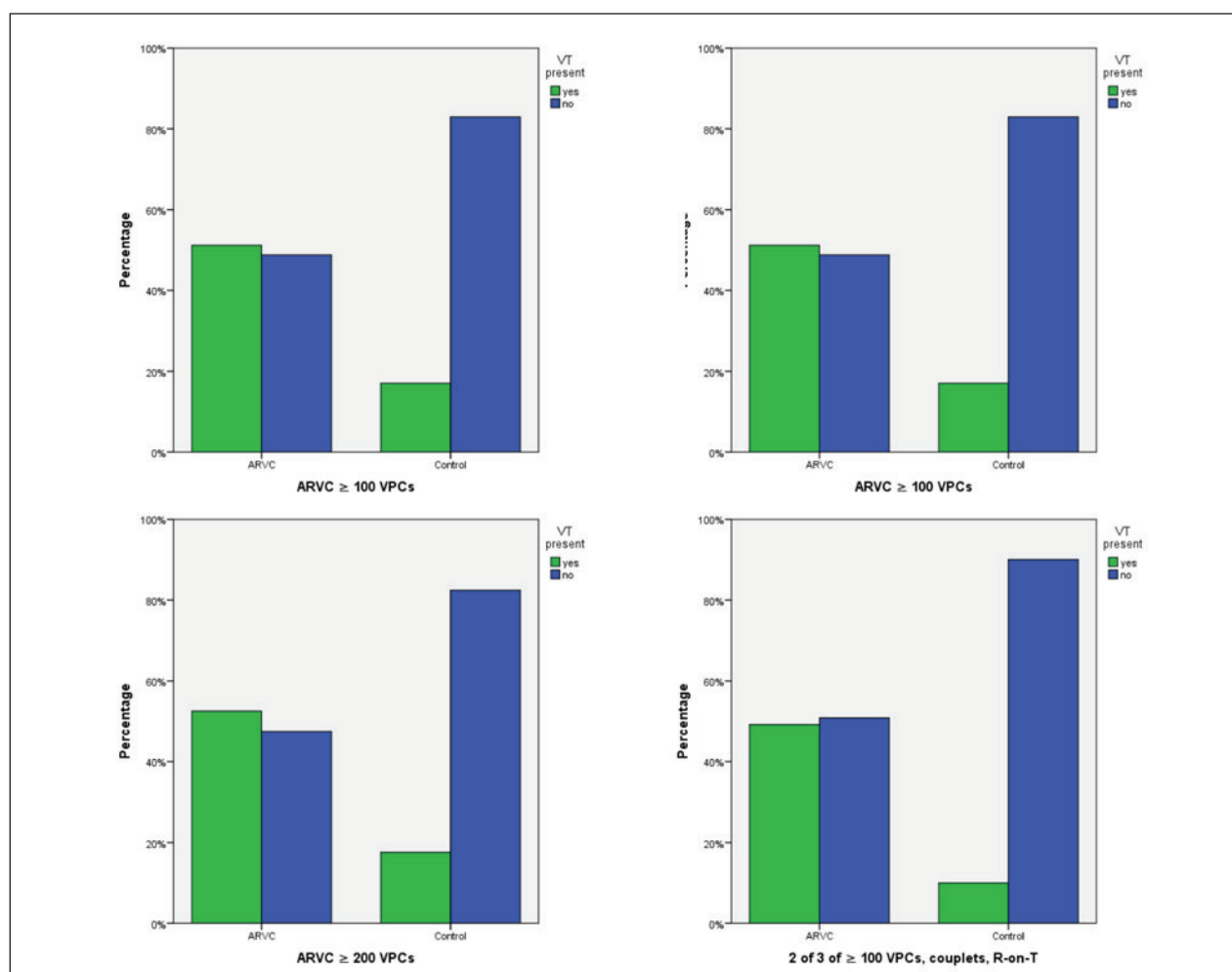


Figure 1. Comparison of prevalence of VT when ARVC is defined as a.) ≥ 100 VPCs, b.) ≥ 50 VPCs, c.) ≥ 200 VPCs, d.) 2 of 3 criteria (≥ 100 VPCs, couplets, R-on-T; only dogs with a 24h-ECG included). All remaining dogs are in Control group.

(Supplemental Material, Table 6) compared to the control group. Addition of one more novel criterion, again without application of echocardiographic exclusion parameters, further refined diagnostic efficacy (Supplemental Material, Table 6 and Fig. 1) and resulted in dogs with AS being moved to the control group (Table 1, Figure 2) and dogs with DCM being moved to the ARVC group (Table 1, Fig. 3). This effect was only marginally more pronounced when all 3 novel criteria were used.

Dogs with RV dilatation, which did not fulfil any of the novel criteria, had either a severe valvular or subvalvular AS, and were therefore correctly assigned to the non-ARVC group, or did not have a 24h-ECG and were therefore not eligible for the correct diagnosis (Supplemental Material, Table 6). Syncope was prevalent in both ARVC and control dogs, however statistically significantly more so in the ARVC group.

Discussion

ARVC in Boxer dogs has been proposed as a useful model for the human disease because of their similarity at the clinical and pathological levels (12). Furthermore the prevalence is estimated to be higher than in humans and disease progression more rapid (21). However, in order to fully exploit this model, clear diagnostic criteria are required. To date, there are no universally accepted diagnostic criteria for ARVC in Boxer dogs, with inclusion criteria in different studies varying considerably, occasionally in a contradictory manner. Diagnosis is traditionally based on the number of VPCs with or without echocardiographic changes (Supplemental Material, Table 1). However, the number of VPCs documented on 24h-ECGs recorded from the same dog may vary as much as 80% (22). We therefore aimed to identify diagnostic criteria, which would describe a more uniform pheno-

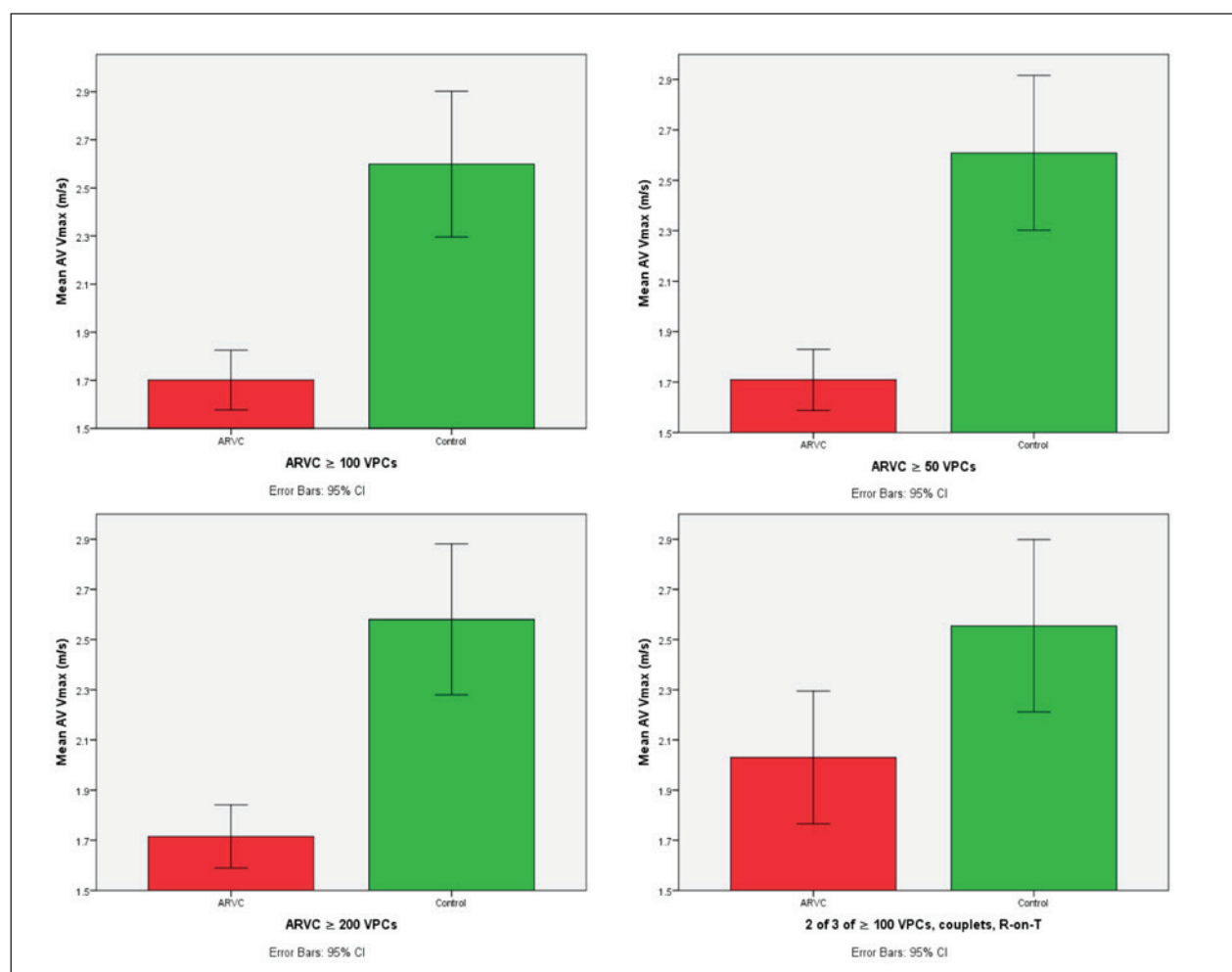


Figure 2. Comparison of mean AV Vmax (m/s), when ARVC is defined as a.) ≥ 100 VPCs, b.) ≥ 50 VPCs, c.) ≥ 200 VPCs, d.) 2 of 3 criteria (≥ 100 VPCs, couplets, R-on-T; only dogs with 24h-ECG included). All remaining dogs are in Control group. Whiskers symbolise 95% confidence intervals.

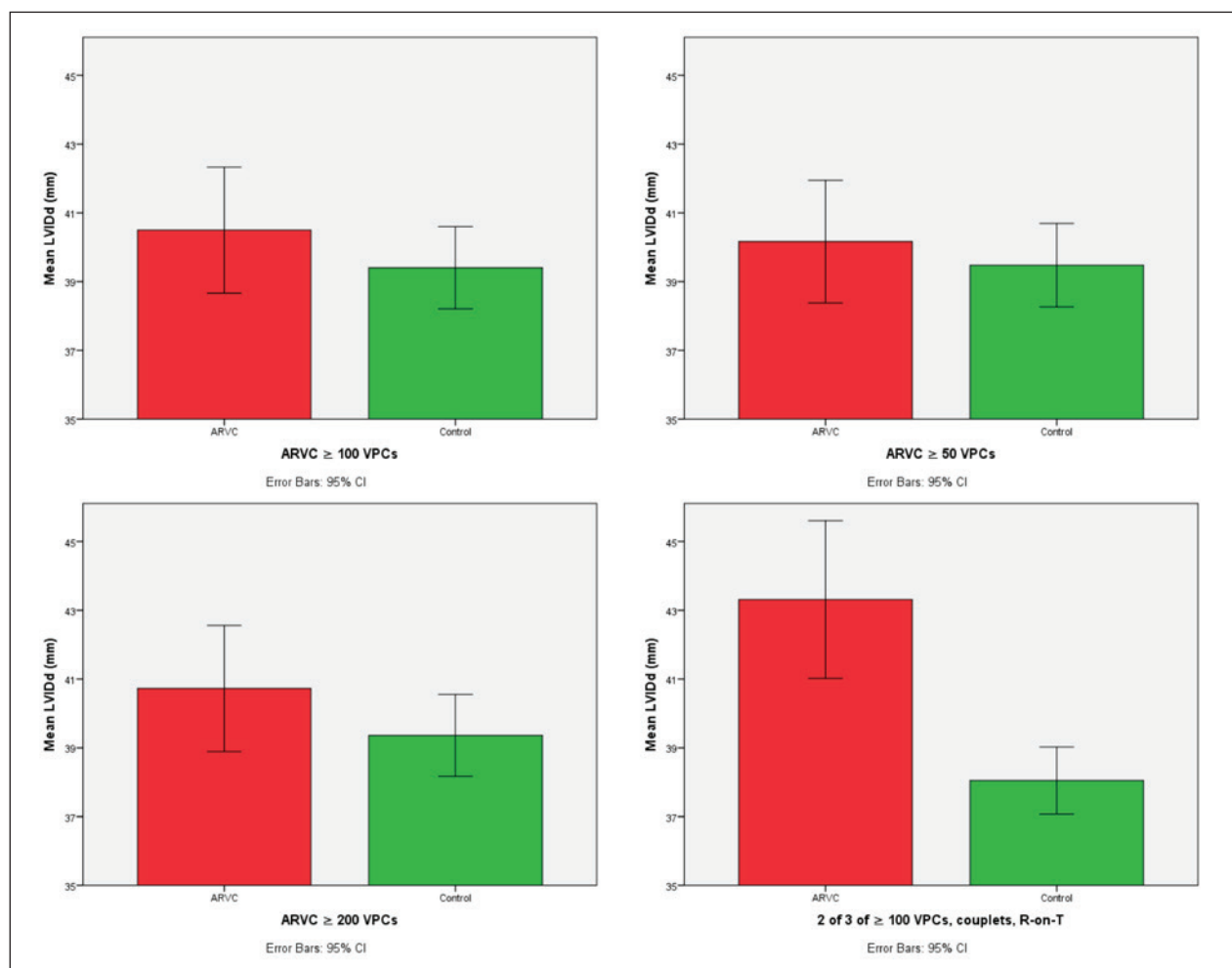


Figure 3. Comparison of mean left ventricular end-diastolic internal diameter (mm), when ARVC is defined as a.) ≥ 100 VPCs, b.) ≥ 50 VPCs, c.) ≥ 200 VPCs, d.) 2 of 3 criteria (≥ 100 VPCs, couplets, R-on-T; only dogs with a 24h-ECG included). All remaining dogs are in Control group. Whiskers symbolise 95% confidence intervals.

type, clinically applicable and not solely related on the number of VPCs on a single 24h-ECG.

Our main findings are that there are significant differences with regard to presentation with syncope, presence of polymorphic VPCs, couplets, triplets, VTs and R-on-T phenomenon in 24h-ECGs, as well as decreased RV function and RV dilatation in echocardiograms between affected and control groups, when using the number of VPCs documented on a 24h-ECG as an inclusion criterion, and echocardiographic signs of AS or DCM as exclusion criteria. Between cut-off values of ≥ 50 , ≥ 100 or ≥ 200 VPCs, a cut-off of ≥ 100 VPCs showed the clearest distinction between the two groups. Multivariable analysis identified couplets and R-on-T phenomenon on 24h-ECGs as clinically useful predictors for ARVC. Therefore, we suggest new criteria for the diagnosis of ARVC consisting of ≥ 100 VPCs, presence of couplets and R-on-T phenomenon on a 24h-ECG.

There is currently no gold standard against which to compare these results. However, when the three diagnostic criteria outlined above are applied without using echocardiographic exclusion criteria, with 2 out of 3 criteria needing to be satisfied for a diagnosis of ARVC, we were able to diagnose a group of dogs presenting with a phenotype closely resembling the phenotype described in human ACM with ventricular arrhythmia, dilatation of the RVOT, presentation with syncope and without signs of valvular disease. Dogs diagnosed with ARVC using only the novel criteria also had larger LV diameters and a lower velocity across the aortic valve in comparison to control dogs, and this finding excludes AS as a common reason for arrhythmia. The use of these three 24h-ECG criteria should enable a clearer description of the phenotype. However, future prospective studies will be required to test their robustness.

ARVC in Boxer dogs is characterized by ventricular tachyarrhythmia, syncope and myocardial dysfunction (12). Necropsies reveal RV chamber dilatation in about a third of cases and histopathological changes closely resembled those seen in human patients (12).

RV dilatation and dysfunction are a mainstay of the diagnosis in humans(8). We identified RV dilatation in a small percentage of Boxer dogs with ARVC, as previously described (23). In humans with ACM, electrical changes often precede structural changes (6). The low prevalence of RV dilatation in Boxer dogs may indicate that RV dilatation is characteristic of more progressive disease and that a proportion of dogs die before these structural changes develop(11). When applying the novel criteria, the mean LV diameter was larger in dogs with ARVC than in the control group. ACM in humans is also known to involve the LV which may have an appearance similar to DCM, however, is generally associated with a more arrhythmic presentation than DCM(10). The finding of biventricular or even left dominant involvement has led to the term “arrhythmogenic cardiomyopathy” (24, 25). The original description of ARVC in Boxer dogs included both an arrhythmic and a dilated phenotype (11). Further studies are required to determine whether both phenotypes are an expression of the same disease. However, based on our results and previous publications commenting on left ventricular involvement in Boxer dogs (12, 13), we recommend the use of the term arrhythmogenic cardiomyopathy in Boxer dogs in view of the condition’s close similarity to the human disease.

In human patients, the diagnostic and prognostic value of couplets is unresolved (26-29). In our study, we identified a correlation between the number of couplets and the number of VPCs. Furthermore, binary logistic regression showed couplets to be an independent predictor for the diagnosis of ARVC in Boxer dogs. The occurrence of the R-on-T phenomenon in Boxer dogs with ARVC has been previously described (30) and this study confirms its diagnostic value.

Our novel criteria, based on knowledge from human ACM with respect to arrhythmia and structural changes, appear robust and therefore likely to have beneficial diagnostic utility. This further refinement of the ARVC phenotype in Boxer dogs should endorse its use as a model of human disease.

Limitations

This is a retrospective study on a heterogeneous and biased cohort of Boxer dogs, which needed to be referred to a tertiary centre for inclusion. Not all dogs were examined with all diagnostic modalities, although dogs without a 24h-ECG were excluded from the ARVC group. Therefore, the control group may have included dogs

with ARVC, which were misdiagnosed. Follow up data in these dogs is lacking, so dogs assigned to the control group may develop ARVC later in life or show an incomplete expression. Also we have not assessed survival data in this study.

The main limitation, however, is, that there is no gold standard for the diagnosis of ARVC. Furthermore, our criteria are based on the hypothesis that ACM in humans and ARVC in Boxer dogs are the same disease (12). Our criteria need confirmation, using prospective longitudinal studies and possibly histological analysis.

Conclusions

We suggest 3 diagnostic criteria, which include ≥ 100 VPCs in 24 hours, presence of couplets and R-on-T phenomenon in a 24h-ECG, of which 2 must be fulfilled as a more robust and straightforward way of diagnosing ARVC in Boxer dogs. ARVC in Boxer dogs progresses more rapidly compared to humans and could therefore serve as an excellent research model for the human disease. Studying the canine version of the disease allows further research on the genetic cause and its therapy, which may be translated into the human clinic. The novel findings of couplets and R-on-T phenomenon will need further evaluation in both Boxer dogs and humans. In view of the close analogy between disease in Boxer dogs and humans and in particular the presence of both right and left ventricular involvement we suggest adopting the term arrhythmogenic cardiomyopathy for the canine condition.

Funding Sources

ASV was funded by the Swiss Heart Rhythm Foundation. WJM was funded by the Higher Education Funding Council for England, British Heart Foundation Program Grant RG/13/19/30568, and Foundation Leducq Transatlantic Networks of Excellence Program: GRANT n° 14 CVD 03. University College London Hospitals NHS Foundation Trust receives funding from the Department of Health’s NIHR Biomedical Research Centre funding scheme. SC was funded by the European Society of Cardiology Research Grant and by the Italian Society of Cardiology with a grant by the MSD Italia-Merck Sharp & Dohme Corporation. DJC, CJC, VLF and AP have nothing to declare.

References

1. Femia G, Hsu C, Singarayar S, et al. Impact of new task force criteria in the diagnosis of arrhythmogenic right ventricular cardiomyopathy. *Int J Cardiol* 2014;171:179-83.

2. Elliott P, Andersson B, Arbustini E, et al. Classification of the cardiomyopathies: a position statement from the European Society Of Cardiology Working Group on Myocardial and Pericardial Diseases. *Eur Heart J* 2008;29:270–276.
3. Basso C, Thiene G, Corrado D, et al. Arrhythmogenic right ventricular cardiomyopathy. Dysplasia, dystrophy, or myocarditis? *Circulation* 1996;94:983–91.
4. Basso C, Corrado D, Marcus FI, et al. Arrhythmogenic right ventricular cardiomyopathy. *Lancet* 2009;373:1289–300.
5. Blomström-Lundqvist C, Beckman-Suurkula M, Wallentin I, et al. Ventricular dimensions and wall motion assessed by echocardiography in patients with arrhythmogenic right ventricular dysplasia. *Eur Heart J* 1988;9:1291–302.
6. Gomes J, Finlay M, Ahmed AK, et al. Electrophysiological abnormalities precede overt structural changes in arrhythmogenic right ventricular cardiomyopathy due to mutations in desmoplakin-A combined murine and human study. *Eur Heart J* 2012;33:1942–53.
7. McKenna WJ, Thiene G, Nava A, et al. Diagnosis of arrhythmogenic right ventricular dysplasia/cardiomyopathy. Task Force of the Working Group Myocardial and Pericardial Disease of the European Society of Cardiology and of the Scientific Council on Cardiomyopathies of the International Society and Federation of Cardiology. *Br Heart J* 1994;71:215–8.
8. Marcus FI, McKenna WJ, Sherrill D, et al. Diagnosis of arrhythmogenic right ventricular cardiomyopathy/dysplasia: proposed modification of the Task Force Criteria. *Eur Heart J* 2010;31:806–14.
9. Groeneweg JA, Bhonsale A, James CA, et al. Clinical presentation, long-term follow-up, and outcomes of 1001 arrhythmogenic right ventricular dysplasia/cardiomyopathy patients and family members. *Circ Cardiovasc Genet* 2015;8:437–46.
10. Sen-Chowdhry S, Syrris P, Prasad SK, et al. Left-dominant arrhythmogenic cardiomyopathy: an under-recognized clinical entity. *J Am Coll Cardiol* 2008;52:2175–87.
11. Harpster NK. Boxer Cardiomyopathy. In: Kirk R, ed. *Current Veterinary Therapy*. VIII. Philadelphia: WB Saunders, 1983, pp. 329–337. Available at: http://www.abcfoundation.org/Harpster_p1.html.
12. Basso C, Fox PR, Meurs KM, et al. Arrhythmogenic right ventricular cardiomyopathy causing sudden cardiac death in boxer dogs: a new animal model of human disease. *Circulation* 2004;109:1180–5.
13. Yamada N, Kitamori T, Kitamori F, et al. Arrhythmogenic right ventricular cardiomyopathy coincided with the cardiac fibrosis in the inner muscle layer of the left ventricular wall in a boxer dog. *J Vet Med Sci* 2015;77:1299–303.
14. Smirk FH. R waves interrupting T waves. *Br Heart J* 1949;11:23–36.
15. Lang RM, Badano LP, Mor-Avi V, et al. Recommendations for cardiac chamber quantification by echocardiography in adults: an update from the American Society of Echocardiography and the European Association of Cardiovascular Imaging. *J Am Soc Echocardiogr* 2015;28:1–39.e14.
16. Schober KE, Fuentes VL. Doppler echocardiographic assessment of left ventricular diastolic function in 74 boxer dogs with aortic stenosis. *J Vet Cardiol Off J Eur Soc Vet Cardiol* 2002;4:7–16.
17. Bussadori C, Amberger C, Le Bobinnec G, et al. Guidelines for the echocardiographic studies of suspected subaortic and pulmonic stenosis. *J Vet Cardiol Off J Eur Soc Vet Cardiol* 2000;2:15–22.
18. Nagueh SF, Appleton CP, Gillebert TC, et al. Recommendations for the evaluation of left ventricular diastolic function by echocardiography. *Eur. J. Echocardiogr. J Work Group Echocardiogr Eur Soc Cardiol* 2009;10:165–93.
19. Scansen BA, Meurs KM, Spier AW, et al. Temporal variability of ventricular arrhythmias in Boxer dogs with arrhythmogenic right ventricular cardiomyopathy. *J Vet Intern Med Am Coll Vet Intern Med* 2009;23:1020–4.
20. Caro-Vadillo A, García-Guasch L, Carretón E, et al. Arrhythmogenic right ventricular cardiomyopathy in boxer dogs: a retrospective study of survival. *Vet Rec*.2013;172:268.
21. Corrado D, Thiene G. Arrhythmogenic right ventricular cardiomyopathy/dysplasia: clinical impact of molecular genetic studies. *Circulation* 2006;113:1634–7.
22. Spier AW, Meurs KM. Evaluation of spontaneous variability in the frequency of ventricular arrhythmias in Boxers with arrhythmogenic right ventricular cardiomyopathy. *J Am Vet Med Assoc* 2004;224:538–41.
23. Palermo V, Stafford Johnson MJ, et al. Cardiomyopathy in Boxer dogs: a retrospective study of the clinical presentation, diagnostic findings and survival. *J Vet Cardiol Off J Eur Soc Vet Cardiol* 2011;13:45–55.
24. Basso C, Bauce B, Corrado D, et al. Pathophysiology of arrhythmogenic cardiomyopathy. *Nat Rev Cardiol* 2011;9:223–33.
25. Pilichou K, Thiene G, Bauce B, et al. Arrhythmogenic cardiomyopathy. *Orphanet J Rare Dis* 2016;11:33.
26. Bigger JT, Fleiss JL, Kleiger R, et al. The relationships among ventricular arrhythmias, left ventricular dysfunction, and mortality in the 2 years after myocardial infarction. *Circulation* 1984;69:250–8.
27. Hinkle LE, Carver ST, Stevens M. The frequency of asymptomatic disturbances of cardiac rhythm and conduction in middle-aged men. *Am J Cardiol* 1969;24:629–50.
28. Paul T, Marchal C, Garson A. Ventricular couplets in the young: prognosis related to underlying substrate. *Am Heart J* 1990;119:577–82.
29. Bethge KP, Bethge D, Meiners G, et al. Incidence and prognostic significance of ventricular arrhythmias in individuals without detectable heart disease. *Eur Heart J* 1983;4:338–46.
30. Oyama MA, Reiken S, Lehnart SE, et al. Arrhythmogenic right ventricular cardiomyopathy in Boxer dogs is associated with calstabin2 deficiency. *J Vet Cardiol Off J Eur Soc Vet Cardiol* 2008;10:1–10.

Appendix

Supplemental Table 1. Topics of previous studies on Boxer dog arrhythmogenic right ventricular cardiomyopathy and the inclusion/exclusion criteria used.

Author	Topic	Inclusion criteria	Exclusion criteria
Spier 2004 ¹	Spontaneous variability in the frequency of ventricular arrhythmias	≥ 2 years old, no evidence of structural heart disease (echo), ≥ 500 VPC/24h	24h-ECG < 20 h
Basso 2004 ²	A new animal model of human ARVC	Substantial ectopy or syncope, died or euthanized	NA
Baumwart 2005 ³	Plasma brain natriuretic peptide concentration	≥ 1000 VPC/24h	Abnormal left ventricular shortening (<25%), increased left ventricular chamber size with respect to body size, notable valvular regurgitation
Meurs 2006 ⁴	Expression of the cardiac ryanodine receptor	> 1000 VPC/24h of RV origin, and, when present, syncope, sudden cardiac death or right heart failure	NA
Baumwart 2007 ⁵	Serum cardiac troponin I concentration	≥ 1000 VPC/24h, echocardiographic variables within reference range limits	24h-ECG < 20 h
Smith 2007 ⁶	Omega-3 fatty acids	≥ 95 VPC/24h	Symptomatic heart disease, concurrent major diseases, left ventricular outflow tract velocity >3 m/s, arrhythmic medication
Oyama 2008 ⁷	Calstabin2 deficiency	> 1000 VPC/24h with LBBB morphology and when present, syncope or SCD	NA
Scansen 2009 ⁸	Temporal variability of ventricular arrhythmias	> 1 year old, ≥100 VPC/24h, normal systolic function (fractional shortening > 25%) in echo	24h-ECG < 24h, current antiarrhythmic medication
Baumwart 2009 ⁹	Magnetic resonance imaging of right ventricular morphology and function	> 1000 VPC/24h and, when present, syncope	NA
Meurs 2010 ¹⁰	Deletion in the 3' untranslated region of striatin	≥ 500 VPC/24h of right ventricular origin and, when present, syncope	Echocardiographic abnormalities suggestive of congenital heart disease or dilated cardiomyopathy
Palermo 2011 ¹¹	Clinical presentation, diagnostic findings and survival	History of syncope or exercise intolerance, presence of ECG and/or 24h-ECG abnormalities	Unavailability of one of the investigations, gross left atrial dilatation, aortic velocity > 2.4 m/s, congenital or other acquired heart diseases, myocardial failure secondary to rapid supraventricular tachycardia, systemic diseases that might affect the cardiovascular system
Oxford 2011 ¹²	Ultrastructural changes in cardiac myocytes	"We used a combination of electrocardiographic and histopathologic characteristics to confirm a phenotypic diagnosis	NA
Caro-Vadillo 2013 ¹³	Retrospective study of survival	> 100 VPC/24h, normal left ventricular chamber on echo (LVEDD/BSA < 4.35 cm/m ² , LVESD <2.91 cm/m ²)	NA
Mötsküla 2013 ¹⁴	Prognostic value of 24-hour ambulatory ECG (Holter) monitoring	Referral for clinical signs	24h-ECG <19 h, documented congenital heart disease, aortic blood flow velocities ≥ 2.25 m/s
Meurs 2013 ¹⁵	Association of dilated cardiomyopathy with the striatin mutation genotype	Adult, frequent ventricular tachyarrhythmias, normal LV systolic function, positive for striatin mutation	NA
Meurs 2014 ¹⁶	Natural history of arrhythmogenic right ventricular cardiomyopathy in the boxer dog: a prospective study	> 1 year old, ≥ 300 VPC/24h without an obvious cause for the arrhythmia, evaluated at least 2 years sequentially	Echocardiographic abnormalities suggestive of congenital heart disease, evidence of serious systemic disease
Oxford 2014 ¹⁷	Change in β-catenin localization suggests involvement of the canonical Wnt pathway	Extensive histopathological examination and striatin mutation OR evidence of cardiac dysfunction on echocardiogram OR > 10% VPC/24h.	NA
Cattanach 2015 ¹⁸	Pedigree-based genetic appraisal	Clinically diagnosed based on echocardiography, 24h-ECG according to the criteria specified by Meurs ¹⁹ , exclusion of other causes of arrhythmia: Supposedly >100 VPC/24h, normal echo	Rescue dogs and other dogs without pedigree

VPC: ventricular premature beat; LBBB: left bundle branch block; SCD: sudden cardiac death; echo: echocardiogram; LVEDD: left ventricular end-diastolic diameter; BSA: body surface area; LVESD: left ventricular end-systolic diameter

Supplemental Table 2. Baseline characteristics of arrhythmogenic right ventricular cardiomyopathy (ARVC) and control group, with a cut-off of ≥ 50 , ≥ 100 and ≥ 200 ventricular premature complexes (VPC), respectively.

Parameter	ARVC: Cut-off ≥ 50 VPC			ARVC: Cut-off ≥ 100 VPC			ARVC: Cut-off ≥ 200 VPC
	ARVC (n = 46)	Controls (n = 218)	p-value	ARVC (n = 43)	Controls (n = 221)	p-value	ARVC (n = 40)
Male Sex	22 (47.8%)	114 (55.0%)	0.417	20 (46.5%)	122 (55.2%)	0.319	18 (45.0%)
Age	7.22 \pm 3.39	4.89 \pm 3.20	0.000	7.31 \pm 3.36	4.91 \pm 3.21	0.000	7.18 \pm 3.35
Echocardiogram	45 (97.8%)	216 (99.0%)	0.438	42 (97.7%)	219 (99.1%)	0.415	39 (97.5%)
24h-ECG	46 (100%)	85 (39.0%)	0.000	43 (100%)	88 (39.8%)	0.000	40 (100%)
(Pre-) Syncope	35 (83.3%) (n = 42)	85 (49.7%) (n = 171)	0.000	33 (84.6%) (n = 39)	87 (50.0%) (n = 174)	0.000	31 (86.1%) (n = 36)
(Pre-) Syncope at exertion	14 (33.3%)	40 (23.4%)	0.234	13 (33.3%)	41 (23.6%)	0.224	12 (33.3%)
BNP	2022 \pm 789 (n = 7)	1673 \pm 1184 (n = 33)	0.462	2022 \pm 789 (n = 7)	1673 \pm 1184 (n = 33)	0.462	2022 \pm 789 (n = 7)
Troponin	1.71 \pm 3.51 (n = 16)	0.72 \pm 2.32 (n = 63)	0.177	1.80 \pm 3.61 (n = 15)	0.72 \pm 2.30 (n = 64)	0.148	1.80 \pm 3.61 (n = 15)

BNP: brain natriuretic peptide.

Supplemental Table 3. 24h-ECG results of arrhythmogenic right ventricular cardiomyopathy (ARVC) and control group, with a cut-off of ≥ 50 , ≥ 100 and ≥ 200 ventricular premature complexes (VPC), respectively.

Parameter	ARVC: Cut-off ≥ 50 VPC			ARVC: Cut-off ≥ 100 VPC			ARVC: Cut-off ≥ 200 VPC		
	ARVC (n = 46)	Controls (n = 85)	p-value	ARVC (n = 43)	Controls (n = 88)	p-value	ARVC (n = 40)	Controls (n = 91)	p-value
Time 24h-ECG (h)	24.4 \pm 1.0	24.4 \pm 1.1	0.821	24.3 \pm 1.0	24.4 \pm 1.0	0.473	24.3 \pm 1.0	24.4 \pm 1.0	0.583
Mean HR (bpm)	92 \pm 17	92 \pm 24	0.902	93 \pm 18	91 \pm 24	0.708	93 \pm 18	91 \pm 24	0.717
VPC present	46 (100%)	79 (92.9)	0.090	43 (100%)	82 (93.2%)	0.177	40 (100%)	85 (93.4%)	0.177
Number VPC	2339 \pm 3129	624 \pm 2051	0.000	2498 \pm 3177	605 \pm 2018	0.000	2673 \pm 3228	590 \pm 1986	0.000
Polymorphic VPC	41 (91.1)	53 (67.1%)	0.002	38 (90.5%)	56 (68.3%)	0.007	35 (89.7%)	59 (69.4%)	0.014
VPC negative lead I	20 (45.5%)	27 (34.2%)	0.248	20 (48.8%)	27 (32.9%)	0.115	19 (50.0%)	28 (32.9%)	0.107
VPC positive lead II	18 (40.9%)	34 (43.0%)	0.851	18 (43.9%)	34 (41.5%)	0.848	18 (47.4%)	34 (40.0%)	0.554
VPC negative lead III	18 (50.0%)	29 (43.9%)	0.678	17 (51.5%)	30 (43.5%)	0.526	14 (46.7%)	33 (45.8%)	1.000
Couplets present	38 (82.6%)	30 (35.3%)	0.000	37 (86.0%)	31 (35.2%)	0.000	34 (85.0%)	34 (37.4%)	0.000
Number Couplets	680 \pm 2183	39 \pm 197	0.008	727 \pm 2252	38 \pm 194	0.005	781 \pm 2327	36 \pm 191	0.003
Polymorphic couplets	15 (40.5%)	12 (41.4%)	1.000	15 (41.7%)	12 (40.0%)	1.000	15 (45.5%)	12 (36.4%)	0.617
Triplets present	24 (52.2%)	15 (17.6%)	0.000	24 (55.8%)	15 (17.0%)	0.000	23 (57.5%)	16 (17.6%)	0.000
Number Triplets	172 \pm 547	10 \pm 63	0.008	184 \pm 565	10 \pm 62	0.005	198 \pm 583	10 \pm 61.0	0.003
Polymorphic triplets	5 (20.0%)	5 (33.3%)	0.457	5 (20.0%)	5 (33.3%)	0.457	5 (21.7%)	5 (29.4%)	0.717
VT present	22 (47.8%)	15 (17.6%)	0.000	22 (51.2%)	15 (17.0%)	0.000	21 (52.5%)	16 (17.6%)	0.000
Number VT	183 \pm 1064	2 \pm 8	0.118	195 \pm 1100	2 \pm 8	0.099	210 \pm 1140	2 \pm 8	0.082
Duration longest VT (beats)	28 \pm 36	14 \pm 17	0.181	28 \pm 36	14 \pm 17	0.181	29 \pm 36	14 \pm 17	0.134
HR fastest VT (bpm)	268 \pm 61	247 \pm 53	0.294	268 \pm 61	247 \pm 53	0.294	270 \pm 62	245 \pm 51	0.197
Polymorphic VT	3 (13.6%)	2 (13.3%)	1.000	3 (13.6%)	2 (13.3%)	1.000	3 (14.3%)	2 (12.5%)	1.000
R-on-T	33 (73.3%)	22 (27.5%)	0.000	32 (76.2%)	23 (27.7%)	0.000	31 (79.5%)	24 (27.9%)	0.000
Number of beats R-on-T	689 \pm 2926	17 \pm 23	0.288	708 \pm 2971	19 \pm 26	0.273	731 \pm 3018	19 \pm 26	0.254
R-on-T % of all beats	26.6 \pm 75.7	36.4 \pm 40.1	0.581	25.0 \pm 76.3	38.3 \pm 40.2	0.447	25.7 \pm 77.4	36.8 \pm 40.1	0.526

HR: heart rate; VT: ventricular tachycardia.

Supplemental Table 4. Echocardiographic results of arrhythmogenic right ventricular cardiomyopathy (ARVC) and control group, with a cut-off of ≥ 50 , ≥ 100 and ≥ 200 ventricular premature complexes (VPC), respectively.

Parameter	ARVC: Cut-off ≥ 50 VPC			ARVC: Cut-off ≥ 100 VPC			ARVC: Cut-off ≥ 200 VPC		
	ARVC (n = 45)	Controls (n = 216)	p-value	ARVC (n = 42)	Controls (n = 219)	p-value	ARVC (n = 47)	Controls (n = 214)	p-value
Decreased RV function	3 (6.7%)	2 (1.0%)	0.045	3 (7.1%)	2 (1.0%)	0.037	3 (7.7%)	2 (1.0%)	0.030
RV dilatation	5 (11.1%)	4 (2.0%)	0.012	5 (11.9%)	4 (2.0%)	0.009	4 (10.3%)	5 (2.4%)	0.039
RV wall motion abnormality	4 (8.9%)	3 (1.5%)	0.023	4 (9.5%)	3 (1.5%)	0.018	4 (10.3%)	3 (1.5%)	0.014
RA dilatation	3 (6.7%)	6 (3.0%)	0.217	3 (7.1%)	6 (3.0%)	0.186	2 (5.1%)	7 (3.4%)	0.638
Aortic diameter (mm)	19.8 \pm 2.2	19.2 \pm 3.3	0.313	19.8 \pm 2.2	19.2 \pm 3.3	0.285	19.8 \pm 2.2	19.2 \pm 3.3	0.345
LA diameter (mm)	33.1 \pm 8.8	30.9 \pm 7.9	0.146	33.6 \pm 9.0	30.9 \pm 7.8	0.066	33.1 \pm 8.0	31.0 \pm 8.1	0.181
LVEF (%)	47.8 \pm 13.2	50.0 \pm 16.5	0.532	47.5 \pm 13.4	50.0 \pm 16.5	0.467	47.0 \pm 13.3	50.2 \pm 16.4	0.365
IVSd (mm)	10.6 \pm 1.7	10.3 \pm 2.0	0.382	10.7 \pm 1.7	10.3 \pm 2.0	0.286	10.6 \pm 1.7	10.4 \pm 2.0	0.469
LVIDd (mm)	40.2 \pm 5.8	39.5 \pm 7.5	0.582	40.5 \pm 5.7	39.4 \pm 7.5	0.390	40.7 \pm 5.6	39.4 \pm 7.5	0.294
LVPWd (mm)	10.6 \pm 1.9	10.8 \pm 1.8	0.497	10.5 \pm 1.9	10.9 \pm 1.8	0.265	10.4 \pm 1.7	10.9 \pm 1.8	0.138
LVIDs (mm)	30.3 \pm 7.2	28.5 \pm 8.6	0.215	30.8 \pm 7.0	28.4 \pm 8.5	0.105	31.0 \pm 7.0	28.4 \pm 8.5	0.086
FS (%)	25.7 \pm 0.5	28.4 \pm 10.3	0.126	25.0 \pm 9.3	28.5 \pm 10.3	0.052	25.0 \pm 9.5	28.5 \pm 10.3	0.059
TAPSE (mm)	15.3 \pm 4.5	15.5 \pm 2.8	0.925	15.3 \pm 4.5	15.5 \pm 2.8	0.925	15.9 \pm 4.5	15.2 \pm 2.9	0.576
MV E Velocity (m/s)	0.80 \pm 0.23	0.82 \pm 0.21	0.625	0.81 \pm 0.23	0.82 \pm 0.21	0.830	0.81 \pm 0.23	0.82 \pm 0.21	0.830
MV Deceleration time (ms)	122 \pm 29	127 \pm 40	0.658	124 \pm 29	126 \pm 40	0.830	124 \pm 29	126 \pm 40	0.830
MV Deceleration slope (m/s ²)	7.2 \pm 3.1	6.4 \pm 2.3	0.311	7.2 \pm 3.1	6.4 \pm 2.3	0.329	7.20 \pm 3.12	6.44 \pm 2.31	0.830
MV A Velocity (m/s)	0.54 \pm 0.15	0.55 \pm 0.15	0.678	0.53 \pm 0.14	0.56 \pm 0.15	0.474	0.53 \pm 0.14	0.55 \pm 0.15	0.329
MV E/A	1.58 \pm 0.79	1.56 \pm 0.53	0.880	1.62 \pm 0.81	1.55 \pm 0.53	0.584	1.62 \pm 0.81	1.55 \pm 0.53	0.584
AV Vmax (m/s)	1.71 \pm 0.33	2.56 \pm 1.27	0.000	1.70 \pm 0.33	2.55 \pm 1.27	0.000	1.71 \pm 0.33	2.54 \pm 1.27	0.001
AV max PG (mmHg)	12 \pm 5	32 \pm 33	0.001	12 \pm 5	31 \pm 33	0.001	12 \pm 5	31 \pm 33	0.002
RVOT PSAX (mm)	25.0 \pm 7.3	24.4 \pm 5.5	0.681	24.7 \pm 7.5	24.5 \pm 5.5	0.866	24.7 \pm 7.6	24.5 \pm 5.4	0.916
RVIT 4CH (mm)	21.8 \pm 10.5	22.7 \pm 4.1	0.692	21.8 \pm 10.9	22.7 \pm 4.0	0.698	21.8 \pm 10.9	22.7 \pm 4.0	0.698
LVIT 4CH (mm)	33.1 \pm 11.6	36.0 \pm 5.7	0.269	32.7 \pm 12.0	36.1 \pm 5.6	0.215	32.7 \pm 12.0	36.1 \pm 5.6	0.215
RVIT/LVIT	0.71 \pm 0.38	0.63 \pm 0.09	0.281	0.72 \pm 0.40	0.63 \pm 0.09	0.225	0.72 \pm 0.40	0.63 \pm 0.09	0.225

RV: right ventricular; RA: right atrium; LA: left atrium; LVEF: left ventricular ejection fraction; IVSd: intraventricular septum measured in diastole; LVIDd: left ventricular internal diameter in diastole; LVPWd: left ventricular posterior wall measured in diastole; LVIDs: left ventricular internal diameter in systole; FS: fractional shortening; TAPSE: tricuspid annular plane systolic excursion; MV: mitral valve; AV: aortic valve; Vmax: maximal velocity; max PG: maximal pressure gradient; RVOT: right ventricular outflow tract; PLAX: parasternal long axis view; PSAX: parasternal short axis view; RVIT: right ventricular inflow tract; 4CH: four-chamber-view; LVIT: left ventricular inflow tract.

Supplemental Table 5 a-c. Simple binary logistic regression predicting likelihood of arrhythmogenic right ventricular cardiomyopathy (ARVC), cut-off a.) ≥ 50 , b.) ≥ 100 , c.) ≥ 200 VPC for diagnosis ARVC.

a.)	B	SE	Wald	df	P	Odds Ratio	95% CI	
							Lower	Upper
Couplets	1.765	0.481	13.468	1	0.000	5.843	2.276	15.000
R on T	1.711	0.448	14.581	1	0.000	5.535	2.300	13.320
Constant	-2.529	0.467	29.283	1	0.000	0.080		

b.)	B	SE	Wald	df	P	Odds Ratio	95% CI	
							Lower	Upper
Couplets	2.051	0.526	15.193	1	0.000	7.779	2.773	21.825
R on T	1.863	0.472	15.551	1	0.000	6.441	2.552	16.257
Constant	-2.975	0.534	31.048	1	0.000	0.051		

c.)	B	SE	Wald	df	P	Odds Ratio	95% CI	
							Lower	Upper
Couplets	1.830	0.532	11.845	1	0.001	6.236	2.199	17.685
R on T	2.052	0.490	17.564	1	0.000	7.783	2.981	20.320
Constant	-3.093	0.552	31.370	1	0.000	0.045		

B: B coefficient; SE: standard error; Wald: Wald test; df: degrees of freedom; P: p value; CI: confidence interval.

Supplemental Table 6. Baseline characteristics of arrhythmogenic right ventricular cardiomyopathy (ARVC) and control group, 1/3, 2/3, 3/3 novel criteria fulfilled necessary for diagnosis, respectively. All dogs included.

Parameter	ARVC: 1 of 3 novel criteria			ARVC: 2 of 3 novel criteria			ARVC: 3 of 3 novel criteria		
	ARVC (n = 89)	Controls (n = 175)	p-value	ARVC (n = 61)	Controls (n = 203)	p-value	ARVC (n = 36)	Controls (n = 228)	p-value
Male Sex	40 (44.9%)	102 (58.3%)	0.050	30 (49.2%)	112 (55.2%)	0.465	20 (55.6%)	122 (53.5%)	0.859
Age	6.55 ± 3.34	4.59 ± 3.16	0.000	7.21 ± 3.07	4.69 ± 3.22	0.000	7.29 ± 2.94	5.00 ± 3.32	0.000
Echocardiogram	88 (98.9%)	173 (98.9%)	1.000	60 (98.4%)	201 (99.0%)	0.547	35 (97.2%)	226 (99.1%)	0.357
24h-ECG	89 (100%)	42 (24.0%)	0.000	61 (100%)	70 (34.5%)	0.000	36 (100%)	95 (41.7%)	0.000
(Pre-) Syncope	63 (79.7%) (n = 79)	57 (42.5%) (n = 134)	0.000	44 (80.0%) (n = 55)	76 (48.1%) (n = 158)	0.000	26 (78.8%) (n = 33)	94 (52.2%) (n = 180)	0.007
(Pre-) Syncope at exertion	31 (39.2%)	23 (17.2%)	0.001	19 (34.5%)	35 (22.2%)	0.075	11 (33.3%)	43 (23.9%)	0.278
BNP	2043 ± 1061 (n = 22)	1356 ± 1112 (n = 18)	0.054	2183 ± 925 (n = 16)	1434 ± 1163 (n = 24)	0.037	2339 ± 574 (n = 7)	1606 ± 1176 (n = 33)	0.118
Troponin	1.68 ± 3.89 (n = 33)	0.38 ± 0.53 (n = 46)	0.028	1.80 ± 4.21 (n = 26)	0.49 ± 1.04 (n = 53)	0.035	1.92 ± 3.85 (n = 13)	0.73 ± 2.28 (n = 66)	0.133

VPC: ventricular premature complexes; BNP: brain natriuretic peptide

Supplemental Table 7. 24h-ECG results of arrhythmogenic right ventricular cardiomyopathy (ARVC) and control group, 1/3, 2/3, 3/3 novel criteria fulfilled necessary for diagnosis, respectively. All dogs included.

Parameter	ARVC: 1 of 3 novel criteria			ARVC: 2 of 3 novel criteria			ARVC: 3 of 3 novel criteria		
	ARVC (n = 89)	Controls (n = 42)	p-value	ARVC (n = 61)	Controls (n = 70)	p-value	ARVC (n = 36)	Controls (n = 95)	p-value
Time 24h-ECG (h)	24.4 ± 1.0	24.5 ± 1.1	0.484	24.4 ± 0.9	24.4 ± 1.1	0.868	24.3 ± 0.8	24.4 ± 1.1	0.429
Mean HR (bpm)	95 ± 24	85 ± 16	0.009	100 ± 26	85 ± 15	0.000	101 ± 29	88 ± 18	0.004
VPC present	88 (98.9%)	37 (88.1%)	0.013	61 (100%)	64 (91.4%)	0.030	36 (100%)	89 (93.7%)	0.123
Number VPC	1802 ± 2996	7 ± 11	0.000	2582 ± 3342	45 ± 167	0.000	2920 ± 3495	585 ± 1821	0.000
Polymorphic VPC	73 (83.9%)	21 (56.8%)	0.002	55 (91.7%)	39 (60.9%)	0.000	35 (97.2%)	59 (67.0%)	0.000
VPC negative lead I	36 (41.9%)	11 (29.7%)	0.230	28 (47.5%)	19 (29.7%)	0.063	20 (55.6%)	27 (31.0%)	0.014
VPC positive lead II	39 (45.3%)	13 (35.1%)	0.325	24 (40.7%)	28 (43.8%)	0.855	14 (38.9%)	38 (43.7%)	0.691
VPC negative lead III	33 (46.5%)	14 (45.2%)	1.000	27 (54.0%)	20 (38.5%)	0.164	17 (56.7%)	30 (41.7%)	0.195
Couplets present	68 (76.4%)	0 (0.0%)	0.000	54 (88.5%)	14 (20.0%)	0.000	36 (100%)	32 (33.7%)	0.000
Number Couplets	388 ± 1601	0 ± 0	0.005	565 ± 1913	2 ± 8	0.015	895 ± 2438	25 ± 150	0.001
Polymorphic couplets	27 (40.9%)	NA	NA	26 (49.1%)	1 (7.7%)	0.006	18 (50.0%)	9 (30.0%)	0.133
Triplets present	38 (42.7%)	1 (2.4%)	0.000	34 (55.7%)	5 (7.1%)	0.000	26 (72.2%)	13 (13.7%)	0.000
Number Triplets	99 ± 403	0 ± 0	0.003	144 ± 481	0 ± 0	0.013	235 ± 613	4 ± 27	0.000
Polymorphic triplets	10 (25.6%)	0 (0.0%)	1.000	10 (28.6%)	0 (0.0%)	0.306	6 (23.1%)	4 (28.6%)	0.718
VT present	33 (37.1%)	4 (9.5%)	0.001	30 (49.2%)	7 (10.0%)	0.000	21 (58.3%)	16 (16.8%)	0.000
Number VT	96 ± 766	0 ± 1	0.421	140 ± 924	0 ± 1	0.209	235 ± 1201	1 ± 4	0.058
Duration longest VT (beats)	24 ± 31	7 ± 4	0.282	26 ± 33	9 ± 6	0.207	32 ± 37	9 ± 5	0.019
HR fastest VT (bpm)	259 ± 60	261 ± 52	0.967	266 ± 59	234 ± 52	0.193	271 ± 56	244 ± 59	0.159
Polymorphic VT	5 (15.2%)	0 (0.0%)	1.000	5 (16.7%)	0 (0.0%)	0.245	4 (19.0%)	1 (6.3%)	0.259
R-on-T	55 (62.5%)	0 (0.0%)	0.000	46 (76.7%)	9 (13.8%)	0.000	36 (100%)	19 (21.3%)	0.000
Number of beats R-on-T	NA	NA	NA	450 ± 2487	13 ± 25	0.563	631 ± 2805	21 ± 31	0.350
R-on-T % of all beats	NA	NA	NA	26.4 ± 68.1	51.9 ± 24.6	0.275	24.0 ± 72.2	43.1 ± 41.7	0.293

VPC: ventricular premature complexes; HR: heart rate; VT: ventricular tachycardia.

Supplemental Table 8. Echocardiographic results of arrhythmogenic right ventricular cardiomyopathy (ARVC) and control group, 1/3, 2/3, 3/3 novel criteria fulfilled necessary for diagnosis, respectively. All dogs included.

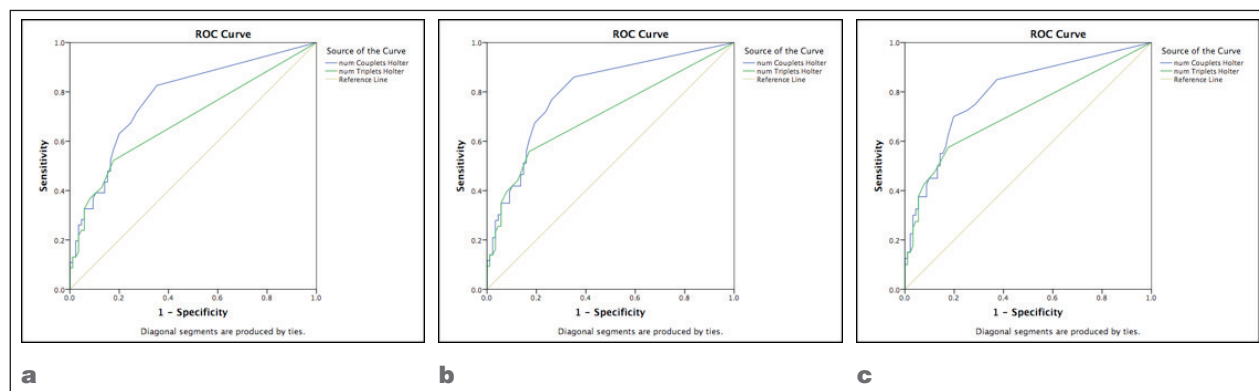
Parameter	ARVC: 1 of 3 novel criteria			ARVC: 2 of 3 novel criteria			ARVC: 3 of 3 novel criteria		
	ARVC (n=88)	Controls (n=173)	p-value	ARVC (n=60)	Controls (n=201)	p-value	ARVC (n=35)	Controls (n=226)	p-value
Decreased RV function	4 (4.7%)	1 (0.6%)	0.032	4 (6.9%)	1 (0.5%)	0.003	4 (11.4%)	1 (0.5%)	0.000
RV dilatation	5 (5.9%)	4 (2.5%)	0.184	5 (8.6%)	4 (2.2%)	0.022	4 (11.4%)	5 (2.4%)	0.009
RV wall motion abnormality	5 (5.9%)	2 (1.3%)	0.039	5 (8.6%)	2 (1.1%)	0.003	5 (14.3%)	2 (1.0%)	0.000
RA dilatation	4 (4.7%)	5 (3.1%)	0.550	4 (6.8%)	5 (2.7%)	0.145	4 (11.4%)	5 (2.4%)	0.008
Aortic diameter (mm)	19.4 ± 3.3	19.3 ± 3.0	0.857	19.5 ± 2.3	19.3 ± 3.4	0.643	19.5 ± 2.3	19.3 ± 3.2	0.707
LA diameter (mm)	33.2 ± 9.3	30.1 ± 6.8	0.010	36.4 ± 0.4	29.3 ± 6.5	0.000	37.5 ± 10.4	30.1 ± 6.9	0.000
LVEF (%)	45.4 ± 15.7	53.1 ± 15.5	0.010	42.0 ± 16.5	53.1 ± 14.0	0.000	40.6 ± 15.9	51.4 ± 15.0	0.005
IVSd (mm)	10.5 ± 1.9	10.3 ± 1.9	0.545	10.6 ± 1.9	10.3 ± 1.9	0.436	10.7 ± 1.9	10.4 ± 1.9	0.412
LVIDd (mm)	41.1 ± 8.3	38.4 ± 5.9	0.009	43.3 ± 8.7	38.0 ± 5.7	0.000	43.7 ± 8.2	38.8 ± 6.6	0.000
LVPWd (mm)	10.8 ± 1.8	10.7 ± 1.8	0.766	10.7 ± 1.9	10.8 ± 1.8	0.770	10.5 ± 1.7	10.8 ± 1.8	0.398
LVIDs (mm)	30.9 ± 9.5	27.4 ± 6.9	0.004	33.5 ± 10.2	27.0 ± 6.4	0.000	34.7 ± 10.4	27.7 ± 7.3	0.000
FS (%)	26.5 ± 10.5	28.8 ± 9.9	0.107	24.1 ± 11.0	29.4 ± 9.4	0.001	22.0 ± 10.7	29.0 ± 9.7	0.000
TAPSE (mm)	15.2 ± 3.8	16.0 ± 2.9	0.601	15.2 ± 3.9	15.8 ± 3.1	0.630	15.5 ± 4.9	15.4 ± 2.9	0.934
MV E Velocity (m/s)	0.84 ± 0.24	0.80 ± 0.18	0.364	0.84 ± 0.26	0.81 ± 0.19	0.482	0.79 ± 0.25	0.82 ± 0.20	0.586
MV Deceleration time (ms)	115 ± 35	134 ± 38	0.035	118 ± 30	128 ± 40	0.348	123 ± 38	126 ± 38	0.798
MV Deceleration slope (m/s ²)	7.0 ± 2.6	6.3 ± 2.4	0.231	6.7 ± 2.5	6.6 ± 2.5	0.872	6.01 ± 2.66	6.67 ± 2.48	0.512
MV A Velocity (m/s)	0.55 ± 0.14	0.55 ± 0.15	0.767	0.52 ± 0.14	0.56 ± 0.15	0.218	0.49 ± 0.13	0.56 ± 0.15	0.057
MV E/A	1.60 ± 0.75	1.54 ± 0.43	0.589	1.67 ± 0.85	1.51 ± 0.44	0.156	1.74 ± 1.00	1.53 ± 0.50	0.199
AV Vmax (m/s)	2.29 ± 1.09	2.47 ± 1.27	0.342	2.03 ± 0.86	2.52 ± 1.28	0.019	1.76 ± 0.54	2.50 ± 1.25	0.007
AV max PG (mmHg)	24 ± 29	30 ± 32	0.246	19 ± 20	31 ± 33	0.032	13 ± 10	30 ± 33	0.015
RVOT PSAX (mm)	25.0 ± 6.8	23.8 ± 4.4	0.421	25.8 ± 7.0	23.6 ± 5.2	0.097	27.1 ± 6.8	23.6 ± 5.6	0.016
RVIT 4CH (mm)	22.8 ± 8.1	22.0 ± 3.6	0.694	23.5 ± 7.7	21.5 ± 5.4	0.316	25.4 ± 9.7	21.6 ± 5.1	0.108
LVIT 4CH (mm)	35.1 ± 9.6	35.1 ± 5.0	0.972	36.0 ± 7.2	34.4 ± 8.4	0.520	38.2 ± 6.8	34.2 ± 8.0	0.158
RVIT/LVIT	0.67 ± 0.28	0.63 ± 0.10	0.515	0.68 ± 0.31	0.63 ± 0.09	0.442	0.72 ± 0.44	0.64 ± 0.09	0.282

RV: right ventricular; RA: right atrium; LA: left atrium; LVEF: left ventricular ejection fraction; IVSd: intraventricular septum measured in diastole; LVIDd: left ventricular internal diameter in diastole; LVPWd: left ventricular posterior wall measured in diastole; LVIDs: left ventricular internal diameter in systole; FS: fractional shortening; TAPSE: tricuspid annular plane systolic excursion; MV: mitral valve; AV: aortic valve; Vmax: maximal velocity; max PG: maximal pressure gradient; RVOT: right ventricular outflow tract; PLAX: parasternal long axis view, PSAX: parasternal short axis view; RVIT: right ventricular inflow tract; 4CH: four-chamber-view; LVIT: left ventricular inflow tract.

Supplemental Table 9. Cases with right ventricular (RV) dilatation: fulfilled criteria, clinical context.

Patient Nr	1 criterion fulfilled	2 criteria fulfilled	3 criteria fulfilled	Clinical context
11	No	No	No	No 24h-ECG, RV dilatation due to fluid overload
25	Yes	Yes	Yes	Progressive abdominal distention, ascites, dilatation of all 4 chambers, systolic dysfunction, moderate TR
35	Yes	Yes	Yes	Recurrent collapses, high arrhythmic burden, mild LV dilatation
56	Yes	Yes	Yes	Syncope during exercise, generalised cardiomegaly, sustained VT during follow up
101	Yes	Yes	No	SVT during routine examination, later presyncope, cough, moderate MR
102	No	No	No	Lethargy, dilatation of all 4 chambers, no 24h-ECG
136	Yes	Yes	Yes	Abdominal distention, ascites, chaotic arrhythmia incl. AF, rapid ventricular runs, severe TR, clinically interpreted as ARVC
155	No	No	No	Murmur at routine examination, syncope during excitement, severe AS, VT in 24h-ECG
222	No	No	No	Murmur detected at first vaccination, severe PS, TR, right heart failure

TR: tricuspid valve regurgitation; LV: left ventricular; VT: ventricular tachycardia; MR: mitral valve regurgitation; AF: atrial fibrillation; ARVC: arrhythmogenic right ventricular cardiomyopathy; AS: aortic stenosis; PS: pulmonic valve stenosis



Supplemental Figure 1. Receiver operated characteristic (ROC) curves for number of couplets and triplets.

- a.)** ROC curve for number of couplets and triplets, diagnosis based on ≥ 50 ventricular premature complexes (VPC). 1.5 couplets are the best cut-off for diagnosis of arrhythmogenic right ventricular cardiomyopathy (ARVC) with a sensitivity of 71.7% and a specificity of 72.9%, area under the curve (AUC) 0.774 (95% confidence interval (CI) 0.689-0.859). 0.5 triplets are the best cut-off for the diagnosis. Sensitivity 52.2%, specificity 82.4%, AUC 0.685 (95% CI 0.584-0.786)
- b.)** ROC Curve for number of couplets and triplets, diagnosis based on ≥ 100 VPC. 1.5 couplets are the best cut-off for diagnosis of ARVC with a sensitivity of 76.7% and a specificity of 73.9%, AUC 0.800 (95% CI 0.718-0.882). 0.5 triplets are the best cut-off for the diagnosis. Sensitivity 55.8%, specificity 83%, AUC 0.707 (95% CI 0.605-0.808)
- c.)** ROC Curve for number of couplets and triplets, diagnosis based on ≥ 200 VPC. 1.5 couplets are the best cut-off for diagnosis of ARVC with a sensitivity of 72.5% and a specificity of 71.4%, AUC 0.796 (95% CI 0.711-0.882). 0.5 triplets are the best cut-off for the diagnosis. Sensitivity 57.5%, specificity 82.4%, AUC 0.717 (95% CI 0.613-0.821).

References for supplemental Material

- Spier AW, Meurs KM. Evaluation of spontaneous variability in the frequency of ventricular arrhythmias in Boxers with arrhythmogenic right ventricular cardiomyopathy. *J Am Vet Med Assoc* 2004;224:538-41.
- Basso C, Fox PR, Meurs KM, et al. Arrhythmogenic right ventricular cardiomyopathy causing sudden cardiac death in boxer dogs: a new animal model of human disease. *Circulation* 2004;109:1180-5.
- Baumwart RD, Meurs KM. Assessment of plasma brain natriuretic peptide concentration in Boxers with arrhythmogenic right ventricular cardiomyopathy. *Am J Vet Res* 2005;66:2086-9.
- Meurs KM, Lacombe VA, Dryburgh K, et al. Differential expression of the cardiac ryanodine receptor in normal and arrhythmogenic right ventricular cardiomyopathy canine hearts. *Hum Genet* 2006;120:111-8.
- Baumwart RD, Orvalho J, Meurs KM. Evaluation of serum cardiac troponin I concentration in Boxers with arrhythmogenic right ventricular cardiomyopathy. *Am J Vet Res* 2007;68:524-8.
- Smith CE, Freeman LM, Rush JE, et al. Omega-3 fatty acids in Boxer dogs with arrhythmogenic right ventricular cardiomyopathy. *J Vet Intern Med Am Coll Vet Intern Med* 2007;21:265-73.
- Oyama MA, Reiken S, Lehnart SE, et al. Arrhythmogenic right ventricular cardiomyopathy in Boxer dogs is associated with calstabin2 deficiency. *J Vet Cardiol Off J Eur Soc Vet Cardiol* 2008;10:1-10.
- Scansen BA, Meurs KM, Spier AW, et al. Temporal variability of ventricular arrhythmias in Boxer dogs with arrhythmogenic right ventricular cardiomyopathy. *J Vet Intern Med Am Coll Vet Intern Med* 2009;23:1020-4.
- Baumwart RD, Meurs KM, Raman SV. Magnetic resonance imaging of right ventricular morphology and function in boxer dogs with arrhythmogenic right ventricular cardiomyopathy. *J Vet Intern Med Am Coll Vet Intern Med* 2009;23:271-4.
- Meurs KM, Mauceli E, Lahmers S, et al. Genome-wide association identifies a deletion in the 3' untranslated region of striatin in a canine model of arrhythmogenic right ventricular cardiomyopathy. *Hum Genet* 2010;128:315-24.
- Palermo V, Stafford Johnson MJ, et al. Cardiomyopathy in Boxer dogs: a retrospective study of the clinical presentation, diagnostic findings and survival. *J Vet Cardiol Off J Eur Soc Vet Cardiol* 2011;13:45-55.
- Oxford EM, Danko CG, Kornreich BG, et al. Ultrastructural changes in cardiac myocytes from Boxer dogs with arrhythmogenic right ventricular cardiomyopathy. *J Vet Cardiol Off J Eur Soc Vet Cardiol* 2011;13:101-13.
- Caro-Vadillo A, García-Guasch L, Carretón E, et al. Arrhythmogenic right ventricular cardiomyopathy in boxer dogs: a retrospective study of survival. *Vet Rec* 2013;172:268.
- Mötsküla PF, Linney C, Palermo V, et al. Prognostic value of 24-hour ambulatory ECG (Holter) monitoring in Boxer dogs. *J Vet Intern Med Am Coll Vet Intern Med* 2013;27:904-12.
- Meurs KM, Stern JA, Sisson DD, et al. Association of dilated cardiomyopathy with the striatin mutation genotype in boxer dogs. *J Vet Intern Med Am Coll Vet Intern Med* 2013;27:1437-40.
- Meurs KM, Stern JA, Reina-Doreste Y, et al. Natural history of arrhythmogenic right ventricular cardiomyopathy in the boxer dog: a prospective study. *J Vet Intern Med Am Coll Vet Intern Med* 2014;28:1214-20.
- Oxford EM, Danko CG, Fox PR, et al. Change in β -catenin localization suggests involvement of the canonical Wnt pathway in Boxer dogs with arrhythmogenic right ventricular cardiomyopathy. *J Vet Intern Med Am Coll Vet Intern Med* 2014;28:92-101.
- Cattanach BM, Dukes-McEwan J, Wotton PR, et al. A pedigree-based genetic appraisal of Boxer ARVC and the role of the Striatin mutation. *Vet Rec* 2015;176:492.
- Meurs KM. Boxer dog cardiomyopathy: an update. *Vet Clin North Am Small Anim Pract* 2004;34:1235-44.

Multi-slice MRI reveals heterogeneity in disease distribution along the length of muscle in Duchenne muscular dystrophy

STEPHEN M. CHRZANOWSKI¹, CELINE BALIGAND¹, REBECCA J. WILLCOCKS², JASJIT DEOL²,
ILONA SCHMALFUSS³, DONOVAN J. LOTT², MICHAEL J. DANIELS⁴, CLAUDIA SENESAC²,
GLENN A. WALTER¹ AND KRISTA VANDENBORNE²

¹ Department of Physiology and Functional Genomics, University of Florida, Gainesville, FL; ² Department of Physical Therapy, University of Florida, Gainesville, FL; ³ Department of Radiology, NF/SG Veterans Administration and University of Florida, Gainesville, FL; ⁴ Department of Statistics, University of Florida, Gainesville, FL, USA

Background. Duchenne muscular dystrophy (DMD) causes progressive pathologic changes to muscle secondary to a cascade of inflammation, lipid deposition, and fibrosis. Clinically, this manifests as progressive weakness, functional loss, and premature mortality. Though insult to whole muscle groups is well established, less is known about the relationship between intramuscular pathology and function.

Objective. Differences of intramuscular heterogeneity across muscle length were assessed using an ordinal MRI grading scale in lower leg muscles of boys with DMD and correlated to patient's functional status.

Methods. Cross sectional T₁ weighted MRI images with fat suppression were obtained from ambulatory boys with DMD. Six muscles (tibialis anterior, extensor digitorum longus, peroneus, soleus, medial and lateral gastrocnemii) were graded using an ordinal grading scale over 5 slice sections along the lower leg length. The scores from each slice were combined and results were compared to global motor function and age.

Results. Statistically greater differences of involvement were observed at the proximal ends of muscle compared to the midbellies. Multi-slice assessment correlated significantly to age and the Vignos functional scale, whereas single-slice assessment correlated to the Vignos functional scale only. Lastly, differential disease involvement of whole muscle groups and intramuscular heterogeneity were observed amongst similar age subjects.

Conclusion. A multi-slice ordinal MRI grading scale revealed that muscles are not uniformly affected, with more advanced disease visible near the tendons in a primarily ambulatory population with DMD. A geographically comprehensive evaluation of the heterogeneously affected muscle in boys with DMD may more accurately assess disease involvement.

Key words: Duchenne Muscular Dystrophy, magnetic resonance imaging, myotendinous junction

Introduction

Duchenne muscular dystrophy (DMD), an X-linked recessive genetic disorder with an incidence of 10.7 to 27.7 per 100,000, is caused by a mutation in the *dystrophin* gene, resulting in an absence or dysfunction of the protein dystrophin (1, 2). Structurally, progressive pathological changes in skeletal muscle resulting from DMD are well described and include inflammation (3), lipid infiltration (4), and fibrotic deposition (5), leading to progressive muscle weakness, loss of functional abilities, and premature mortality (6-8).

Magnetic resonance imaging (MRI) has developed to be a safe, sensitive, non-invasive, and effective method to investigate patterns of disease pathology within muscle in DMD (9-16). To evaluate quality of muscle, Mercuri and colleagues developed an ordinal scale to qualitatively assess severity and disease distribution in congenital muscular dystrophy using T₁ weighted MRI imaging (17). This scale has been utilized and modified for a number of studies of various muscular dystrophies and myopathies (16, 18-27). Traditionally, most MRI protocols analyze muscle data from either single or few consecutive slices, selecting slices based on anatomical landmarks of a muscle (14, 15). Such evaluation may have limitations as, published by Vidt and collaborators, who demonstrated that single-image assessment using T₁ weighted MRI are not predictive of 3-D measurements of fatty infiltration in patients with rotator cuff tears [28]. Additionally, using water/fat separation MRI, Hooijmans et al. demonstrated heterogeneous fat fractions throughout the length of mus-

cle in DMD (26). In DMD, where muscle injury leads to variable fatty deposition within and between muscles, a 3-D evaluation may provide greater insight into the understanding of the disease process (10, 14-16, 26).

To date, only one group has published data regarding differences of disease involvement along the length of muscles in DMD individuals as visible with MRI, suggesting that the proximal and distal regions of muscle may be preferentially affected when compared to the muscle belly [26]. This phenomenon is in concordance with pre-clinical studies that showed geographic vulnerabilities to disease pathology, specifically an increased susceptibility to disease at the muscle-tendon junction. Furthermore, using a modified Mercuri scale, Polavarapu et al. also reported differences in geographic involvement of different muscles of the thigh, with preferential involvement of the superficial posterior and lateral muscles groups and sparing of the deep posterior and anterior muscle groups in DMD patients (16). Importantly, they also correlated their single-slice findings to the Muscular Dystrophy Functional Rating Scale, demonstrating a relationship between function and MRI observations in the thigh muscles (16). Such observation of heterogeneous disease distribution in axial and craniocaudal directions is critical for understanding the pathophysiology of muscular dystrophies and the natural progression of such diseases.

In this study, we confirm and expand upon the current knowledge base of DMD pathophysiology and the recently published work by Hooijmans and Polavarapu by performing a multi-slice T_1 weighted ordinal evaluation of individual lower leg muscles in a larger and primarily ambulant DMD patient population. In addition, we compare proximodistal disease distribution per MRI with clinical functionality and age. The objectives of the present study were (a) to utilize multi-slice MRI in lower legs of boys with DMD to study tendon to muscle differences of disease involvement (fatty changes and fibrosis) within and between individual lower leg muscles and (b) to determine if evaluation in a multi-slice fashion reveals stronger correlations to age and function than single-slice analyses in boys with DMD.

Methods

Study design

In this cross sectional study, 30 boys (age, 9.9 ± 2.7 years; range, 6.2-15.2; height, 1.27 ± 0.3 m; weight, 34.0 ± 2.6 kg; ambulatory, 27/30; glucocorticoid positive, 30/30; Vignos median score, 25 IQR%, and 75 IQR% = 2, 1, 2.5) with DMD confirmed by molecular genetic testing (PCR amplification, but specific genetic mutations

not available) and/or immunohistochemistry from biopsy. In addition, 6 unaffected control males (age, 7.7 ± 1.9 years; range, 6.3-13.9 height, 1.31 ± 0.11 m; weight, 26.2 ± 4.1 kg; ambulatory, 6/6; glucocorticoid positive, 0/6; Vignos median score, 25 IQR%, and 75 IQR% = 1, 1, 1) volunteered to participate in the study. All participants were functionally scored on the Vignos lower extremity functional scale (29). This study was HIPAA compliant and approved by the Institutional Review Board at the University of Florida. Upon thorough description of the study, written consent was provided by a parent or legal guardian and written assent was provided by the pediatric subjects.

Magnetic resonance acquisition and measures

Subjects were asked to avoid any vigorous physical activity for two days prior to the study and to use a wheelchair or equivalent mobility device when traveling to avoid excessive walking. Acquisitions were performed on a 3.0 Tesla whole body human system (Achieva, Philips Medical Systems, Best, Netherlands) at the McKnight Brain Institute at the University of Florida. With a parent and study staff member accompanying the subjects in the testing room, subjects were placed in a supine position within the magnet without sedation. Each subjects' right lower leg was placed in an eight-channel SENSE receive-only extremity coil (Invivo, Gainesville, FL, USA) with the proximal end of the coil aligned with the fibular head and tibial tuberosity. Padded weights were utilized to maintain the leg in a fixed position for the duration of the scan. Commercially available T_1 weighted 3D gradient echo images were acquired (field of view, 12-24 x 12-14 cm², voxel size = $0.75 \times 0.75 \times 2.8$ mm³, 50 slices, flip angle = 20°, TR/TE = 24/1.8, number of averages = 2). Acquisitions were made with fat suppression using spectral presaturation with inversion recovery (SPIR). During data collection, subjects were shown a movie of their choice on an in-magnet video display system to facilitate compliance and minimize movement artifacts during the scanning.

MRI and function data evaluation

Six muscles (tibialis anterior [TA], extensor digitorum logus [EDL], peroneus [Per], soleus [Sol], medial gastrocnemius [MG], and lateral gastrocnemius [LG]) were analyzed by two blinded reviewers, RW and CB, with 5 and 10 years of experience assessing muscle on MRI, respectively. When the two reviewers were not in agreement (< 5% of slices), selected slices were reviewed together with the principal investigator who served as a tie breaker.

For each subject, 5 fat-saturated axial images were

selected along the length of the leg for image analysis. Slice selection was acquired based on the lower leg length percentage distal from the tibial head to account for differences in age and height between participants: proximal: $10 \pm 2\%$, mid-proximal: $19 \pm 2\%$, middle: $26 \pm 2\%$, mid-distal: $35 \pm 2\%$ and distal: $43 \pm 2\%$ from the tibial plateau as shown in Figure 1. MRI assessment (Fig. 2) of each muscle was obtained using the Mercuri grading scale, previously used for a variety of muscular dystrophies (10, 11, 14-17, 30-32).

To demonstrate the distribution of disease within all muscles, an ordinal scale MRI score was assigned to individual muscles, based on disease involvement (Figure 2). Note that in T_1 -weighted fat suppressed images, hypointense regions may be composed of either lipid infiltrate or fibrosis though the major contributor responsible for hypointense signal is fatty replacement. Further, MRI scores were binned in the following categories for evaluation purposes: not affected (MRI Score = 0), moderately affected (MRI Score = 1-2), or severely affected (MRI Score = 3-5). To assess the overall disease involvement of the lower leg muscles, MRI scores for all 6 muscles were summed to obtain both an overall leg MRI score and a single middle slice leg MRI score. MRI scores were

then normalized to the total number of slices, accounting for muscle data missing from slices, creating comparable normalized multi-slice scores and slice scores. Similarly, Vignos scores were binned into four categories: 1 (able to walk and climb stairs without assistance), 2 (able to walk and climb stairs with aid of railing), 3-4 (walks, climbs stairs slowly, < 25s for 8 standard steps with railing or not at all), and 5+ (unable to rise from chair, unable to walk independently, or unable to walk at all). Furthermore, subjects' ages and functional ability were compared to normalized multislice and single-slice scores.

Statistical evaluation

To compare the differences of ordinal MRI scores, Wilcoxon matched-pairs signed rank tests were performed, comparing the proximal to middle and distal to middle slices of all muscles. To quantify the relationship between age and MRI scores, Spearman's rank correlation was computed. A Kruskal-Wallis test with adjustment for multiple comparisons was used to compare MRI scores across Vignos score categories. Statistical analyses were conducted using GraphPad Prism (version 6.0d; La Jolla, CA, USA). Statistical significance was set at $p < 0.05$ (two-tailed).

Results

Non-uniform distribution of muscular involvement in DMD

In order to assess spatial heterogeneity and pathology within and between muscles, MR images were acquired along the length of lower legs of boys with DMD (Fig. 1). Representative cross sectional images (Fig. 3) showed variability of disease involvement between muscles, with the Per muscle being the most affected, and with different degrees of involvement between proximal, midbelly, and distal portions of muscles (Fig. 3). Furthermore, while boys with DMD typically demonstrated worse pathology at the myotendinous junctions, not all subjects revealed identical patterns of disease affliction. The spectrum of MRI scores and how different pathology manifests along various spatial regions of the same muscle are shown in two similarly aged representative subjects (aged 10.0 and 10.7 years) in Figure 4. When investigating pathology along the length of muscles, variability was observed, with greater evidence of disease at the most proximal and distal ends of muscle as compared to the midbelly (Fig. 5). Through presentation of each subjects' muscle MRI scores (Fig. 5), one can appreciate the differences in severity of disease based on location within individual muscles and between specific muscle groups for all subjects. Furthermore, when proximal versus middle single

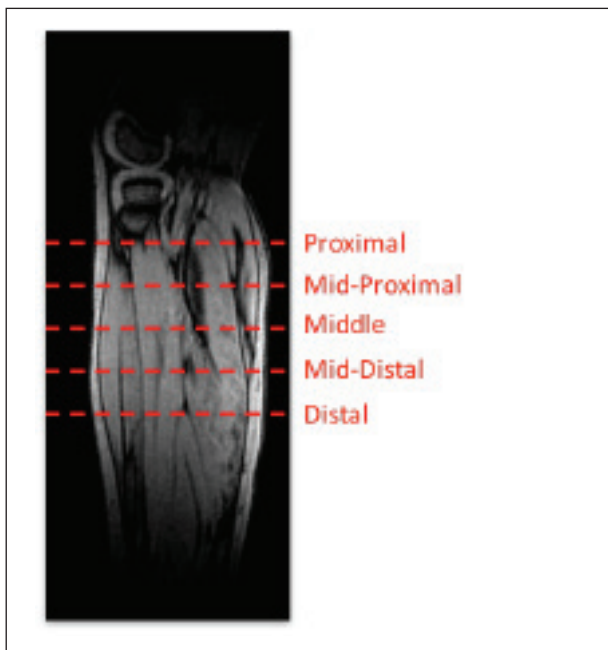


Figure 1. Schematic representation of slice selections along the length of the lower leg. Representation of the slice positions based the percentage distance along the tibia (starting at the tibial plateau) along the longitudinal axis: proximal (P): ~ 10 - 12% , mid-proximal (MP): ~ 17 - 21% , middle (M): 25 - 28% , mid-distal (MD): 33 - 37% , distal (D): 41 - 45% inferior of the tibial plateau.











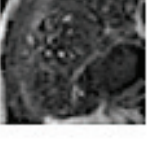

Grade	Description	Examples	
		Peroneus	Soleus
0	No Involvement: normal appearance		
1	Minimal involvement: increase in number and thickness of septate		
2	Numerous discrete areas of decreased signal, comprising less than 30% of the muscle area		
3	Numerous discrete areas of decreased signal, comprising 30-60% of muscle area		
4	Washed-out fuzzy appearance comprising more than 60% muscle area		
5	Muscle replaced with connective tissue and fat, with only a rim of muscle and neurovascular structure distinguishable		

Figure 2. Descriptions of the ordinal MRI scores to describe disease involvement of muscle.

slices were compared of each of the muscles, significant differences were observed in five out of the six muscles (Table 1). No significant differences were observed when comparing the middle versus distal slices (Table 1).

Relationship between MRI scores, function and age

Additionally, a goal of this study was to see if a comprehensive multi-slice assessment could better correlate with clinical measures than single-slice analyses. Overall, the study subjects with DMD demonstrated comparable functional capability to patients of similar ages in other studies (33, 34). Specifically for our study,

Table 1. Intramuscular heterogeneity statistical differences

	Proximal v. middle	Distal v. middle
Per	p = 0.72, ns	p = 0.48, ns
EDL	p = 0.002**	p > 0.99, ns
TA	p = 0.0007***	p = 0.43, ns
Sol	p = 0.004**	p = 0.25, ns
MG	p = 0.03*	N/A
LG	p < 0.0001****	N/A

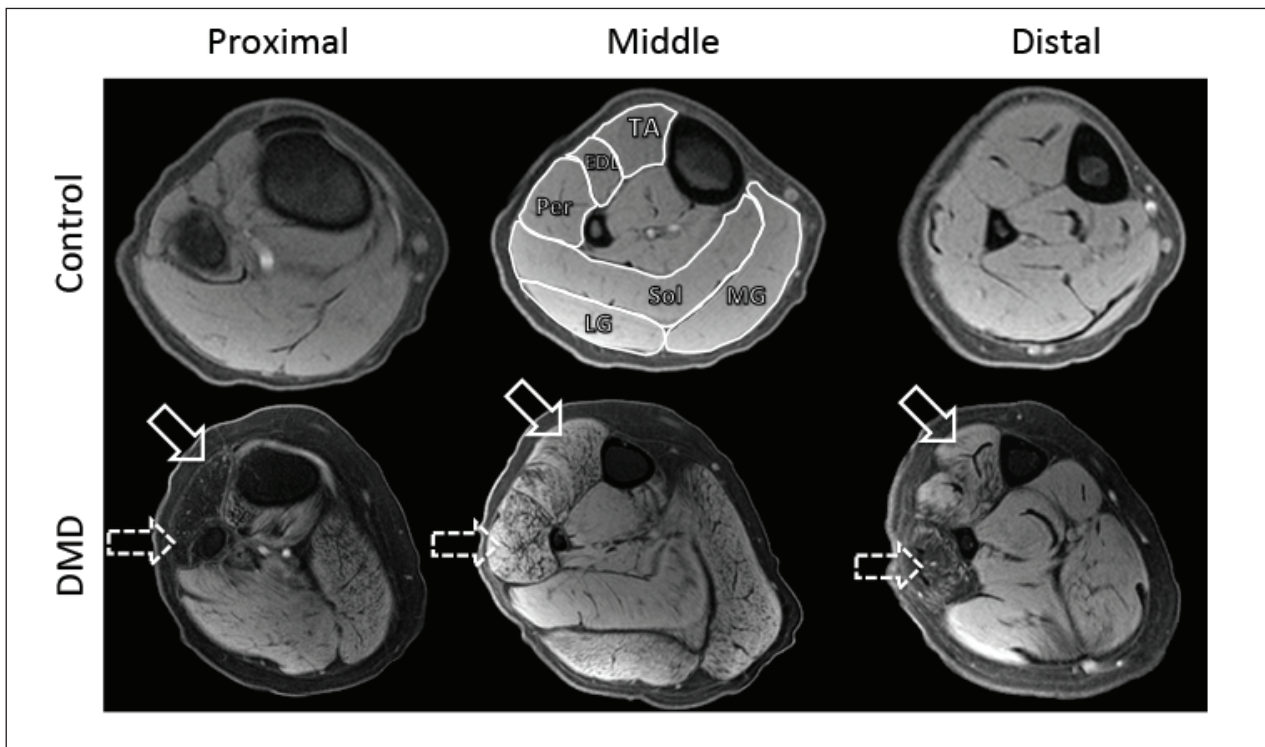


Figure 3. Representative transverse T_1 -weighted MR images with fat suppression of the lower leg of a control subject (top row) and subject with DMD (bottom row). MR imaging evaluation of the TA, EDL, Per, Sol, MG, and LG (labeled on the middle control image) was performed on all muscle groups in a manner described in Figure 2. Note the differences in the Per (dashed arrow) and TA (solid arrow) muscles at the proximal and distal compared to the middle slices in the DMD patient.

with increasing ages of subjects, normalized multi-slice MRI score concurrently increased ($\rho = 0.69$, $p < 0.0001$), confirming that disease involvement within muscle increases as children age (Fig. 6A), whereas normalized single-slice MRI scores (Fig. 6C) did not correlate with the age of the subjects ($\rho = -0.23$, $p = 0.25$). Additionally, functional status was measured by Vignos scoring [29] to assess if MRI grading may be related to functional capabilities. Increases in both normalized multi slice scores ($p = 0.003$, Fig. 6B) and normalized single-slice scores ($p = 0.01$, Fig. 6D) were observed with decreased functional status.

Discussion

The primary purpose of this work was to investigate intramuscular heterogeneity of disease involvement (fatty replacement) in the lower legs of 6-15 year old boys with DMD through a simple multi-slice MRI acquisition that can be performed on most clinical MRI scanners using an established muscle grading scale that can be easily utilized to assess heterogeneous disease involvement. Building upon developments of MRI as

a feasible modality to investigate muscle pathology in DMD, continuing to understand the heterogeneous nature of DMD is critical to further advance our knowledge of this lethal disease (9-11, 13-15).

Through this investigation, we confirmed that a multi-slice MRI acquisition of subjects with DMD reveals differential disease involvement within muscles of the lower leg, most prominently at the myotendinous junction, as demonstrated by Hooijmans and colleagues (26). Next, we investigated the relationship between our multi-slice MRI findings to functional status and patients' ages. Also, we provide evidence of heterogeneity of muscular involvement between DMD subjects of similar age that has not been, to our knowledge, explicitly reported yet.

Previously, Mercuri et al. developed an ordinal grading scheme for neuromuscular disorders (17), and adopted by several studies investigating disease progression in DMD (9, 10, 14, 15). Unique to our study was the use of a multi-slice acquisition along the lower leg, allowing for investigation of intramuscular differences in disease pathology. Hooijmans and colleagues similarly addressed geographic differences along the muscle length of DMD patients by assessing the lipid deposition using Dixon

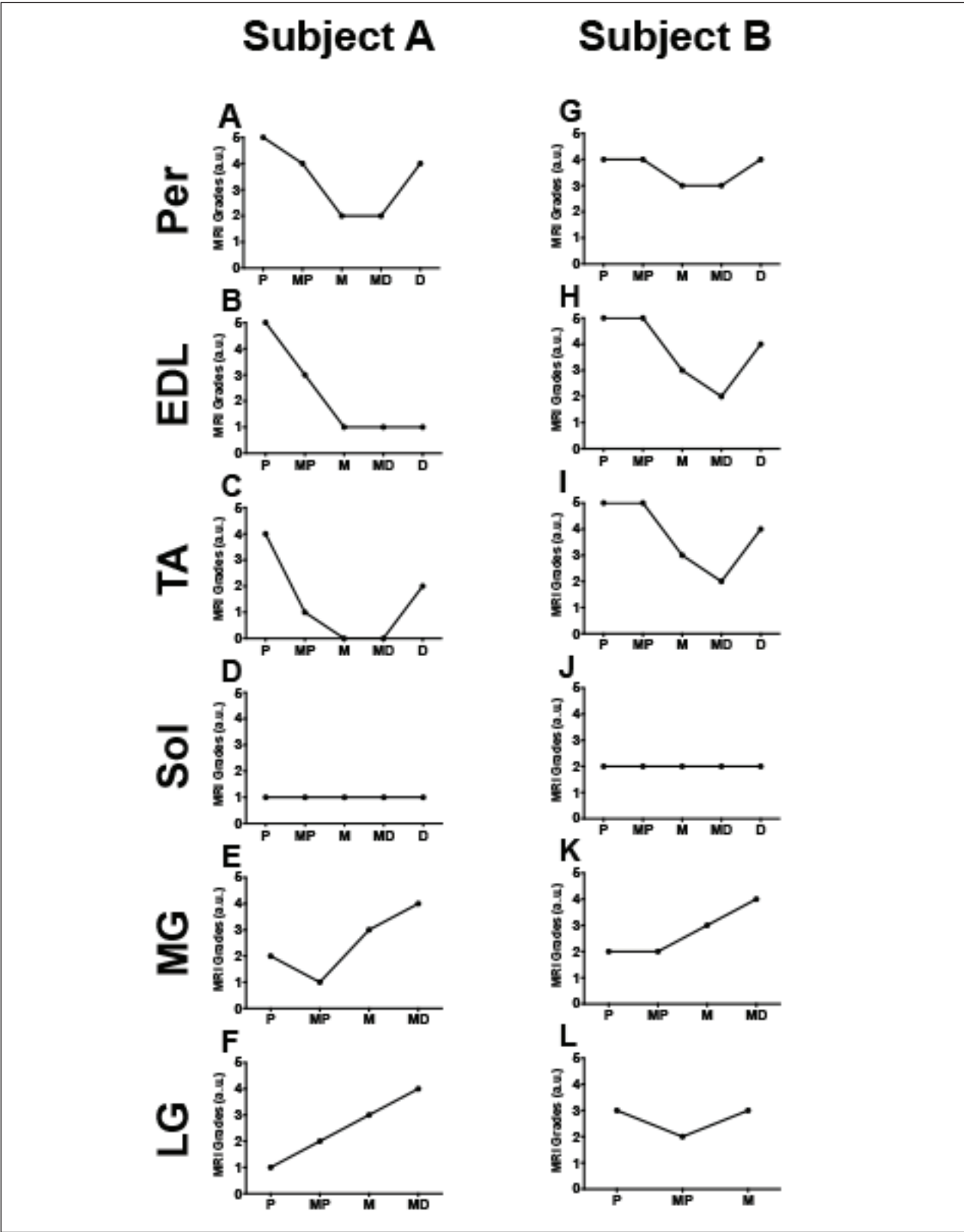


Figure 4. Ordinal MRI Scores from two representative DMD patients (A = 10.0 years, B = 10.7 years) demonstrating differences in involvement along the length of six lower leg muscle groups. X axes are labeled with P (proximal), MP (mid-proximal), M (middle), MD (mid-distal), and D (distal).

techniques to calculate fat fraction [26]. Through our investigation, we show that semi-quantitative assessment based on scoring of T_1 weighted images allows for appreciation of differences between the myotendinous region versus midbelly of several muscles, highlighted specifically in the Per, as observed in Figure 3. A strength of the fat suppressed T_1 weighted imaging implemented in this study is that it highlights fatty replacement changes of muscle secondary to DMD.

Our study also revealed that disease involvement is heterogeneous between DMD subjects of similar age as emphasized in Figure 4. Such non-uniformity of disease distribution within muscle(s) and between DMD patients emphasizes how critical the location of a biopsy or MR slice selections is for evaluation of disease progression. This is well illustrated in the two similarly aged DMD patients in Figure 4. Specifically, Figure 4 shows how contradicting the results of disease involvement could be when the entire muscle length is not used for assessment of disease extent as minimal disease is appreciated in the midbelly of Subject A's TA, whereas advanced disease is noted at the myotendinous ends. This contrasts with advanced disease involvement in the midbelly of Subject B's TA. This is of special importance when studying the pathophysiology and natural progression of DMD, as different regions of muscle have different rates of disease progression. As shown in Figure 4, assessment of single slices of muscle may lead to contradicting interpretations of disease progression. Taking into account the remainder of the subject population, a broad distribution of disease involvement was observed throughout the length of lower leg muscle (Fig. 5), with statistical confirmation seen in Table 1. Interestingly, the Per did not show significant differences between either the proximal versus middle, nor middle versus distal muscle slices. This may be attributed to the already advanced state of disease in the Per muscle, as previously reported. Additionally, the lack of a significant difference observed between the middle and distal slices may be due to the limited field of view, missing the distal myotendinous junctions. A general trend was detected in that an increase of disease pathology can be observed closer to the myotendinous junctions as also reported by Hooijmans et al. (26). These results highlight the differences of muscle pathology that individuals with DMD can present with.

The final analyses performed in this study were to see if the MRI scores generated could be related to standard clinical measures of disease progression. As individuals with DMD age, muscles continually accumulate insults of the disease, evident by the clinical progression of DMD (6, 10, 14, 35). While our normalized multi-slice score positively correlated with the age of subjects, normalized single-slice score at muscle midbelly did not,

suggesting that a multi-slice assessment more accurately reflects clinical disease progression. Increases in the Vignos lower extremity scoring demonstrated progressive decline in functional ability that paralleled increasing MRI grading scores. There was however no difference in the correlation of the functional scores between normalized multi-slice and single-slice MRI scores in contrast with the age correlations. Effectively, this demonstrates that with increasing age and decreasing function, lower leg muscles of boys with DMD have increasingly progressive disease involvement, as previously reported by Polavarapu et al. (16).

The exact cause of the heterogeneous pattern of involvement observed in our study, both across different muscles and along the proximodistal direction of each muscle, is still unknown. However, a number of pre-clinical studies have explored mechanical and biological properties of muscles that may be linked to a possible vulnerability or predisposition to faster disease progression in the context of DMD. Though muscles are initially rendered susceptible to damage as a result of dystrophin lacking, further properties may influence the ability of tissue to succumb to the progression of the disease, including the biological composition of tissue (36, 37), the distribution of strain (38), the cross sectional area (39), speed and type of contractions (40), and other passive viscoelastic properties (41).

Differing amounts of eccentric contractions that muscles experience during gait have been shown to strongly correlate with lower limb fat fraction, a marker of disease progression (9, 42). In the *mdx* mouse, the stress relaxation rate of the EDL was found to be increased in *mdx* mice compared to healthy counterparts, and recoverable upon micro and mini dystrophin treatment, suggesting that dystrophic muscle itself has different passive properties than healthy muscle (43, 44). In other studies, strain measures of the gastrocnemii belly (20-30%) were found to be greater than those of the aponeurosis (1-5%) (38) and the tapered myotendinous junction experienced greater stress than the muscle belly (40). This suggests that different passive mechanical properties exist between different geographical segments of muscles, rendering the myotendinous junctions more vulnerable to the pathologic insult observed in DMD. Sun et al. elegantly demonstrated microfailure of the muscle-tendon unit using peroneus longus muscles of rabbits, suggesting that the weakest region of muscle is at the myotendinous junction, which may provide rationale for the observations made in our patient cohort and from the study by Hooijmans et al. (27, 40). Many of these pre-clinical experiments are not feasible in clinical subjects because of their invasive nature; therefore, extrapolation of pre-clinical findings to

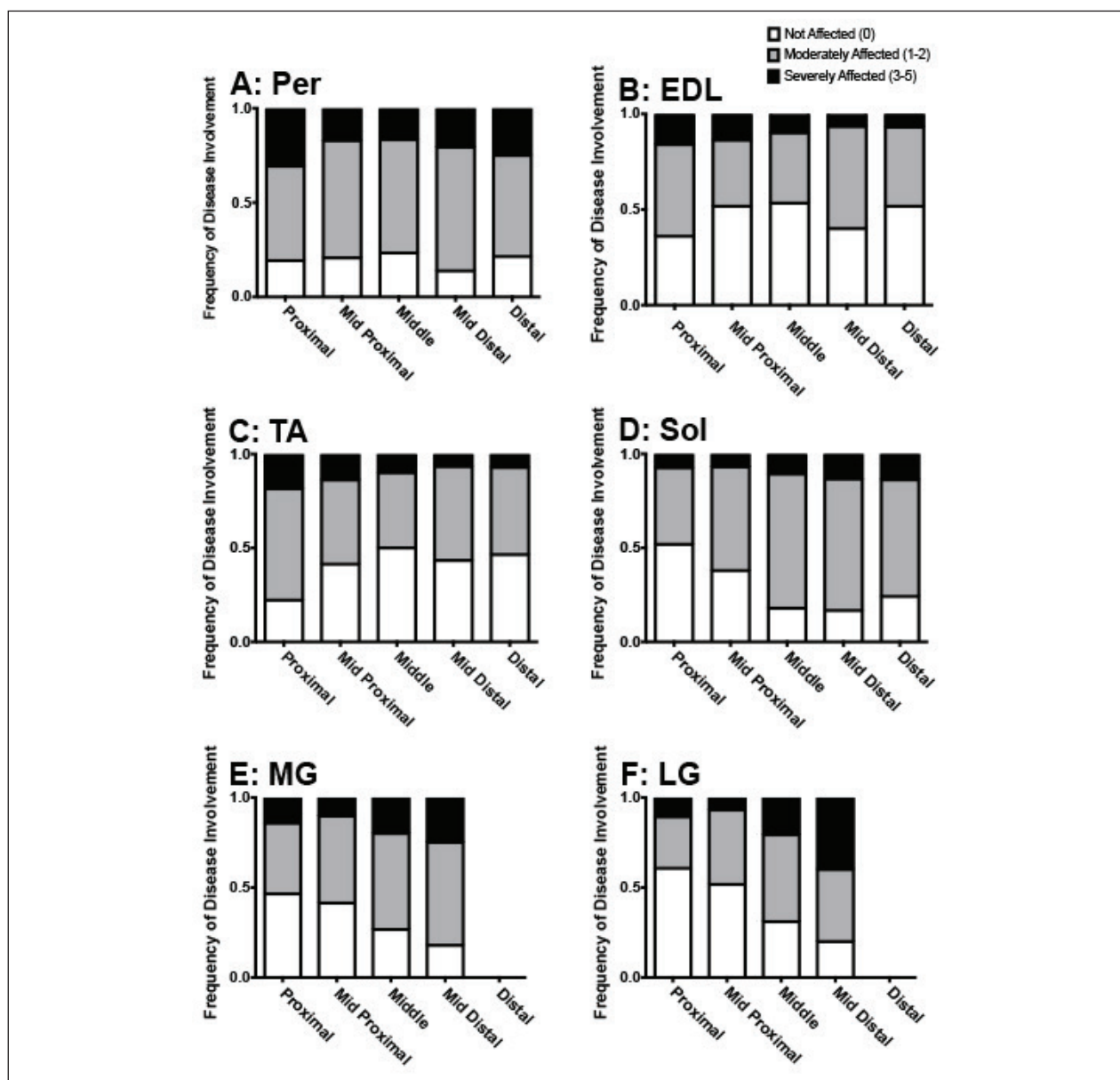


Figure 5. Frequency of involvement of six muscles in lower legs of boys with DMD. Shown are A: Peroneus, B: Extensor Digitorum Longus, C: Tibialis Anterior, D: Soleus, E: Medial Gastrocnemius, F: Lateral Gastrocnemius with differing MRI scores based on slice location. MRI scores of 0 were considered to be “not affected,” scores of 1 and 2 were considered to be “moderately affected,” and scores of 3-5 were considered to be “severely affected”.

humans have to be made with caution.

Limitations and future directions

A primary limitation of this study is the lack of full geographic capture of muscle from tendon to tendon. This study is a subset of a larger study (RO1, AR0569373, PI: Vandenborne), and images were captured to meet the needs to the larger study. The ordinal grading scale utilized in this study, though previously demonstrated to be effective

and able to collect data in a much more time sensitive manner, is not as quantitative as possible with other MRI techniques, such as the Dixon sequence, T_2 mapping, or magnetic resonance spectroscopy (15, 16, 26, 45, 46). Because disease involvement of DMD muscle includes both T_1 shortening fibrotic effects and T_1 lengthening lipid effects on muscle, we employed T_1 weighting with fat suppression techniques to address both fatty infiltration and fibrotic changes to muscle as previously demonstrated in

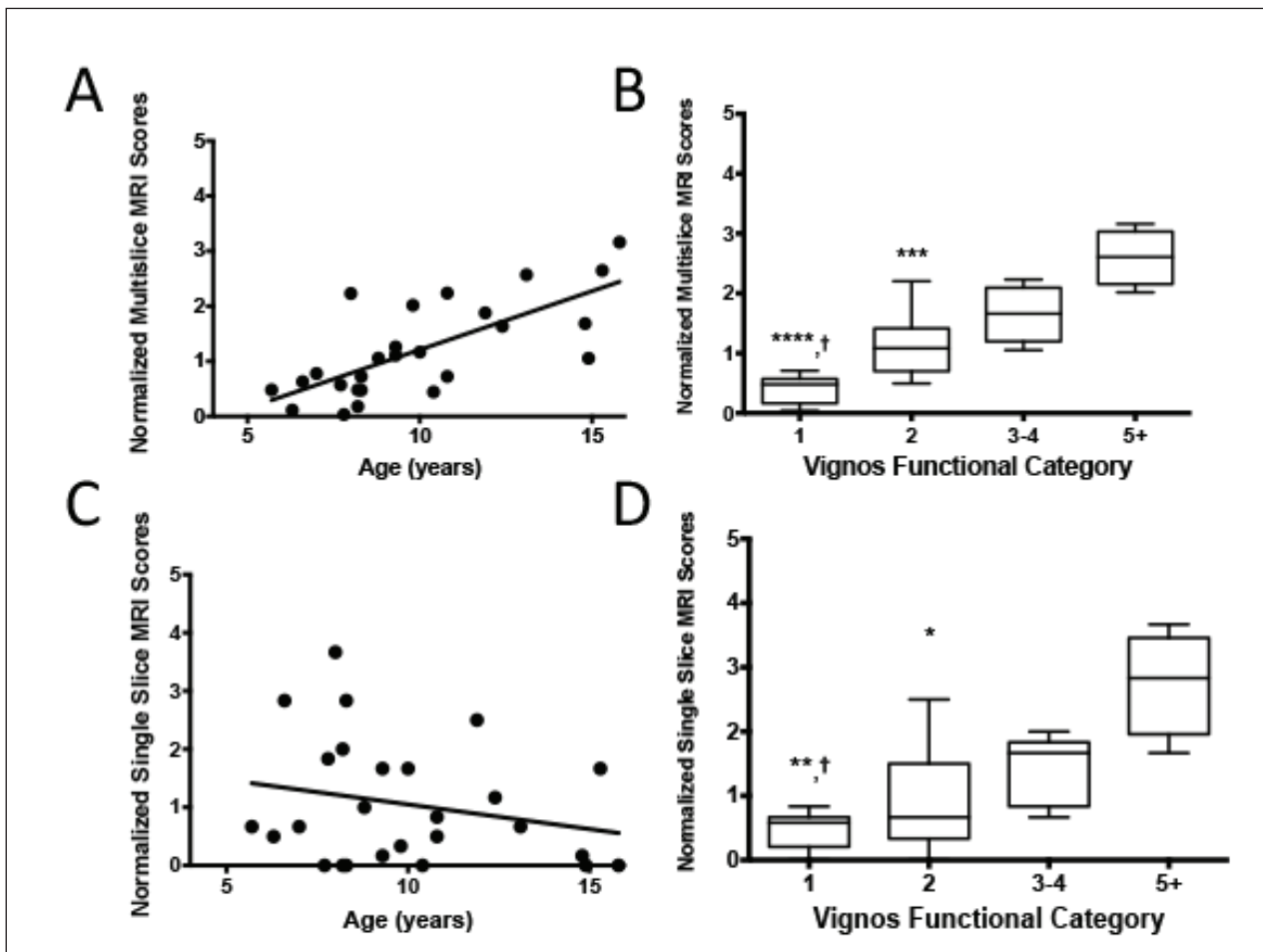


Figure 6. Age and function are compared to MRI scores. The sum of the scores of the multi-slice (Fig. 6a; $\rho = 0.69$, $p < 0.0001$) and middle slices (Fig. 6c; $\rho = -0.23$, $p = 0.25$) MRI scores are plotted correlated to the age of subjects. Figure 6b and 6d show the relationship between subjects binned by their Vignos score and the summative multi-slice and middle slice MRI scores, respectively, by median and 25th and 75th percentiles. In Figures 6b and 6d, comparison to Vignos grade 5+ is indicated by asterisks where * indicates $p < 0.05$, ** indicates $p < 0.01$, **** indicates $p < 0.0001$, and comparison to Vignos grade 3-4 is indicated by daggers, where † indicates $p < 0.05$.

muscular dystrophies, though fatty accumulation accounts for the majority of signal change (16, 31). Lastly, the Vignos score may be a non-optimal functional impairment scale and even though it is still used in the clinic, more sensitive instruments have been developed and validated for use in the DMD population (47, 48).

The localization of slices by distance in centimeters or inches is challenging in a pediatric population because of different leg lengths between participating subjects. Therefore, percentage length was selected in our study as it more appropriately accounts for differences in physical stature and age of subjects. Future studies looking at intra-muscular heterogeneity would greatly benefit from larger anatomical coverage of slice selection, anatomically based alignment of slices (e.g. insertions of vari-

ous tendons) and investigating differences in composition throughout muscle. In addition, the low number of control subjects in our study could be considered a limitation; however, several studies have identified that unaffected healthy male subjects do not demonstrate substantial fatty muscle replacement, deviating the need for higher numbers of control subjects (35, 46, 49, 50).

Further studies are warranted in other neuromuscular disorders to see if other diseases demonstrate unique intra-muscular heterogeneity, as observed in DMD in this study. In addition, further investigation of the different genetic types of DMD as well as longitudinal studies are necessary to determine if unique patterns of disease involvement in the different DMD subtypes exist and what pattern of progression of involvement occurs over time.

Expansion of the MRI studies to the other parts of the body might also be beneficial to better understand which muscle parts are affected when and to what extent. For better understanding of the pathophysiology of DMD disease, it would be also interesting to evaluate the degree of fatty infiltration versus fibrotic changes and how they relate to each other in the different stages of the disease, patient age and functional status.

Conclusions

In this investigation, we utilized a modified version of the previously established ordinal Mercuri scale using multi-slice fat-saturated T_1 weighting MR imaging to evaluate the pathology of lower leg muscles of boys with DMD. Overall, we demonstrate that a multi-slice composite score may provide a more comprehensive characterization of disease severity along the length of dystrophic muscle. Specifically, there were four major conclusions from this study: (i) the six individual muscles of the lower leg were not affected equally by the disease; (ii) there was more muscle involvement at the myotendinous junctions rather than the midbelly of muscle; (iii) differential disease involvement was found between subjects of similar age; and (iv) MRI mutislice scores are related to age and functional ability. In summary, our results show a unique distribution of involvement both inter- and intra- muscularly in the lower legs of boys with DMD. Knowledge of such geographic differences is critical for assessing the natural progression and elucidating the pathophysiology of DMD. Caution may be warranted when using single- slice acquisitions, as they may not appropriately represent overall disease status in individuals with DMD as outlined above.

Acknowledgements

This study was supported in part by the following organizations: Muscular Dystrophy Association (MDA4170), and Parent Project Muscular Dystrophy (PPMD8509), and was supported by NIH (R01 AR056973) as a subset of the larger ImagingDMD study. We thank William Triplett and Kami Veltri for assistance with imaging evaluation and Tammy Nicholson for operation of the clinical scanner.

References

- Hoffman EP, Brown RH Jr., Kunkel LM. Dystrophin: the protein product of the Duchenne muscular dystrophy locus. *Cell* 1987;51:919-28.
- Mah JK, Korngut L, Dykeman J, et al. A systematic review and meta-analysis on the epidemiology of Duchenne and Becker muscular dystrophy. *Neuromuscul Disord* 2014;24:482-91.
- McDouall RM, Dunn MJ, Dubowitz V. Nature of the mononuclear infiltrate and the mechanism of muscle damage in juvenile dermatomyositis and Duchenne muscular dystrophy. *J Neurol Sci* 1990;99:199-217.
- Bongers H, Schick F, Skalej M, et al. Localized in vivo 1H spectroscopy of human skeletal muscle: normal and pathologic findings. *Magn Reson Imaging* 1992;10:957-64.
- Kharraz Y, Guerra J, Pessina P, et al. Understanding the process of fibrosis in Duchenne muscular dystrophy. *Bio Med Res Int* 2014;2014:e965631.
- Bushby K, Finkel R, Birnkrant DJ, et al. Diagnosis and management of Duchenne muscular dystrophy, part 1: diagnosis, and pharmacological and psychosocial management. *Lancet Neurol* 2010;9:77-93.
- Bushby K, Finkel R, Birnkrant DJ, et al. Diagnosis and management of Duchenne muscular dystrophy, part 2: implementation of multidisciplinary care. *Lancet Neurol* 2010;9:177-89.
- Flanigan KM. Duchenne and Becker muscular dystrophies. *Neurol Clin* 2014;32:671-88.
- Baudin PY, Marty B, Robert B, et al. Qualitative and quantitative evaluation of skeletal muscle fatty degenerative changes using whole-body Dixon nuclear magnetic resonance imaging for an important reduction of the acquisition time. *Neuromuscul Disord* 2015;25:758-63.
- Kinali M, Arechavala-Gomez V, Cirak S, et al. Muscle histology vs MRI in Duchenne muscular dystrophy. *Neurology* 2011;76:346-53.
- Liu GC, Jong YJ, Chiang CH, et al. Duchenne muscular dystrophy: MR grading system with functional correlation. *Radiology* 1993;186:475-80.
- Mercuri E, Pichiecchio A, Allsop J, et al. Muscle MRI in inherited neuromuscular disorders: past, present, and future. *J Magn Reson Imaging JMRI* 2007;25:433-40.
- Schreiber A, Smith WL, Ionasescu V, et al. Magnetic resonance imaging of children with Duchenne muscular dystrophy. *Pediatr Radiol* 1987;17:495-7.
- Torriani M, Townsend E, Thomas BJ, et al. Lower leg muscle involvement in Duchenne muscular dystrophy: an MR imaging and spectroscopy study. *Skeletal Radiol* 2012;41:437-45.
- Wokke BH, Bos C, Reijnierse M, et al. Comparison of dixon and T_1 -weighted MR methods to assess the degree of fat infiltration in duchenne muscular dystrophy patients. *J Magn Reson Imaging* 2013;38:619-24.
- Polavarapu K, Manjunath M, Preethish-Kumar V, et al. Muscle MRI in Duchenne muscular dystrophy: Evidence of a distinctive pattern. *Neuromuscul Disord NMD* 2016;26:768-74.
- Mercuri E, Talim B, Moghadaszadeh B, et al. Clinical and imaging findings in six cases of congenital muscular dystrophy with rigid spine syndrome linked to chromosome 1p (RSM1). *Neuromuscul Disord* 2002;12:631-8.
- Sarkozy A, Deschauer M, Carlier RY, et al. Muscle MRI findings in limb girdle muscular dystrophy type 2L. *Neuromuscul Disord NMD* 2012;22(Suppl 2):S122-129.

19. Stramare R, Beltrame V, Dal Borgo R, et al. MRI in the assessment of muscular pathology: a comparison between limb-girdle muscular dystrophies, hyaline body myopathies and myotonic dystrophies. *Radiol Med (Torino)* 2010;115:585-99.
20. Willis TA, Hollingsworth KG, Coombs A, et al. Quantitative magnetic resonance imaging in limb-girdle muscular dystrophy 2I: a multinational cross-sectional study. *PLoS One* 2014;9:e90377.
21. Janssen BH, Voet NB, Nabuurs CI, et al. Distinct disease phases in muscles of facioscapulohumeral dystrophy patients identified by MR detected fat infiltration. *PLoS ONE*, 2014;9:e85416.
22. Leung DG, Carrino JA, Wagner KR, et al. Whole-body magnetic resonance imaging evaluation of facioscapulohumeral muscular dystrophy. *Muscle Nerve* 2015;52,:512-20.
23. Tasca G, Monforte M, Ottaviani P, et al. Magnetic resonance imaging in a large cohort of facioscapulohumeral muscular dystrophy patients: Pattern refinement and implications for clinical trials. *Ann Neurol* 2016;79:854-64.
24. Fischmann A, Hafner P, Fasler S, et al. Quantitative MRI can detect subclinical disease progression in muscular dystrophy. *J Neurol* 2012;259:1648-54.
25. Mahjneh I, Bashir R, Kiuru-Enari S, et al. Selective pattern of muscle involvement seen in distal muscular dystrophy associated with anoctamin 5 mutations: a follow-up muscle MRI study. *Neuromuscul Disord* 2012;22 (Suppl 2):S130-136.
26. Hooijmans MT, Niks EH, Burakiewicz J, et al. Non-uniform muscle fat replacement along the proximodistal axis in Duchenne muscular dystrophy. *Neuromuscul Disord* 2017;27:458-64.
27. Fischer D, Kley RA, Strach K, et al. Distinct muscle imaging patterns in myofibrillar myopathies. *Neurology* 2008;71:758-65.
28. Vidt ME, Santago AC 2nd, Tuohy CJ, et al. Assessments of fatty infiltration and muscle atrophy from a single magnetic resonance image slice are not predictive of 3-dimensional measurements. *Arthroscopy* 2016;32:128-39.
29. Lue Y-J, Lin R-F, Chen S-S, et al. Measurement of the functional status of patients with different types of muscular dystrophy. *Kaohsiung J Med Sci* 2009;25:325-33.
30. Fischer D, Kley RA, Strach K, et al. Distinct muscle imaging patterns in myofibrillar myopathies. *Neurology* 2008;71:758-65.
31. Leung DG, Carrino JA, Wagner KR, et al. Whole-body magnetic resonance imaging evaluation of facioscapulohumeral muscular dystrophy. *Muscle Nerve* 2015;52:512-20.
32. Mahjneh I, Bashir R, Kiuru-Enari S, et al. Selective pattern of muscle involvement seen in distal muscular dystrophy associated with anoctamin 5 mutations: a follow-up muscle MRI study. *Neuromuscul Disord* 2012;22(Suppl 2):S130-136.
33. Akima H, Lott D, Senesac C, et al. Relationships of thigh muscle contractile and non-contractile tissue with function, strength, and age in boys with Duchenne muscular dystrophy. *Neuromuscul Disord* 2012;22:16-25.
34. Henricson EK, Abresch RT, Cnaan A, et al. The cooperative international neuromuscular research group Duchenne natural history study: glucocorticoid treatment preserves clinically meaningful functional milestones and reduces rate of disease progression as measured by manual muscle testing and other commonly used clinical trial outcome measures. *Muscle Nerve* 2013;48:55-67.
35. Willcocks RJ, Arpan IA, Forbes SC, et al. Longitudinal measurements of MRI-T2 in boys with Duchenne muscular dystrophy: effects of age and disease progression. *Neuromuscul Disord* 2014;24:393-401.
36. Babic J, Lenarcic J. In vivo determination of triceps surae muscle-tendon complex viscoelastic properties. *Eur J Appl Physiol* 2004;92:477-84.
37. Suydam SM, Soulas EM, Elliott DM, et al. Viscoelastic properties of healthy achilles tendon are independent of isometric plantar flexion strength and cross-sectional area. *J Orthop Res* 2015;33:926-31.
38. van Bavel H, Drost MR, Wielders JDL, et al. Strain distribution on rat medial gastrocnemius (MG) during passive stretch. *J Biomech*, 1996;29:106974.
39. Sun JS, Tsaung YH, Hou SM, et al. Microfailure of peroneus longus muscle during passive extension. *Proc Natl Sci Coun Repub China B* 1994;18:24-9.
40. Sharafi B, Ames EG, Holmes JW, et al. Strains at the myotendinous junction predicted by a micromechanical model. *J Biomech* 2011;44,:2795-801.
41. Pasternak C, Wong S, Elson EL. Mechanical function of dystrophin in muscle cells. *J Cell Biol* 1995;128:355-61.
42. Hu X, Blemker SS. Musculoskeletal simulation can help explain selective muscle degeneration in duchenne muscular dystrophy. *Muscle Nerve* 2015;52:174-82.
43. Hakim CH, Duan D. A marginal level of dystrophin partially ameliorates hindlimb muscle passive mechanical properties in dystrophin-null mice. *Muscle Nerve* 2012;46:948-50.
44. Hakim CH, Duan D. Truncated dystrophins reduce muscle stiffness in the extensor digitorum longus muscle of mdx mice. *J Appl Physiol Bethesda Md* 1985;114:482-9.
45. Triplett WT, Baligand C, Forbes SC, et al. Chemical shift-based MRI to measure fat fractions in dystrophic skeletal muscle. *Magn Reson Med* 2014;72:8-19.
46. Forbes SC, Walter GA, Rooney WD, et al. Skeletal muscles of ambulant children with Duchenne muscular dystrophy: validation of multicenter study of evaluation with MR imaging and MR spectroscopy. *Radiology* 2013;269:198-207.
47. Ricotti V, Ridout DA, Pane M, et al. The NorthStar Ambulatory Assessment in Duchenne muscular dystrophy: considerations for the design of clinical trials. *J Neurol Neurosurg Psychiatry* 2016;87:149-55.
48. Pane M, Mazzone ES, Sivo S, et al. Long term natural history data in ambulant boys with Duchenne muscular dystrophy: 36-month changes. *PLoS One* 2014;9:e108205.

49. Torriani M, Townsend E, Thomas BJ, et al. Lower leg muscle involvement in Duchenne muscular dystrophy: an MR imaging and spectroscopy study. *Skeletal Radiol* 2012;41:437-45.
50. Wokke BH, Bos C, Reijnierse M, et al. Comparison of dixon and T1-weighted MR methods to assess the degree of fat infiltration in duchenne muscular dystrophy patients. *J Magn Reson Imaging* 2013;38:619-24.

Leber's hereditary optic neuropathy (LHON) in an Apulian cohort of subjects

ANGELICA BIANCO¹, LUIGI BISCEGLIA², PAOLO TREROTOLI³, LUCIANA RUSSO¹, LEONARDO D'AGRUMA², SILVANA GUERRIERO¹ AND VITTORIA PETRUZZELLA¹

¹ Dipartimento di Scienze Mediche di Base, Neuroscienze e Organi di Senso, Università degli Studi Aldo Moro, Bari, Italia;

² Ospedale Casa Sollievo della Sofferenza IRCCS, UOC Genetica Medica, San Giovanni Rotondo, Foggia, Italia;

³ Dipartimento di Scienze Biomediche ed Oncologia Umana, Università degli Studi Aldo Moro, Bari, Italia

Leber's hereditary optic neuropathy (LHON) is a maternally inherited disorder that causes severe loss of sight in young adults, and is typically associated to mitochondrial DNA (mtDNA) mutations. Heteroplasmy of primary LHON mutations, presence of 'ancillary' mtDNA mutations, and mtDNA copy number are probably correlated with the penetrance and the severity of the disease. In this study, we performed a mutational screening in an Apulian cohort of LHON patients and we found that 41 out of 54 subjects harbored the m.11778G>A mutation, and 13 harbored the m.3460G>A mutation. Whole mtDNA sequencing was performed in three affected subjects belonging to three unrelated m.11778G>A pedigrees to evaluate the putative synergistic role of additional mtDNA mutations in determining the phenotype. Our study suggests to include haplogroup T as a possible genetic background influencing LHON penetrance and to consider the increase of mtDNA copy number as a protective factor from vision loss regardless the hetero/homoplasmic status of LHON primary mutations.

Key words: LHON; heteroplasmy; homoplasmy; Mitochondrial DNA mutation; mtDNA copy number

Introduction

Leber hereditary optic neuropathy (LHON, MIM#535000) is the most frequent inherited mitochondrial disorder due to mitochondrial DNA (mtDNA) mutations, with a prevalence ranging between 0.2 to 0.4 cases per 100,000 in Europe (1-5). Typically, LHON arises in males (6) during young adulthood with painless loss of central vision in one eye followed by loss of vision in the second eye within a short time (7, 8). LHON is most frequently associated to one of three mtDNA point mutations affecting NADH-ubiquinone oxidoreductase

(complex I; EC 1.6.5.3) subunits, *i.e.* m.3460G>A in MT-ND1; m.11778G>A in MT-ND4; m.14484T>C in MT-ND6 (9). Fifteen further mutations have been identified as pathogenic for LHON (<http://www.mitomap.org/MITOMAP>) with some of them affecting MT-ND subunits of complex I, and associating with phenotypes overlapping MELAS (10), Leigh syndrome (11) and deafness (12-14). Unlike the majority of mtDNA mutations which are heteroplasmic (a mixture of both mutant and normal molecules) in mitochondrial diseases, LHON mutations are frequently homoplasmic (only mutant mtDNA); nonetheless, heteroplasmic mutations, particularly the m.3460G>A, have been detected in about 14% of the families observed (15-19). Although LHON has been the first disease to be identified as caused by mutations in the mtDNA, there are several puzzling features of LHON, *i.e.* the incomplete penetrance. All the matrilineal members of a LHON pedigree harbor mtDNA mutations, but only some individuals develop blindness implying that the primary mutation is a necessary but not sufficient condition to develop optic neuropathy. Among the genetic factors affecting penetrance, the homo/heteroplasmic condition is one of the pathological features which still needs to be completely elucidated (20). It was suggested that a contributing factor to the complexity of LHON is determined by additional mtDNA mutations, defined as 'secondary', that may well act in synergy with the primary ones – so far several nucleotide variants have been reported as such (21-25) – though the significance of such variants still remains controversial. Furthermore, as mtDNA is a multicopy genome, it has been proposed that the fine-tuning of mtDNA 'copy number' (20-26) may respond to an alteration of the bioenergetics request (27). Other genetic

risk factors as well as environmental triggers – e.g. smoking – have been reported as significantly associated with increased risk of visual loss (28, 29).

Herein, we present molecular and genetic data of a cohort of LHON patients collected from the Apulia Region and we propose some ‘ancillary’ mtDNA mutations and mtDNA copy number as putative factors that may significantly affect LHON penetrance.

Materials and methods

Ophthalmologic examination and sample collection

A total of 54 subjects were enrolled in the study: 46 subjects were from the Ophthalmology Clinic, Policlinico Hospital of Bari, and 8 subjects were from the I.R.C.C.S. Casa Sollievo Della Sofferenza Hospital, San Giovanni Rotondo, Italy. Prior written and informed consent was obtained from each subject according to Institutional Guidelines. Among 54 subjects, 31 had already been partially analyzed in previous studies (20, 26). The control group consisted of 90 unrelated Italian subjects. Slit-lamp biomicroscopy dilated stereoscopic examination of the optic nerve head and *fundus*, visual field (VF) test (when possible), optical coherence tomography (OCT) (when possible) and fluorescein angiography were performed. The peripapillary RNFL thickness was measured using a spectral-domain Cirrus HD-OCT. The results from the VF tests were considered reliable if the fixation losses were less than 20% and false positive and false negative rates were less than 15%.

Mitochondrial genetics and statistical analysis

Total genomic DNA was extracted by standard methods from peripheral blood of the patients and their relatives with suspicion of LHON and from healthy control subjects. To detect the m.3460G>A, m.11778G>A and m.14484T>C mutations, convenient fragments were amplified by PCR performing a final last cycle of super-extension for 5 min at 72°C, to minimize the possible formation of heteroduplexes between mutant and wild-type strands. The presence of mutations was detected by PCR-RFLP (30) in all the subjects and, when present, confirmed by direct sequencing (ABI prism 310, Applied Biosystems). Entire mtDNA sequencing was performed in three affected individuals as described previously (31). All sequences were analyzed by comparison with mitochondrial reference sequence (*Reconstructed Sapiens Reference Sequence – RSRS*) (32). Mitochondrial haplogroups were defined by the web-based bioinformatic platform Mitochondrial Disease Sequence Data Resource (<https://mseqdr.org/>). Relative quantification of mtDNA

copy number was performed (33). All the data were analyzed by GraphPad Prism and Medcalc (MedCalc Statistical Software version 17.5.5 (MedCalc Software bvba, Ostend, Belgium) applying the chi-square test or the Fisher’s exact test as appropriate to compare percentages of independent groups. To compare quantitative variables ANOVA test in conjunction with Bonferroni test was used and description was done by means and standard deviation if data approach Gaussian distribution. If data were not Gaussian distributed description was done by median and interquartile range, Kruskal-Wallis non parametric analysis of variance were applied to compare groups and non-parametric test according to Conover was used for post-hoc comparisons. Statistical significance was set at $P < 0.05$.

Results

Population and clinical features

The cohort consisted of 54 subjects including 42 subjects belonging to 12 families, and 12 unrelated subjects. Male: female ratio was overall 28:26, 19: 8 for patients and 9: 18 for unaffected subjects. We counted 28 LHON affected subjects, representing the 52% of the entire cohort, in which the molecular genetic diagnosis was positive for one of the primary mutations (Table 1). All the clinical findings, sex, age and age at onset, molecular genetics test, and therapy as Idebenone administration, risk factors and recovery of vision for all the subjects, when available, are reported in Table 1. Among the 54 subjects tested, 6 (II-1 FAM-A1; II-1 FAM-A8; I-1 FAM-A14; I-1 FAM-A14; III-1 FAM-B2; I-1 FAM-B3) were examined at the acute phase and the diagnosis of LHON was clinically based on the unilateral and severe visual decline followed by a declining vision in the contralateral eye within a few weeks. Alteration of the visual field for the presence of a centrocecal scotoma, an ophthalmoscopic appearance of the *fundus* with the presence of an edematous, hyperemic optic nerve head, vascular tortuosity and telangiectasia were examined. Fluorescein angiography was performed in all affected subjects, and highlighted vascular telangiectasia in those examined during the acute phase without phenomena of leakage or staining, whereas it showed non-specific alterations in those observed during the atrophic stage. Interestingly, three m.11778G>A patients and one m.3460G>A patient experienced visual recovery: one (II-1 FAM-A2) homoplasmic and one (II-5 FAM-A4) heteroplasmic patient without Idebenone treatment, and two (I-1 FAM-A14; I-1 FAM-B3) homoplasmic patients, including an m.3460G>A, out of the 13 Idebenone treated-affected subjects. In all the cases, the diagnosis was confirmed by mtDNA genetic analysis.

Since LHON patients were characterized by a sudden and devastating vision loss, the asymptomatic carriers, who had normal vision, were considered unaffected by the disease. Hereafter, we will refer to the subjects as *Carriers*, *Affected* and *Controls*. The control group consisted of 90 (male: female ratio 47:43) unrelated subjects who did not show any sign of optic neuropathy. The mean age resulted significantly different among LHON subjects, aged $45.3 \text{ ys} \pm 15.9$, *Carriers* aged 47.8 ± 20.5 and *Controls* aged $37.9 \text{ ys} \pm 11.9$ ($F = 5.675$; $p = 0.004$).

Genetic analysis of mtDNA

If we consider a total of 54 LHON mutation-positive subjects, they represent an overall observed prevalence of 1: 75,503 in the Apulia population with sex proportion of 29 males (1: 68,250 male) versus 25 females (1: 83,916 female) (December 31, 2016). On the basis of clinical features and genetic mitochondrial analysis, we diagnosed 28 subjects as *Affected* and 26 as *Carriers*. Among the 54 subjects, 76% harbored the m.11778A mutation and 24% carried the m.3460G>A mutation. Moreover, the 95% of subjects who harbored m.11778G>A were homoplasmic (51% *Affected*; 49% *Carriers*) and 5% were heteroplasmic (all *Affected*); whereas among the subjects who harbored m.3460G>A, 70% were homoplasmic (56% *Affected*; 44% *Carriers*) and 30% were heteroplasmic (25% *Affected*; 75% *Carriers*). The difference of frequency of homoplasmic subjects between m.11778G>A and m.3460G>A resulted statistically significant at Fisher exact test ($p = 0.0248$). Among the heteroplasmic *Affected*, I-1 FAM-A5 and II-5 FAM-A4 (*Family 11*) were both heteroplasmic for m.11778G>A with mutant load estimated to be ~75% (34) and ~60%, respectively; I-1 FAM-B4 was heteroplasmic for m.3460G>A with an estimated load of ~15%. Among the heteroplasmic *Carriers*, I-2, II-2, III-4 all belonging to FAM-B2 harbored the m.3460G>A with a mutant load estimated as ~30%, ~40%, and ~40%, respectively. None of them carried the m.14484T>C primary mutation. Among all 54 LHON subjects, 33 (Table 1) were reported in our previous study (20, 26) and the relatives of FAM-B2 (Table 1) will be described in the near future (Manuscript in preparation).

The penetrance rate of both LHON mutations in our cohort was: 52% (28/54), i.e. 71% (20/28) in males and 29% (8/28) in females. Among the 41 subjects (22 males; 19 females) who harbored the m.11778G>A mutation, 24 (16 males; 8 females) developed typical optic neuropathy thus showing 59% phenotype penetrance. In the remaining 13 subjects (7 males; 6 females) who harbored m.3460G>A mutation, 6 (4 males; 2 female) were *Affected* thus showing 46% phenotype penetrance. The penetrance rate did not result significantly different (chi-square = 1.375; $p = 0.2409$), but there was a difference

of percentage of affected between males and females respectively 32% (8/25) vs 68.97% (20/29) that resulted statistically significant (chi-square = 7.348, $p = 0.0067$).

We performed Sanger sequencing of the entire mtDNA genome of three *Affected* carrying homoplasmic m.11778G>A mutation: II-1 FAM-A1; II-1 FAM-A2; I-1 FAM-A3. The criterion of selection of these three patients was based on the fact that they showed a quite peculiar manifestation. II-1 FAM-A1 reported a history of alcohol, tobacco, and drug abuse and he had been diagnosed as psychotic following psychiatric examination. II-1 FAM-A2 had reported visual recovery without having been treated with Idebenone; I-1 FAM-A3 had experienced an early onset of LHON with an acute and painless loss of central vision already at 4 ys of age.

All the mtDNA nucleotide variants identified in the three patients were analyzed by MtoolBox which performs prioritization taking into account the pathogenicity of each mutated allele with different algorithms, and the nucleotide variability of each variant site (34). For all three patients the m.11778G>A mutation was prioritized with a high score of pathogenicity (Supplemental Table 1). II-1 FAM-A1 showed 56 additional variants of which 45 mutational events help to define the sample haplogroup (K1a). The prioritization process recognized 7 variants annotated in Mitomap and they were predicted as not having a deleterious effect (Supplemental Table 1A). II-1 FAM-A2 showed 61 variants, of which 38 contributed to defining the sample haplogroup (T2e2a) and 8 further variants were prioritized (Supplemental Table 1B). We focused on two out of the eight variants: m.4136A>G/*MT-ND1* (p.Y277C) and m.9139G>A/*MT-ATPase6* were predicted to have a deleterious effect (Supplemental Table 1B) and already reported as associated to LHON disease (<http://www.mitomap.org/MITOMAP>). We noticed that the patient carried two additional mutations, m.4216T>C/*MT-ND1* (p.Y304H) and m.4917A>G/*MT-ND1* (p.N150D), previously defined as 'secondary' LHON mutations (35), that were not prioritized because they are indeed polymorphic variants and also T2e2a haplogroup markers (<http://www.phylotree.org/>). I-1 FAM-A3 showed 78 variants, of which 64 contributed to defining the sample haplogroup (T2e2a) and 9 variants were further prioritized (Supplemental Table 1C). Among the nine mutations, the m.4136A>G/*MT-ND1* and m.9139G>A/*MT-ATPase6* mutations are the same deleterious variants also identified in the above mentioned II-1 FAM-A2. In the I-1 FAM-A3 patient we noticed the presence of m.4216T>C and m.4917A>G mutations which define the same haplogroup T2e2a. Interestingly, the same MT-ND1 variants defining haplogroup T2e2a had been identified also in I-1 FAM-A5 (36). None of the *Affected* fitted to haplogroup J previously suggested as increasing the penetrance of the m.11778 LHON mutation (37).

Table 1. Clinical and genetic findings in subjects carrying the primary LHON mutations. Ophthalmological findings, sex, age, possible exposure to environmental triggers (i.e. alcohol, smoking and illicit drugs) and mtDNA LHON mutations, percentage of heteroplasmy and copy number are indicated. M, male; F, female; RE, right eye; LE, left eye; LP, light perception; N, no; Y, yes; n.a., not available; HOM, Homoplasmic; HET, Heteroplasmic. Number in brackets near Subject ID indicates the reference of papers where the mtDNA copy number was previously reported.

Subject ID	Family ID	Relation	Sex	Age (ys)	Visual condition at the first examination		Currently visual condition		Level of Visual Loss	Recovery	Idebenone treatment	Age at test (ys)	Age at onset (ys)	Clinical Features	Risk factors	Primary mtDNA mutation	mtDNA Mutation type (%mut)	Copy number (mtDNA/nDNA)
					RE	LE	RE	LE										
I-1 (26)	FAM-A1	Relative	F	62	20/20	20/20	20/20	20/20	Normal vision	-	-	56	-	Normal vision	-	m.11778G>A	HOM	431 ± 49
II-1 (26)		Proband	M	38	20/200	20/40	LP	LP	Profound	N	Y	32	32	Bilateral optic atrophy; RNFL: LE 80.17µm; psychotic	Illicit drug and tobacco abuse	m.11778G>A	HOM	196 ± 16
II-2 (26)		Relative	M	36	20/20	20/20	20/20	20/20	Normal vision	-	-	30	-	Normal vision RNFL: RE 87µm; LE 88µm	-	m.11778G>A	HOM	256 ± 47
I-1 (26)	FAM-A2	Relative	F	61	20/20	20/20	20/20	20/20	Normal vision	-	-	58	-	Normal vision	-	m.11778G>A	HOM	685 ± 271
II-1 (26)		Proband	M	35	20/200	20/200	20/200	20/200	Moderate	Y	N	24	n.a.	Bilateral optic atrophy	-	m.11778G>A	HOM	348 ± 35
I-1	FAM-A3	Proband	F	66	na	na	20/40	LP	Moderate	N	Y	54	4	RE optic subatrophy LE optic atrophy	-	m.11778G>A	HOM	177 ± 46
II-1 (26)		Relative	M	30	20/20	20/20	20/20	20/20	Normal vision	n.a.	n.a.	29	n.a.	Normal vision	-	m.11778G>A	HOM	316 ± 62
II-5 (20)	FAM-A4	Proband	M	51	n.a.	n.a.	20/20	20/20	Normal vision	Y	N	47	n.a.	Bilateral optic subatrophy	Alcohol	m.11778G>A	HET (60%)	149 ± 40
III-2 (20)		Proband	M	n.a.	n.a.	n.a.	LP	LP	Profound	n.a.	N	n.a.	n.a.	Bilateral optic subatrophy	-	m.11778G>A	HOM	n.a.
I-1 (20)	FAM-A5	Proband	M	67	20/300	20/300	LP	LP	Profound	N	Y	60	56	Bilateral optic subatrophy	-	m.11778G>A	HET (70%)	n.a.
I-1 (26)	FAM-A6	Proband	F	51	20/25	20/32	20/25	20/32	Mild	N	Y	39	30	Bilateral optic subatrophy with hemeralopia; psychiatric signs	-	m.11778G>A	HOM	311 ± 30
II-1 (26)		Proband	F	25	20/40	20/32	20/40	20/40	Mild	N	Y	13	11	RE optic atrophy, LE optic subatrophy	-	m.11778G>A	HOM	366 ± 43
I-1 (26)	FAM-A7	Proband	M	66	LP	LP	LP	LP	Profound	n.a.	N	65	28	Bilateral optic atrophy	-	m.11778G>A	HOM	183 ± 35
I-2 (26)		Proband	M	45	LP	20/1000	LP	20/800	Severe	n.a.	N	44	25	Bilateral optic atrophy	-	m.11778G>A	HOM	429 ± 75
I-1	FAM-A8	Proband	F	52	n.a.	n.a.	20/40	20/200	Moderate	N	N		n.a.	Bilateral optic subatrophy	-	m.11778G>A	HOM	486 ± 56
II-1		Proband	M	21	20/200	20/200	LP	20/800	Severe	N	Y	20	20	Bilateral optic atrophy; RNFL: RE 95.12µm; LE 98.34µm	-	m.11778G>A	HOM	190 ± 33
II-2		Relative	F	15	20/20	20/20	20/20	20/20	Normal vision	-	-	-	-	Normal vision	-	m.11778G>A	HOM	221 ± 48
I-1	FAM-A9	Relative	F	61	20/20	20/20	20/20	20/20	Normal vision	-	-	-	n.a.	Normal vision	-	m.11778G>A	HOM	510 ± 77
II-1		Proband	M	45	20/200	20/40	LP	20/200	Severe	n.a.	n.a.	-	n.a.	Bilateral optic atrophy	-	m.11778G>A	HOM	327 ± 45
II-2		Relative	F	n.a.	20/20	20/20	20/20	20/20	Normal vision	n.a.	-	-	n.a.	Normal vision	-	m.11778G>A	HOM	430 ± 94



Subject ID	Family ID	Relation	Sex	Age (ys)	Visual condition at the first examination		Currently visual condition		Level of Visual Loss	Recovery	Idebenone treatment	Age at test (ys)	Age at onset (ys)	Clinical Features	Risk factors	Primary mtDNA mutation	mtDNA Mutation type (%mut)	Copy number (mtDNA/nDNA)
					RE	LE	RE	LE										
I-2	FAM-A10	Relative	F	89	20/20	20/20	20/20	20/20	Normal vision	-	-	-	-	Normal vision	-	m.11778G>A	HOM	453 ± 52
II-2		Relative	F	59	20/20	20/20	20/20	20/20	Normal vision	-	-	-	-	Normal vision	-	m.11778G>A	HOM	562 ± 68
III-1		Proband	M	34	n.a	n.a.	LP	LP	Mild	n.a.	n.a.	-	n.a	Bilateral optic subatrophy	-	m.11778G>A	HOM	334 ± 29
III-2		Relative	M	28	20/20	20/20	20/20	20/20	Normal vision	-	-	-	-	Normal vision	-	m.11778G>A	HOM	484 ± 85
I-1	FAM-A11	Relative	M	74	20/20	20/20	20/20	20/20	Normal vision	-	-	-	-	Normal vision	-	m.11778G>A	HOM	165 ± 47
I-2		Relative	F	68	20/20	20/20	20/20	20/20	Normal vision	-	-	-	-	Normal vision	-	m.11778G>A	HOM	161 ± 39
I-3		Relative	F	66	20/20	20/20	20/20	20/20	Normal vision	-	-	-	-	Normal vision	-	m.11778G>A	HOM	167 ± 25
I-4		Relative	F	58	20/20	20/20	20/20	20/20	Normal vision	-	-	-	-	Normal vision	-	m.11778G>A	HOM	241 ± 73
I-5		Relative	F	55	20/20	20/20	20/20	20/20	Normal vision	-	-	-	-	Normal vision	-	m.11778G>A	HOM	182 ± 59
II-1		Relative	M	34	20/20	20/20	20/20	20/20	Normal vision	-	-	-	-	Normal vision	-	m.11778G>A	HOM	380 ± 18
II-2		Proband	M	38	n.a.	n.a.	LP	LP	Profound	n.a.	Y	-	n.a.	Bilateral optic atrophy	-	m.11778G>A	HOM	201 ± 45
II-3		Relative	F	38	20/20	20/20	20/20	20/20	Normal vision	-	-	-	-	Normal vision	-	m.11778G>A	HOM	263 ± 55
I-1 (26)	FAM-A12	Proband	F	55	20/40	20/25	20/40	20/25	Mild	N	N	51	26	Bilateral optic subatrophy with hemeralopia	-	m.11778G>A	HOM	246 ± 31
I-1 (26)	FAM-A13	Proband	F	42	20/25	20/32	20/25	20/32	Mild	N	Y	40	30	Bilateral optic subatrophy with hemeralopia	-	m.11778G>A	HOM	187 ± 26
I-1 (26)	FAM-A14	Proband	M	41	20/80	20/160	20/200	20/40	Mild	Y	Y	28	28	Bilateral optic subatrophy	Tobacco and alcohol abuse	m.11778G>A	HOM	739 ± 121
I-1	FAM-A15	Proband	M	34	n.a.	n.a.	n.a.	n.a.	Severe	n.a.	n.a.	21	n.a.	Bilateral optic atrophy	-	m.11778G>A	HOM	n.a.
I-1 (26)	FAM-A16	Proband	M	41	20/20	20/200	20/200	20/800	Severe	Y	Y	33	33	Bilateral optic Subatrophy	-	m.11778G>A	HOM	136 ± 36
I-1 (26)	FAM-A17	Proband	M	26	20/20	20/200	LP.	LP.	Profound	N	Y	19	19	Bilateral optic atrophy	-	m.11778G>A	HOM	313 ± 44
I-1 (26)	FAM-A18	Proband	M	53	20/800	20/800	20/800	20/800	Profound	N	N	50	20	Bilateral optic atrophy	-	m.11778G>A	HOM	268 ± 108
I-1 (26)	FAM-A19	Unrelated	M	n.a.	20/20	20/20	20/20	20/20	Normal vision	-	-	-	-	Normal vision	-	m.11778G>A	HOM	582 ± 76
I-1 (26)	FAM-A20	Unrelated	F	n.a.	20/20	20/20	20/20	20/20	Normal vision	-	-	-	-	Normal vision	-	m.11778G>A	HOM	303 ± 78
I-1 (26)	FAM-B1	Proband	F	61	20/32	20/28	20/32	20/28	Mild	N	N	54	40	Bilateral optic subatrophy	-	m.3460G>A	HOM	279 ± 36
I-2 (26)		Proband	F	70	20/40	20/32	20/40	20/32	Mild	N	Y	63	35	Bilateral optic subatrophy	-	m.3460G>A	HOM	259 ± 27
II-1 (26)		Proband	M	49	20/40	20/40	20/40	20/40	Mild	N	Y	42	27	Bilateral optic subatrophy, severe visual impairment with hemeralopia	-	m.3460G>A	HOM	305 ± 38



Subject ID	Family ID	Relation	Sex	Age (ys)	Visual condition at the first examination		Currently visual condition		Level of Visual Loss	Recovery	Idebenone treatment	Age at test (ys)	Age at onset (ys)	Clinical Features	Risk factors	Primary mtDNA mutation	mtDNA Mutation type (%mut)	Copy number (mtDNA/nDNA)
					RE	LE	RE	LE										
I-2	FAM-B2	Relative	F	71	20/20	20/20	20/20	20/20	Normal vision	-	-	70	-	Normal vision	-	m.3460G>A	HET (35%)	206 ± 15
II-1 (26)		Relative	F	47	20/20	20/20	20/20	20/20	Normal vision	-	-	39	-	Mild mental retardation	-	m.3460G>A	HOM	636 ± 74
II-2		Relative	F	46	20/20	20/20	20/20	20/20	Normal vision	-	-	38	-	Borderline mental functioning	-	m.3460G>A	HET (40%)	713 ± 144
II-3 (26)		Relative	M	44	20/20	20/20	20/20	20/20	Normal vision	-	-	43	-	Normal vision	Tobacco abuse	m.3460G>A	HOM	213 ± 9
III-1 (26)		Proband	M	25	20/200	20/200	20/800	L.P.	Profound	N	Y	17	n.a.	Bilateral optic atrophy epilepsies, mild mental retardation	-	m.3460G>A	HOM	240 ± 86
III-2 (26)		Relative	M	21	20/20	20/20	20/20	20/20	Normal vision	-	-	17	-	Hyperemic optic disk, borderline mental functioning	-	m.3460G>A	HOM	604 ± 149
III-3 (26)		Relative	F	18	20/25	20/25	20/25	20/25	Normal vision	-	-	12	-	Borderline mental functioning	-	m.3460G>A	HOM	667 ± 72
III-4		Relative	M	18	20/20	20/20	20/20	20/20	Normal vision	-	-	10	-	Borderline mental functioning	Tobacco abuse	m.3460G>A	HET (40%)	739 ± 184
I-1 (26)	FAM-B3	Proband	M	16	20/80	20/200	20/40	20/80	Moderate	Y	Y	13	13	Bilateral optic subatrophy; several maternal relatives with optic atrophy	-	m.3460G>A	HOM	140 ± 38
I-1 (20)	FAM-B4	Proband	M	77	20/32	20/25	20/32	20/25	Mild	N	Y	69	30	Bilateral optic subatrophy with hemeralopia	Illicit drug Alcohol and tobacco abuse	m.3460G>A	HET (15%)	285 ± 24

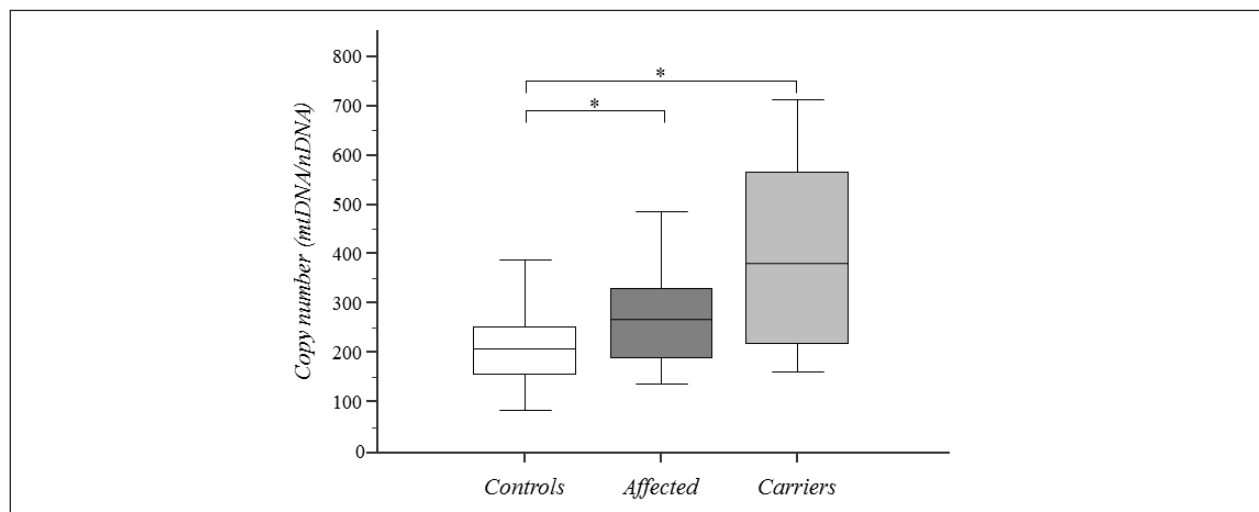


Figure 1. Analysis of mtDNA content in LHON subjects. Box-plot of mtDNA copy number (mtDNA/nDNA) by Affected, Carriers and Controls. Experiments were performed in triplicates for all samples; for thirty-one LHON mutation carriers mtDNA content was evaluated in previous works (20, 26) and herein included. Asterisks indicate statistical significance (p -value <0.05) at post-hoc comparisons.

Analysis of mtDNA copy number in LHON subjects

The evaluation of mtDNA copy numbers was performed independently from the type of primary mutations in 25 *Affected* (23 homoplasmic; 2 heteroplasmic) and 26 *Carriers* (24 homoplasmic; 3 heteroplasmic) (Table 1). mtDNA copy number of thirty-one LHON subjects was evaluated in previous works (20, 26). Mitochondrial copy number values were measured either using MT-ND1 or MT-ND4 as target genes. The analysis of the MT-ND4 region was indeed implemented after assessing the presence of an ancient polymorphism, m.3480A>G/ND1, just within the annealing region of ND1 primers in I-1, II-1, II-2 (FAM-A1), I-2, II-2, III-1, III-2 (FAM-A10) I-1 FAM-B4 LHON subjects, and unexpectedly led to very low values of copy number. Three *Affected* (I-1 FAM-A5, III-2 FAM-A4 and I-1 FAM-A15) were diagnosed, but we could not perform the quantitation of the mtDNA content due to the scarcity of DNA samples. The values of the mtDNA copy number showed a statistically significant difference (KW = 24.828, $p = 0.000004$) and the peak of mtDNA content shifted progressively towards higher values from *Controls* (median 207; interquartile range 155.5-251.25) to *Affected* (median 268; interquartile range 189.25-328.75) to *Carriers* (median 380; interquartile range 219-567). The post-hoc analysis showed a statistically significant difference between *Controls versus Affected* and *Controls versus Carriers* (Fig. 1). Among the *Carriers*, we noticed that the relatives belonging to *Family11* showed a quite low mtDNA content below the mean of *Carriers*. Indeed, the age of the *Family11* mem-

bers is relatively higher than the age of the other *Carriers* and we reasoned that this may explain the lower amount of mtDNA according to the decrease of mtDNA copy number with aging (38); additionally, the age of the oldest women of the family (FAM-A11) was over 60ys which is compatible with a low estrogens condition thus confirming *in vivo* the loss of the protective role by estrogens in activating mitochondrial biogenesis and mtDNA content in LHON (39). On the other hand, the comparison between the mtDNA copy number of *Affected* subjects, whose blood samples were obtained in the acute phase of the disease (II-1 FAM-A8, I-1 FAM-A14, I-1 FAM-A17, III-1 FAM B2), and mtDNA copy number of those subjects already affected by optic atrophy in the chronic stage (II-1 FAM-A2, I-1 FAM-A7, I-2 FAM-A7, I-1 FAM-A18), did not reveal any difference.

Discussion

In the present study, we report on the genetic and molecular characterization of LHON subjects born and living in Apulia, Southern Italy. From our data, the prevalence of subjects carrying the LHON primary mutations can be estimated to be approximately 1 case in 75,503 thus, if compared to the prevalence in the North of England (1/31,000), the Netherlands (1/39,000) (2) and Finland (1/50,000) (19,40), it may indicate that in our Region the disease is very low or remains underestimated. Probably, the reason is that some patients may not be adequately diagnosed or are misdiagnosed or are diagnosed outside the Region. Our mutational screening disclosed two out

of the three most common primary LHON mutations, i.e. m.11778G>A and m.3460G>A, either homoplasmic or heteroplasmic. Interestingly, we found that heteroplasmy is present for both primary mutations but it is more frequent for the m.3460G>A than for m.11778G>A mutation, according to a previous estimation in different countries (2, 41). Among the mitochondrial diseases, LHON is notable for the incomplete penetrance since not all the *Carriers* will develop loss of sight and it is expected that additional genetic and environmental factors may play a role in LHON penetrance (42). As in the majority of mitochondrial disorders, it has been suggested that a certain amount of wild-type mtDNA can compensate for the mutant mtDNA in a cell of a LHON individual (18). In our cohort we found no difference in the LHON manifestations among the *Affected*, either homoplasmic or heteroplasmic, since there was no clear-cut segregation with either more severe or benign clinical course of the disease, respectively. This finding is supported by a study performed specifically in a LHON heteroplasmic population (20).

With the aim of better investigating LHON penetrance we performed the whole mtDNA sequencing of three *Affected* who had a different course of disease: the first one was a man (II-1 FAM-A1) who was diagnosed as psychotic and, although after the disease onset he had started Idebenone treatment, he did not experience any visual recovery; the second one (II-1 FAM-A2) was a man who experienced visual recovery without Idebenone treatment; the third one (I-1 FAM-A3) was a woman who had an early acute and painless loss of central vision at four years of age. Unexpectedly, the latter two cases who manifested a less severe and a more severe LHON phenotype respectively, shared the co-occurrence of two mutations (m.4136A>G, m.9139G>A), thus suggesting that both mutations do not have an unequivocal effect in worsening the LHON manifestation, although both mutations had been previously reported to play a synergistic role when occurring with the LHON primary mutation (43). Furthermore, we identified the co-occurrence of the m.4136A>G with two haplogroup markers, m.4216T>C and m.4971A>G, in two out of three sequenced patients; the same genotype with the three variants had been previously reported in other three unrelated patients harboring the m.11778G>A mutation, coming from the Apulia Region, described by La Morgia et al. and Torroni et al. (43, 44). Interestingly, the three Apulian patients previously described (43, 44), similarly to our patients, belonged to haplogroup T2. The shared Apulian origin of these families supports the hypothesis that the m.11778G>A together with m.4136A>G, 4216T>C and 4917A>G are indeed associated and acquired by descent from a common maternal ancestor. Several studies have

identified the haplogroup J as a risk genetic background for patients with m.11778G>A and m.14484T>C (44-46) and haplogroup K for patients with m.3460G>A; conversely, haplogroup H seemed to have a protective role in patients with m.11778G>A (47). On the basis of the data herein discussed, we suggest that also haplogroup T may play a role in LHON penetrance; this might not be unexpected since haplogroup T, like haplogroup J, belongs to the same macro-haplogroup JT (<http://www.phylotree.org/tree/index.htm>). Regarding the II-1 FAM-A1 case, the patient did not show any significant or prioritized mutation implying that his extraocular signs (i.e. psychotic trait) might be probably due more to his drug and alcohol addiction.

According to recent evidences (20, 26, 27) supporting the concept that the increase in mitochondrial mass differentiates the LHON unaffected from the affected, we measured mtDNA content in either heteroplasmic or homoplasmic LHON subjects. With the aim of evaluating the mtDNA copy number of the overall cohort of LHON subjects, we also included thirty-one subjects already reported (20, 26), and we found an increase in the number of mtDNA molecules in peripheral blood of *Carriers versus Affected* despite the homo- or heteroplasmy of LHON mutations. We may claim that such increase can be considered as a compensatory response to the decline in the respiratory function and a way to protect from vision loss. On the other hand, in agreement with previous studies (39, 48) we found that environmental triggers such as tobacco, alcohol, as well as low estrogen conditions and age itself are all contributing factors that affect mitochondrial biogenesis. We cannot rule out that among the *Carriers* those subjects showing low content of mtDNA might be considered at a high risk of developing the disease. But, of course, this should be monitored over time.

In conclusion, our study on Apulian LHON subjects, despite the small number, suggests the haplogroup T as a possible genetic background influencing LHON penetrance. Furthermore, mtDNA content may be considered as a protective factor from vision loss regardless the hetero/homoplasmic *status* of LHON primary mutations.

Funding

The Authors thank the patients and their families for participating. They would particularly like to thank Barbara Pasculli, Ms, for valuable comments and Maria Rosa De Bellis, MS, for proofing the manuscript. The Authors have no competing interests. This work was supported by 2010 grants from the University of Bari (Fondi ex-60%, 2009-2011) and Petruzzella00724113Prin – Finanziamento Università Prin 30 2009.

References

- Chinnery PF, Thorburn DR, Samuels DC, et al. The inheritance of mitochondrial DNA heteroplasmy: random drift, selection or both? *Trends Genet* 2000;16:500-5.
- Man PY, Griffiths PG, Brown DT, et al. The epidemiology of Leber hereditary optic neuropathy in the North East of England. *Am J Hum Genet* 2003;72:333-9.
- Puomila A, Viitanen T, Savontaus ML, et al. Segregation of the ND4/11778 and the ND1/3460 mutations in four heteroplasmic LHON families. *J Neurol Sci* 2002;205:41-5.
- Mascialino B, Leinonen M, Meier T. Meta-analysis of the prevalence of Leber hereditary optic neuropathy mtDNA mutations in Europe. *Eur J Ophthalmol* 2012;22:461-5.
- Spruijt L, Kolbach DN, de Coe RF, et al. Influence of mutation type on clinical expression of Leber hereditary optic neuropathy. *Am J Ophthalmol* 2006;141:676-82.
- Dimitriadis K, Leonhardt M, Yu-Wai-Man P, et al. Leber's hereditary optic neuropathy with late disease onset: clinical and molecular characteristics of 20 patients. *Orphanet J Rare Dis* 2014;9:158.
- Newman NJ, Bioussé V, David R, et al. Prophylaxis for second eye involvement in leber hereditary optic neuropathy: an open-labeled, nonrandomized multicenter trial of topical brimonidine purite. *Am J Ophthalmol* 2005;140:407-15.
- Barboni P, Carbonelli M, Savini G, et al. Natural history of Leber's hereditary optic neuropathy: longitudinal analysis of the retinal nerve fiber layer by optical coherence tomography. *Ophthalmology* 2010;117:623-7.
- Newman NJ. Hereditary optic neuropathies: from the mitochondria to the optic nerve. *Am J Ophthalmol* 2005;140:517-23.
- Pulkes T, Eunson L, Patterson V, et al. The mitochondrial DNA G13513A transition in ND5 is associated with a LHON/MELAS overlap syndrome and may be a frequent cause of MELAS. *Ann Neurol* 1999;46:916-19.
- Fruhman G, Landsverk ML, Lotze TE, et al. Atypical presentation of Leigh syndrome associated with a Leber hereditary optic neuropathy primary mitochondrial DNA mutation. *Mol Genet Metab* 2011;103:153-60.
- Wei QP, Zhou X, Yang L, et al. The coexistence of mitochondrial ND6 T14484C and 12S rRNA A1555G mutations in a Chinese family with Leber's hereditary optic neuropathy and hearing loss. *Biochem Biophys Res Commun* 2007;357:910-6.
- Zhang AM, Jia X, Yao YG, et al. Co-occurrence of A1555G and G11778A in a Chinese family with high penetrance of Leber's hereditary optic neuropathy. *Biochem Biophys Res Commun* 2008;376:221-4.
- Khan MR, Bashir R, Naz S. SLC26A4 mutations in patients with moderate to severe hearing loss. *Biochem Genet* 2013;51:514-23.
- Newman NJ, Lott MT, Wallace DC. The clinical characteristics of pedigrees of Leber's hereditary optic neuropathy with the 11778 mutation. *Am J Ophthalmol* 1991;111:750-62.
- Smith KH, Johns DR, Heher KL, et al. Heteroplasmy in Leber's hereditary optic neuropathy. *Arch Ophthalmol* 1993;111:1486-90.
- Nikoskelainen EK, Marttila RJ, Huoponen K, et al. Leber's "plus": neurological abnormalities in patients with Leber's hereditary optic neuropathy. *J Neurol Neurosurg Psychiatry* 1995;59:160-4.
- Chinnery PF, Andrews RM, Turnbull DM, et al. Leber hereditary optic neuropathy: Does heteroplasmy influence the inheritance and expression of the G11778A mitochondrial DNA mutation? *Am J Med Genet* 2001;98:235-43.
- Puomila A, Viitanen T, Savontaus ML, et al. Segregation of the ND4/11778 and the ND1/3460 mutations in four heteroplasmic LHON families. *J Neurol Sci* 2002;205:41-45.
- Bianco A, Bisceglia L, Russo L, et al. High mitochondrial DNA copy number is a protective factor from vision loss in heteroplasmic Leber's Hereditary Optic Neuropathy (LHON). *Invest Ophthalmol Vis Sci* 2017;58:2193-7.
- Sartore M, Grasso M, Piccolo G, et al. Leber's hereditary optic neuropathy (LHON)-related mitochondrial DNA sequence changes in Italian patients presenting with sporadic bilateral optic neuritis. *Biochem Mol Med* 1995;56:45-51.
- Chinnery PF, Howell N, Andrews RM, et al. Mitochondrial DNA analysis: polymorphisms and pathogenicity. *J Med Genet* 1999;36:505-10.
- Brown MD, Starikovskaya E, Derbeneva O, et al. The role of mtDNA background in disease expression: a new primary LHON mutation associated with Western Eurasian haplogroup. *J Human Genetics* 2002;110:130-8.
- Bi R, Logan I, Yao YG. Leber Hereditary Optic Neuropathy: a mitochondrial disease unique in many ways. *Handb Exp Pharmacol* 2016.
- Lodi R, Montagna P, Cortelli P, et al. 'Secondary' 4216/ND1 and 13708/ND5 Leber's hereditary optic neuropathy mitochondrial DNA mutations do not further impair in vivo mitochondrial oxidative metabolism when associated with the 11778/ND4 mitochondrial DNA mutation. *Brain* 2000;123(Pt 9):1896-902.
- Bianco A, Martinez-Romero I, Bisceglia L, et al. Mitochondrial DNA copy number differentiates the Leber's hereditary optic neuropathy affected individuals from the unaffected mutation carriers. *Brain* 2016;139.
- Giordano C, Iommarini L, Giordano L, et al. Efficient mitochondrial biogenesis drives incomplete penetrance in Leber's hereditary optic neuropathy. *Brain* 2014;137(Pt 2):335-53.
- Hudson G, Keers S, Yu-Wai-Man P, et al. Identification of an X-chromosomal locus and haplotype modulating the phenotype of a mitochondrial DNA disorder. *Am J Hum Genet* 2005;77:1086-91.
- Kirkman MA, Korsten A, Leonhardt M, et al. Quality of life in patients with leber hereditary optic neuropathy. *Invest Ophthalmol Vis Sci* 2009;50:3112-5.
- Guerriero S, Vetrugno M, Ciraci L, et al. Bilateral progressive visual loss in an epileptic, mentally retarded boy. *Middle East Afr J Ophthalmol* 2011;18:67-70.

31. Tommasi S, Favia P, Weigl S, et al. Mitochondrial DNA variants and risk of familial breast cancer: an exploratory study. *Int J Oncol* 2014;44:1691-8.
32. Behar DM, van Oven M, Rosset S, et al. A “Copernican” reassessment of the human mitochondrial DNA tree from its root. *Am J Hum Genet* 2012;90:675-84.
33. Zoccolella S, Artuso L, Capozzo R, et al. Mitochondrial genome large rearrangements in the skeletal muscle of a patient with PMA. *Eur J Neurol* 2012;19:e63-4.
34. Calabrese C, Simone D, Diroma MA, et al. MToolBox: a highly automated pipeline for heteroplasmy annotation and prioritization analysis of human mitochondrial variants in high-throughput sequencing. *Bioinformatics* 2014;30:3115-7.
35. Johns DR, Berman J. Alternative, simultaneous complex I mitochondrial DNA mutations in Leber’s hereditary optic neuropathy. *Biochem Biophys Res Commun* 1991;174:1324-30.
36. Zoccolella S, Petruzzella V, Prascina F, et al. Late-onset Leber hereditary optic neuropathy mimicking Susac’s syndrome. *J Neurol* 2010;257:1999-2003.
37. Carelli V, Achilli A, Valentino ML, et al. Haplogroup effects and recombination of mitochondrial DNA: novel clues from the analysis of Leber hereditary optic neuropathy pedigrees. *Am J Hum Genet* 2006;78:564-74.
38. Mengel-From J, Thinggaard M, Dalgard C, et al. Mitochondrial DNA copy number in peripheral blood cells declines with age and is associated with general health among elderly. *Human Genetics* 2014;133:1149-59.
39. Giordano L, Deceglie S, d’Adamo P, et al. Cigarette toxicity triggers Leber’s hereditary optic neuropathy by affecting mtDNA copy number, oxidative phosphorylation and ROS detoxification pathways. *Cell Death Dis* 2015;6.
40. Huoponen K, Vilkkilä J, Aula P, et al. A new mtDNA mutation associated with Leber hereditary optic neuroretinopathy. *Am J Hum Genet* 1991;48:1147-53.
41. Brown MD, Trounce IA, Jun AS, et al. Functional analysis of lymphoblast and cybrid mitochondria containing the 3460, 11778, or 14484 Leber’s hereditary optic neuropathy mitochondrial DNA mutation. *J Biol Chem* 2000;275:39831-6.
42. Meyerson C, Van Stavern G, McClelland C. Leber hereditary optic neuropathy: current perspectives. *Clin Ophthalmol* 2015;9:1165-76.
43. La Morgia C, Achilli A, Iommarini L, et al. Rare mtDNA variants in Leber hereditary optic neuropathy families with recurrence of myoclonus. *Neurology* 2008;70:762-70.
44. Torroni A, Petrozzi M, D’Urbano L, et al. Haplotype and phylogenetic analyses suggest that one European-specific mtDNA background plays a role in the expression of Leber hereditary optic neuropathy by increasing the penetrance of the primary mutations 11778 and 14484. *Am J Hum Genet* 1997;60:1107-21.
45. Hudson G, Carelli V, Spruijt L, et al. Clinical expression of Leber hereditary optic neuropathy is affected by the mitochondrial DNA-haplogroup background. *Am J Hum Genet* 2007;81:228-33.
46. Carelli V, Achilli A, Valentino ML, et al. Haplogroup effects and recombination of mitochondrial DNA: Novel clues from the analysis of Leber hereditary optic neuropathy pedigrees. *Am J Hum Genet* 2006;78:564-74.
47. Howell N, Herrnstadt C, Shults C, et al. Low penetrance of the 14484 LHON mutation when it arises in a non-haplogroup J mtDNA background. *American Journal of Medical Genetics Part A* 2003;119A:147-51.
48. Giordano C, Montopoli M, Perli E, et al. Oestrogens ameliorate mitochondrial dysfunction in Leber’s hereditary optic neuropathy. *Brain* 2011;134(Pt 1):220-34.

Supplemental Table 1. List of mtDNA mutations prioritized by MToolBox in three LHON patients. All variants identified in each LHON subject were prioritized as potentially deleterious (score closer to 1 is more likely to be damaging) the mutations which do not contribute to the macro-haplogroup definition and, if non-synonymous, can be predicted as disease-associated by at least one of the pathogenicity prediction methods. A. II-1 FAM-A1; B. II-1 FAM-A2; C. I-1 FAM-A3.

A. II-1 FAM-A1										
Variant Allele	Locus	Nt Variability	Codon Position	AA Change	AA Variability	Disease Score	Mitomap Associated Disease(s)	Somatic Mutations	dbSNP ID	Haplogroup
11179G	MT-ND4	0.00021	3	syn	1.0					K1a
15653T	MT-CYB	0.00149	1	M303L	0.0028	0.124				
309.CCT	MT-DLOOP	0.00196								
11778A	MT-ND4	0.00368	2	R340H	0.0605	0.853	LHON/Progressive Dystonia		rs199476112	
513.CA	MT-DLOOP	0.0681								
5046A	MT-ND2	0.079	1	V193I	0.21	0.127				
310C	MT-DLOOP	0.283						Normal buccal swab	rs66492218	
150T	MT-DLOOP	0.419					Longevity / Cervical Carcinoma / HPV infection risk	Elderly fibroblasts/leukocytes, lung, thyroid, prostate tumors	rs62581312	
B. II-1 FAM-A2										
Variant Allele	Locus	Nt Variability	Codon Position	AA Change	AA Variability	Disease Score	Mitomap Associated Disease(s)	Somatic Mutations	dbSNP ID	Haplogroup
309.CT	MT-DLOOP	0.00196								T2e2a
11778A	MT-ND4	0.00368	2	R340H	0.0605	0.853	LHON/Progressive Dystonia		rs199476112	
9139A	MT-ATP6	0.00431	1	A205T	0.0051	0.893	LHON			
4136G	MT-ND1	0.00641	2	Y277C	0.0226	0.76	LHON		rs199476121	
6026A	MT-CO1	0.0479	3	syn	0.0				rs41474553	
16293G	MT-DLOOP	0.106						Glioblastoma		
310C	MT-DLOOP	0.283						Normal buccal swab	rs66492218	
150T	MT-DLOOP	0.419					Longevity / Cervical Carcinoma / HPV infection risk	Elderly fibroblasts/leukocytes, lung, thyroid, prostate tumors	rs62581312	
C. I-1 FAM-A3										
Variant Allele	Locus	Nt Variability	Codon Position	AA Change	AA Variability	Disease Score	Mitomap Associated Disease(s)	Somatic Mutations	dbSNP ID	Haplogroup
11778A	MT-ND4	0.00277	2	R340H	0.0402	0.853	LHON / Progressive Dystonia		rs199476112	T2e2a
9139A	MT-ATP6	0.00376	1	A205T	0.0043	0.893	LHON			
309.CT	MT-DLOOP	0.0043								
4136G	MT-ND1	0.00639	2	Y277C	0.0232	0.76	LHON		rs199476121	
8222C	MT-CO2	0.0147	1	syn	0.0021					
16153A	MT-DLOOP	0.038							rs2853512	
6026A	MT-CO1	0.0718	3	syn	0.0				rs41474553	
16293G	MT-DLOOP	0.098						Glioblastoma		
310C	MT-DLOOP	0.215						Normal buccal swab		
150T	MT-DLOOP	0.414					Longevity / Cervical Carcinoma / HPV infection risk	Elderly fibroblasts/leukocytes, lung, thyroid, prostate tumors	rs62581312	

CASE REPORT

Bethlem myopathy in a Portuguese patient – case report

ANA INÊS MARTINS¹, CRISTINA MARQUES², JORGE PINTO-BASTO³ AND LUIS NEGRÃO¹

¹ Neuromuscular Disease Unit, Neurology Department, Coimbra University and Hospital Center, Coimbra, Portugal; ² Radiology Department, Coimbra University and Hospital Centre, Coimbra, Portugal; ³ Centro de Genética Clínica, Porto, Portugal

Mutations of the encoding genes of collagen VI (*COL6A1*, *COL6A2* and *COL6A3*), are responsible for two classical phenotypes (with a wide range of severity), the Ullrich congenital muscular dystrophy (UCMD) and the Bethlem myopathy (BM). We present a male patient of 49 years old, with symptoms of muscle weakness beginning in childhood and of very slowly progression. At the age of 42, the neurological examination revealed proximal lower limb muscle weakness and contractures of fingers flexors muscles, positive Gowers manoeuvre and a waddling gait. Serum creatine kinase (CK) values were slightly elevated, electromyographic study revealed myopathic changes and muscle MRI of the lower limbs showed a specific pattern of muscle involvement, with peripheral fat infiltration in vastus lateralis and intermedius and anterocentral infiltration in rectus femoris. Respiratory and cardiac functions were unremarkable. Whole exome sequencing identified the homozygous mutation c.1970-9G>A in *COL6A2* gene.

Key words: congenital muscular dystrophy, Bethlem myopathy, collagen VI

Introduction

Type VI collagen, a nonfibrillar collagen, is a major component of microfibrils in many connective tissues including tendons, ligaments, muscle, skin, cornea, cartilage, bone tissue and periosteum. Collagen VI is a heterotrimeric protein consisting of three different alpha-chains and it is involved in various cellular interactions such as cell adhesion, migration and apoptosis, through its binding to cell-surface molecules (1).

Mutations of the collagen VI coding genes (*COL6A1*, *COL6A2* and *COL6A3*) are responsible for two clinical phenotypes, the Ullrich congenital muscular dystrophy (UCMD) and Bethlem myopathy (BM). In UCMD, the

symptoms are usually present at birth and are characterized by the presence of a pronounced and progressive muscle weakness, hyperlaxity and contractures of proximal joints, with early loss of ambulation and decrease in life expectancy (2). The BM phenotype is associated with mild proximal muscular weakness and typical distal contractures of the fingers and ankles joints. There is usually a slow progression, with preserved ambulation in adult life, and respiratory function is typically unremarkable. Cardiac and cognitive functions are not affected and the patient has a normal life expectancy (3). BM has an autosomal dominant mode of inheritance, although a few cases of autosomal recessive inheritance have been reported (4). CK levels are usually slightly elevated (below 1000 UI/L) (3). Concentric fatty infiltration in vastus lateralis and intermedius, and an anterocentral infiltration in rectus femoris, corresponding to a “central shadow” or a “U-shaped” infiltration may be found in the MRI muscle of BM patients (5).

We report the first Portuguese patient with molecular confirmed BM.

Clinical case

The patient is a 49 years old male, with a normal social and professional life. He was born of a consanguineous couple (third degree cousins) and familial history was negative for neuromuscular disorders. He began walking at 2 years of age and experienced a slight difficulty in running and competing with his peers at school. At the age of 40 he reported increasing motor difficulties. Neurological examination at the age of 42, revealed mild proximal lower limb muscle weakness (grade 4, MRC score), a waddling gait with lumbar hyperlordosis, contractures of

fingers flexors muscles and shortening of the Achilles tendons. Gowers manoeuvre was positive. Myotatic reflexes were abolished throughout and sensory examination was normal.

Laboratory studies revealed a slightly elevated CK value (472 UI/L). Respiratory parameters and cardiac evaluation (eco and electrocardiogram) were unremarkable. Electromyography presented myopathic features with normal nerve conduction studies. Left deltoid muscle biopsy identified a nonspecific moderate dystrophic pattern with effaced architecture and adipose tissue infiltration, increased fibre diameter variability and internal nuclei (Fig. 1). Immunostaining with monoclonal antibodies against dysferlin, dystrophin, calpain and sarcoglycans (α , β , γ , and δ) revealed normal staining pattern.

Lower limb muscle MRI – thigh level – (Fig. 2), showed a specific pattern on the anterior thigh muscles with concentric fatty infiltration in vastus lateralis and intermedius, and an anteroventral infiltration in rectus femoris, corresponding to a “central shadow” or a “U-shaped” infiltration.

Molecular studies, using the whole genome sequencing technology, identified the homozygous mutation c.1970-9G>A in *COL6A2* gene, with the parents being heterozygous for the mutation (Fig. 3).

Discussion

We present a typical case of BM, with slowly progressive proximal muscle weakness and distal contractures, beginning in childhood and with preserved ambulation in adulthood.

BM was first described in 1976 by Bethlem and Wijngaarden based on 28 patients from different families (6). It is a rare disease, with an estimated frequency of 0.77/100.000 habitants on European countries (7). However, its benign and slowly progressive course may lead to under diagnosing. BM corresponds to the milder end of a collagen pathology spectrum, with UCMD at the other end of clinical severity. Muscular weakness associated to contractures are also present in other diseases, such as *Emery Dreifuss* muscular dystrophy (EDMD) (8) and some variants of early onset limb girdle muscular dystrophy (LGMD) (9). In EDMD, the presence of cardiac electrical abnormalities and eventual dilated cardiomyopathy, help to differentiate it from BM. Muscle MRI abnormalities are also useful in making the distinction, with a predominantly posterior compartment involvement, while in BM the anterior muscles of the thigh are the most affected (2). BM may resemble some LGMD when the prominent clinical signs are related to proximal muscle weakness. Immunohistochemistry with specific antibodies is of special importance in making the differential diagnosis. Also, serum CK levels might be use-

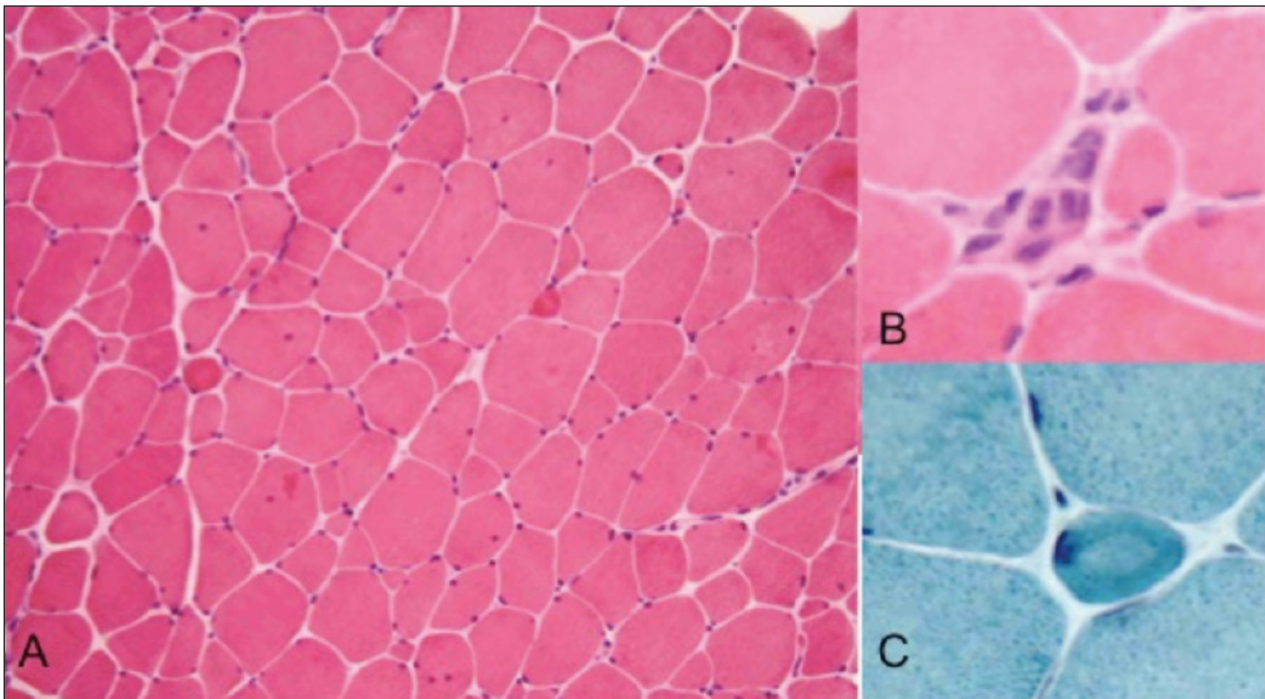


Figure 1. A) Increased variability of fiber diameter and internal nuclei (HE 200x); B) necrotic fiber (HE 400x); C) ring fiber (modified Gomori Trichrome 400x).

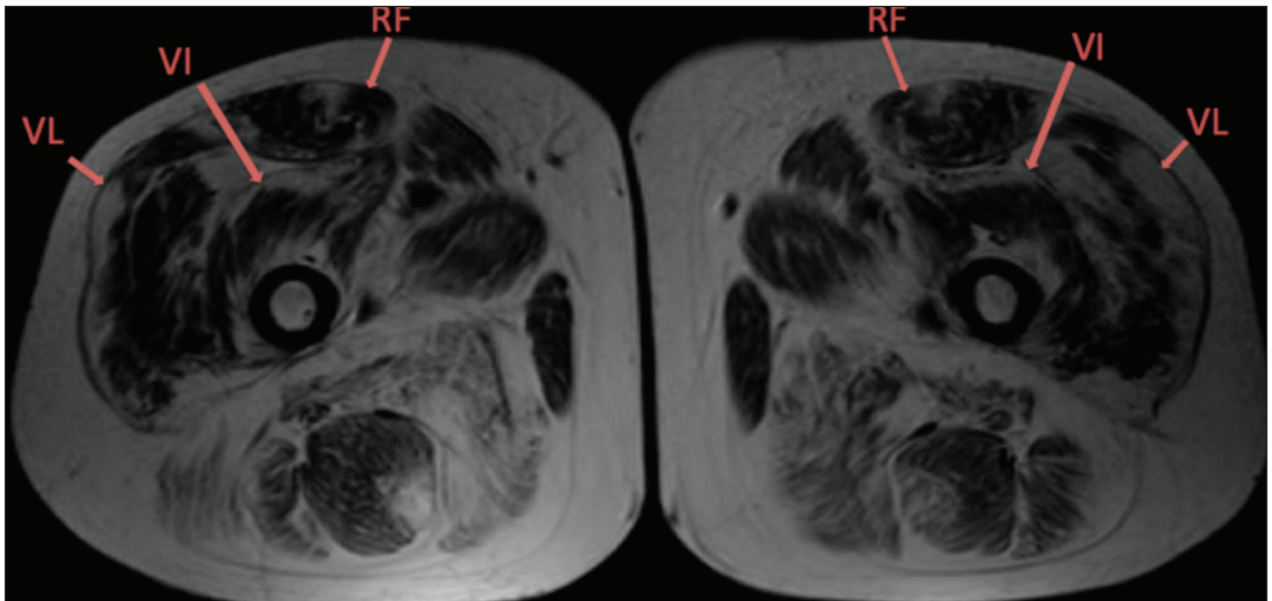


Figure 2. Lower limb muscle MRI, axial thigh level: concentric fatty infiltration in vastus lateralis (VL) and intermedius (VI) and an anterocentral infiltration in rectus femoris (RF), corresponding to a “central shadow” or a “U-shaped” infiltration.

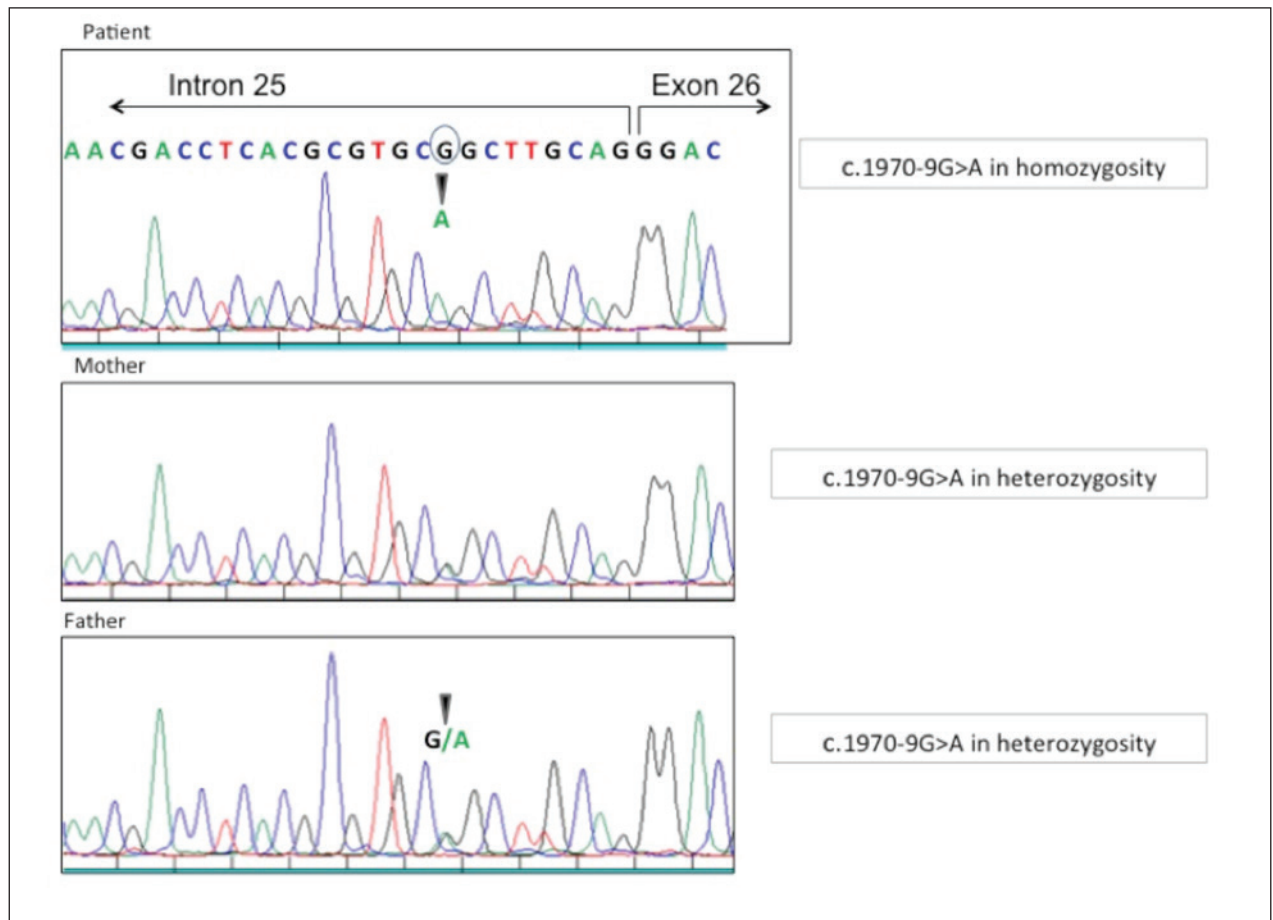


Figure 3. Mutation analysis (electropherogram) of *COL6A2* gene (Chromosome 21).

ful in making the distinction, as in BM they are mildly elevated, while most of the LGMD have CK levels are significantly elevated, like sarcoglycanopathies and dysferlinopathies (9). In the presence of joint laxity, *Ehlers-Danlos* syndrome should also be suspected, particularly in a teenager or adult patient. However, the presence of the characteristic skin hyperlaxity helps to differentiate it from BM. Keloids and hyperkeratosis, which are frequently reported in BM, were not present in our patient, but they are not essential to BM clinical diagnose (3). Muscle biopsy and immunostaining techniques with antibodies to collagen VI and also to sarcoglycans, caveolin, dysferlin, α -dystroglycan and merosin are usually normal in BM patients. Conversely, in UCMD, these techniques reveal a decreased/total absence of collagen VI immunostaining, being a striking difference between the two phenotypes (1).

Muscle MRI findings have been used to characterize some specific muscle diseases and those described in our patient have been considered specific of BM.

The molecular findings of our patient have been already identified in other patients with similar clinical characteristics and prognosis (10) and its pathogenic role is certain. Although BM is mostly inherited dominantly, recessive inheritance has also been described (4) – as occurred in our patient.

To our knowledge, this is the first Portuguese patient diagnosed with BM, a rare cause of benign and slowly progressive muscular dystrophy.

Acknowledgements

We would like to acknowledge Maria Rosário Almeida and Olinda Rebelo for their important scientific contribution.

References

1. Hu J, Higuchi I, Shiraishi T, et al. Fibronectin receptor reduction in skin and fibroblasts of patients with Ullrich's disease. *Muscle Nerve* 2002;26:696-701.
2. Bonnemann CG. The collagen VI-related myopathies: muscle meets its matrix. *Nat Rev Neurol* 2011;7:379-90.
3. Hicks D, Lampe AK, Barresi R, et al., A refined diagnostic algorithm for Bethlem myopathy. *Neurology* 2008;70:1192-9.
4. Gualandi F, Urciuolo A, Martoni E, et al. Autosomal recessive Bethlem myopathy. *Neurology* 2009;73:1883-91.
5. Mercuri E, Lampe A, Allsop J, et al. Muscle MRI in Ullrich congenital muscular dystrophy and Bethlem myopathy. *Neuromuscul Disord* 2005;15:303-10.
6. Bethlem J, Wijngaarden GK. Benign myopathy, with autosomal dominant inheritance. A report on three pedigrees. *Brain* 1976;99:91-100.
7. Norwood FL, Harling C, Chinnery PF, et al. Prevalence of genetic muscle disease in Northern England: in-depth analysis of a muscle clinic population. *Brain* 2009;132:3175-86.
8. Pillers DA, Von Bergen NH. Emery-Dreifuss muscular dystrophy: a test case for precision medicine. *Appl Clin Genet* 2016;9:27-32.
9. Mahmood OA, Jiang XM. Limb-girdle muscular dystrophies: where next after six decades from the first proposal (Review). *Mol Med Rep* 2014;9:1515-32.
10. Deconinck N, Richard P, Allamand V, et al., Bethlem myopathy: long-term follow-up identifies COL6 mutations predicting severe clinical evolution. *J Neurol Neurosurg Psychiatry* 2015;86:1337-46.

ERRATA

Acta Myologica • 2017; XXXVI: p. 19-24-

Integrated care of muscular dystrophies in Italy. Part 1. Pharmacological treatment and rehabilitative interventions

LUISA POLITANO¹, MARIANNA SCUTIFERO¹, MELANIA PATALANO², ALESSANDRA SAGLIOCCHI²,
ANTONELLA ZACCARO², FEDERICA CIVATI³, ERIKA BRIGHINA³, GIANLUCA VITA⁴, SONIA MESSINA⁴,
MARIA SFRAMELI⁴, MARIA ELENA LOMBARDO⁵, ROBERTA SCALISE⁵, GIULIA COLIA⁶, MARIA CATTERUCCIA⁶,
ANGELA BERARDINELLI⁷, MARIA CHIARA MOTTA⁷, ALESSANDRA GAIANI⁸, CLAUDIO SEMPLICINI⁸,
LUCA BELLO⁸, GUJA ASTREA⁹, GIULIA RICCI⁹, MARIA GRAZIA D'ANGELO³, GIUSEPPE VITA⁴,
MARIKA PANE⁵, ADELE D'AMICO⁶, UMBERTO BALOTTIN⁷, CORRADO ANGELINI⁸,
ROBERTA BATTINI⁹ AND LORENZA MAGLIANO²

¹ Cardiology and Medical Genetics, Department of Experimental Medicine, Campania University "Luigi Vanvitelli" (former denomination: Second University of Naples), Italy; ² Department of Psychology, Campania University "Luigi Vanvitelli", Italy; ³ NeuroMuscular Unit, Department of NeuroRehabilitation, IRCCS "E. Medea", Bosisio Parini (LC), Italy; ⁴ Department of Neurosciences, University of Messina; ⁵ Department of Paediatric Neurology, Catholic University, Rome, Italy; ⁶ Unit of Neuromuscular and Neurodegenerative Diseases, Bambin Gesù Children's Hospital, Rome, Italy; ⁷ Child Neuropsychiatry Unit, Department of Brain and Behavioral Sciences, University of Pavia, Pavia, Italy; ⁸ Department of Neurosciences, University of Padova, Italy; ⁹ Developmental Neuroscience, IRCCS Stella Maris, Pisa Italy; ¹⁰ Department of Brain and Behavioural Sciences, Child Neuropsychiatry Unit, University of Pavia, Italy

CORRIGE

Integrated care of muscular dystrophies in Italy. Part 1. Pharmacological treatment and rehabilitative interventions

LUISA POLITANO¹, MARIANNA SCUTIFERO¹, MELANIA PATALANO², ALESSANDRA SAGLIOCCHI²,
ANTONELLA ZACCARO², FEDERICA CIVATI³, ERIKA BRIGHINA³, GIANLUCA VITA⁴, SONIA MESSINA⁴,
MARIA SFRAMELI⁴, MARIA ELENA LOMBARDO⁵, ROBERTA SCALISE⁵, GIULIA COLIA⁶, MARIA CATTERUCCIA⁶,
ANGELA BERARDINELLI⁷, MARIA CHIARA MOTTA^{8,9}, ALESSANDRA GAIANI¹⁰, CLAUDIO SEMPLICINI¹⁰,
LUCA BELLO¹⁰, GUJA ASTREA¹¹, GIULIA RICCI¹¹, MARIA GRAZIA D'ANGELO³, GIUSEPPE VITA⁴,
MARIKA PANE⁵, ADELE D'AMICO⁶, UMBERTO BALOTTIN^{8,9}, CORRADO ANGELINI¹⁰,
ROBERTA BATTINI¹¹ AND LORENZA MAGLIANO²

¹ Cardiology and Medical Genetics, Department of Experimental Medicine, Campania University "Luigi Vanvitelli" (former denomination: Second University of Naples), Italy; ² Department of Psychology, Campania University "Luigi Vanvitelli", Italy; ³ NeuroMuscular Unit, Department of NeuroRehabilitation, IRCCS "E. Medea", Bosisio Parini (LC), Italy; ⁴ Department of Neurosciences, University of Messina; ⁵ Department of Paediatric Neurology, Catholic University, Rome, Italy; ⁶ Unit of Neuromuscular and Neurodegenerative Diseases, Bambin Gesù Children's Hospital, Rome, Italy; ⁷ Unit of Child and Adolescence Neurology, C. Mondino National Neurological Institute, Pavia; ⁸ Child Neuropsychiatry Unit, C. Mondino National Neurological Institute, Pavia; ⁹ University of Pavia; ¹⁰ Department of Neurosciences, University of Padova, Italy; ¹¹ Developmental Neuroscience, IRCCS Stella Maris, Pisa Italy

ERRATA

Acta Myologica • 2017; XXXVI: p. 41-45-

Integrated care of muscular dystrophies in Italy. Part 2. Psychological treatments, social and welfare support, and financial costs

LORENZA MAGLIANO¹, MARIANNA SCUTIFERO², MELANIA PATALANO¹, ALESSANDRA SAGLIOCCHI¹,
ANTONELLA ZACCARO¹, FEDERICA CIVATI³, ERIKA BRIGHINA³, GIANLUCA VITA⁴, SONIA MESSINA⁴,
MARIA SFRAMELI⁴, MARIA ELENA LOMBARDO⁵, ROBERTA SCALISE⁵, GIULIA COLIA⁶, MARIA CATTERUCCIA⁶,
ANGELA BERARDINELLI⁷, MARIA CHIARA MOTTA⁷, ALESSANDRA GAIANI⁸, CLAUDIO SEMPLICINI⁸,
LUCA BELLO⁸, GUJA ASTREA⁹, GIULIA RICCI⁹, MARIA GRAZIA D'ANGELO³, GIUSEPPE VITA⁴,
MARIKA PANE⁵, ADELE D'AMICO⁶, UMBERTO BALOTTIN⁷, CORRADO ANGELINI⁸,
ROBERTA BATTINI⁹ AND LUISA POLITANO²

¹ Department of Psychology, Campania University "Luigi Vanvitelli", (former denomination: Second University of Naples), Italy; ² Cardiomyology and Medical Genetics, Department of Experimental Medicine, Campania University "Luigi Vanvitelli", Italy; ³ NeuroMuscular Unit, Department of NeuroRehabilitation, IRCCS "E. Medea", Bosisio Parini (Lc), Italy; ⁴ Department of Neurosciences, University of Messina; ⁵ Department of Paediatric Neurology, Catholic University, Rome, Italy; ⁶ Unit of Neuromuscular and Neurodegenerative Diseases, Bambin Gesù Children's Hospital, Rome, Italy; ⁷ Child Neuropsychiatry Unit, Department of Brain and Behavioral Sciences, University of Pavia, Italy; ⁸ Department of Neurosciences, University of Padova, Italy; ⁹ Developmental Neuroscience, IRCCS Stella Maris, Pisa Italy; ¹⁰ Department of Brain and Behavioural Sciences, Child Neuropsychiatry Unit, University of Pavia, Italy

CORRIGE

Integrated care of muscular dystrophies in Italy. Part 2. Psychological treatments, social and welfare support, and financial costs

LORENZA MAGLIANO¹, MARIANNA SCUTIFERO², MELANIA PATALANO¹, ALESSANDRA SAGLIOCCHI¹,
ANTONELLA ZACCARO¹, FEDERICA CIVATI³, ERIKA BRIGHINA³, GIANLUCA VITA⁴, SONIA MESSINA⁴,
MARIA SFRAMELI⁴, MARIA ELENA LOMBARDO⁵, ROBERTA SCALISE⁵, GIULIA COLIA⁶, MARIA CATTERUCCIA⁶,
ANGELA BERARDINELLI⁷, MARIA CHIARA MOTTA^{8,9}, ALESSANDRA GAIANI¹⁰, CLAUDIO SEMPLICINI¹⁰,
LUCA BELLO¹⁰, GUJA ASTREA¹¹, GIULIA RICCI¹¹, MARIA GRAZIA D'ANGELO³, GIUSEPPE VITA⁴,
MARIKA PANE⁵, ADELE D'AMICO⁶, UMBERTO BALOTTIN^{8,9}, CORRADO ANGELINI¹⁰,
ROBERTA BATTINI¹¹ AND LUISA POLITANO²

¹ Department of Psychology, Campania University "Luigi Vanvitelli", (former denomination: Second University of Naples), Italy; ² Cardiomyology and Medical Genetics, Department of Experimental Medicine, Campania University "Luigi Vanvitelli", Italy; ³ NeuroMuscular Unit, Department of NeuroRehabilitation, IRCCS "E. Medea", Bosisio Parini (Lc), Italy; ⁴ Department of Neurosciences, University of Messina; ⁵ Department of Paediatric Neurology, Catholic University, Rome, Italy; ⁶ Unit of Neuromuscular and Neurodegenerative Diseases, Bambin Gesù Children's Hospital, Rome, Italy; ⁷ Unit of Child and Adolescence Neurology, C. Mondino National Neurological Institute, Pavia; ⁸ Child Neuropsychiatry Unit, C. Mondino National Neurological Institute, Pavia; ⁹ University of Pavia; ¹⁰ Department of Neurosciences, University of Padova, Italy; ¹¹ Developmental Neuroscience, IRCCS Stella Maris, Pisa Italy

NEWS FROM AROUND THE WORLD

AIM

The 17th Congress of the Italian Myology Association (AIM) took place in Syracuse from 31 May to 3 June 2017. The participation of the specialists in the field reached remarkably high levels with a presence of about 300 participants from all over Italy and foreign countries. The recent scientific advances in diagnosis, therapy and care have been illustrated by the best Italian scientists and by German, French, Danish, British, Portuguese and American speakers. It should also be noted that more than half of the participants were young researchers under 35, some of whom were awarded for their brilliant scientific contributions.

The AIM Web site has recently been updated in content and graphics and can be consulted at www.miologia.org. Within the site, all the AIM clinical centers were recently censused and were reported in a comprehensive list in order to clearly provide national reference centers to patients and physicians.

In order to promote research on neuromuscular diseases among young physicians, AIM, in collaboration with some patient associations, has recently promoted two fellowships for young researchers engaged in mitochondrial diseases and muscle glycogenosis research, respectively. With the intent of obtaining a closer collaboration with the patient's associations, AIM is supporting and cooperating with CAMN (Neuromuscular Disease Association Coordination), which put together the main patient/Family's Italian Associations.

The next AIM Congress will take place in Genoa in Spring 2018. Further information on the event and other activities of the association can be viewed on the new website.

GCA

During the Gala dinner of the 13th Congress of the Mediterranean Society of Myology the 2018 Gaetano Conte Prizes will be assigned for basic and clinical research.

MSM

The 13th Congress of the Mediterranean Society of Myology will be held in Turkey in 2018, organised by Prof. Haluk Topaloglu. The symposium was in the traditional two-days MSM format with selected topics (see brochure).

WMS

The 22nd International WMS Congress will be held in Saint Malo, France from 3 to 7 October 2017. The symposium will follow the traditional format with 3 selected topics:

1. Excitation-contraction coupling: basic aspects and related disorders.
2. Extra-muscular manifestations in NMD.
3. Advances in the treatment of neuromuscular disorders

Contributions will also be welcome on new advances across the neuromuscular field.

FORTHCOMING MEETINGS

2017

September 5-9

IDMC-11. San Francisco, CA, USA. Information: website: <http://www.idmc11.org>

September 13-15

Global Biobank Week. Towards harmony in biobanking. Stockholm, Sweden. Information: website: <http://globalbiobankweek.org>

September 14-16

International Academy of Cardiology Scientific Sessions—World Congress on Heart Disease Vancouver, Canada. Information: website: <http://www.cardiologyonline.com/wchd2017/>

September 14-17

Asia Pacific Heart Rhythm Society (APHRS). Yokohama, Japan. Information: website: <http://www.aphrs.org/>

October 3-7

22nd Congress of World Muscle Society. St. Malo, France. Information: website: www.worldmusclesociety.org

October 17-21

ASHG Annual Meeting. Orlando, Florida, USA. Information: website: www.ashg.org

October 25-27

15th edition of Venice Arrhythmias. Venice, Italy. Information: website: <http://www.venicearrhythmias.org/>

November 22-24

Imaging in Neuromuscular Disease 2017. Berlin, Germany. Information: www.myo-mri.eu

2018

June 28-30

XIII Congress of Mediterranean Society of Myology. Uçhisar – Cappadocia, Turkey. Information: [Haluk Topaloglu htopaloglu@hacettepe.edu.tr](mailto:Haluk.Topaloglu@hacettepe.edu.tr)

August 25-29

European Society of Cardiology (ESC). Munich, Germany. Information: website: <https://www.escardio.org/>

October 2-6

23rd Congress of World Muscle Society. Mendoza, Argentina. Information: website: www.worldmusclesociety.org

October 16-20

ASHG Annual Meeting. San Diego, CA, USA. Information: website: www.ashg.org

October 17-21

Asia Pacific Heart Rhythm Society (APHRS). Taipei, Taiwan. Information: website: <http://www.aphrs.org/>

October 31- November 2

World Congress on Human Genetics. Valencia, Spain. Information: website: <http://humangenetics.conferenceseries.com/>

November 9-10

9th International Conference & Exhibition on Tissue Preservation and Biobanking at Atlanta, USA during, 2018. Information: website: <http://biobanking.conferenceseries.com/>

2019

May 2019

Heart Rhythm 40th Annual Scientific Sessions (HRS). Chicago, IL. Information: website: <http://www.hrssessions.org/>

September 24-28

24th Congress of World Muscle Society. Copenhagen, Denmark. Information: website: www.worldmusclesociety.org

October 22-26

ASHG Annual Meeting. Toronto, Canada. Information: website: www.ashg.org

To be announced

Asia Pacific Heart Rhythm Society (APHRS). Bangkok, Thailand. Information: website: <http://www.aphrs.org/>

2020

October 27-31

ASHG Annual Meeting. San Diego, CA, USA. Information: website: www.ashg.org

To be announced

25th Congress of World Muscle Society. Toronto, Canada. Information: website: www.worldmusclesociety.org



13th Meeting of the Mediterranean Society of Myology



in connection with the

2nd Congress of the Turkish Neuromuscular Society

**28-30 June 2018
Avanos, Cappadocia, Turkey**



Topics of the congress: Limb-girdle muscular dystrophies, Advances in the field
Extra activity 1: 26-27 June 2017, Clinical neuromuscular course for physicians
Extra activity 2: 27 June 2017, Outcome measures course for physiotherapists



ORGANIZING SECRETARIAT

Topkon Congress & Event Management

Zühtüpaşa Mh. Rifat Bey Sok. No: 24

34724 Kalamış-Kadıköy-İstanbul

Phone : +90 216 330 90 20

Fax : +90 216 330 90 05



13th Meeting of the Mediterranean Society of Myology in connection with the 2nd Congress of the Turkish Neuromuscular Society

28-30 June 2018 | Avanos, Cappadocia, Turkey

ORGANIZING COMMITTEE

Congress Presidents

Giovanni Nigro, Haluk Topaloğlu

Local Organizing Committee

İpek Alemardoğlu (secretary)

Sevim Erdem

Gökür Haliloğlu

Ayşe Karaduman

Piraye Oflazer

Müjgan Sönmez

Beril Talim

Ersin Tan

Öznur Yılmaz

Uluç Yiş

Board of the Mediterranean Society of Myology

President

G. Nigro

President Elect

H. Topaloglu

Vice-Presidents

L.T. Middleton and G. Siciliano

Secretary

K. Christodoulou

Treasurer

L. Politano

Members

E. Abdel-Salam

M. Dalakas

F. Deymeer

F. Hentati

G. Meola

Y. Shapira

E. Tizzano

A. Toscano

J. Zidar

Board of the Turkish Neuromuscular Society

President

G. Kale

Secretary

M. Sönmez

Treasurer

Ö. Yılmaz

Members

H. Topaloğlu

B. Talim

A. Karaduman

Dear Colleagues,

Thirty-six years ago, a group of researchers with interest in the field of muscular dystrophies felt the need to promote a mutual cooperation among the people of the Mediterranean area, and created the Mediterranean Society of Myology in 1993, in Ischia.

The initiative had a rapid success with the accession of the representatives of 22 Mediterranean Countries and was a model to establish other International Societies of Myology, such as the European NeuroMuscular Center-ENMC (established in 1992 by Ysbrandt Portman, Reinhardt Rudel and myself) and the Word Muscle Society (established in 1995 by Victor Dubowitz, Luciano Merlini and myself)

The presence of the Turkish delegates has always enriched the value of the Society, and the organization of the 13th Congress attests their contribution.

Therefore I am very pleased and grateful to Prof. Haluk Topaloglu for accepting the task (and load) of the Congress organization, and I'm convinced it will be a successful event.

I hope that many of you will be present next year in Cappadocia.

Giovanni Nigro

President of the
Mediterranean Society of Myology

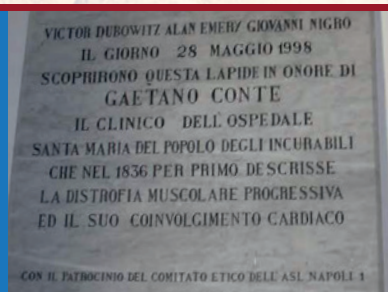
Dear Colleagues,

We invite you to attend the 13th Meeting of the Mediterranean Society of Myology (MSM) in Cappadocia, Turkey, June 28 - 30 2018. MSM has been originated in Italy, rapidly escalated, and within a decade has become an internationally renowned group of enthusiasts. Bi-annual meetings have been traditional. With the spirit we have received from the past congresses of the Society, it will be our aim to bring researchers together with interest in basic and clinical science. The special topic for this congress has been chosen as "limb-girdle muscular dystrophies". We shall try our best to create an exciting programme. This congress will jointly be done with the 2nd Turkish Myology meeting.

Cappadocia which was the population zone of the Assyrian civilization later has hosted the Hittite, Frig, Pers, Byzantine, Seljuk and Ottoman civilizations. Cappadocia is an important tourism site in Turkey.

We think that your visit to Cappadocia in the summer of 2018 will be rewarding academically and educationally, and also from the social aspects.

Prof. Haluk Topaloglu



For application or renewal to MSM

MEDITERRANEAN SOCIETY OF MYOLOGY* (MSM)

G. Nigro, *Honorary President*
H. Topaloglu, *President Elected*
L.T. Middleton, G. Siciliano, *Vice-Presidents*
K. Christodoulou, *Secretary*
L. Politano, *Treasurer*

APPLICATION/RENEWAL FORM

Application/Renewal for 1yr 2 yrs

Prof. Luisa Politano, MSM Treasurer, Viale dei Pini 101, 80131, Napoli, Italy
Fax: 39 081 5665100 E-mail: actamyologica@gmail.com • luisa.politano@unicampania.it
Fax or Mail to the above address. Type or print.

Name _____ Degree(s) _____

Last First

Department _____


Institution _____

Street Address _____

City, State, zip, country _____

Tel () Fax ()
Area code Area code

* Amount payable:	1 year	Euro 100
	2 years	Euro 150

 I enclose copy of the bank transfer to:

Bank name: Banco di Napoli – Filiale 00660
Bank address: Via Riviera di Chiaia, 131 – 80122 Napoli, Italy
Account holder: MSM – Mediterranean Society of Myology
IBAN code: IT48T0101003488100000100680
BIC code (for foreign countries): IBSPITNA

INSTRUCTIONS FOR AUTHORS

Acta Myologica publishes articles related to research in and the practice of primary myopathies, cardiomyopathies and neuromyopathies, including observational studies, clinical trials, epidemiology, health services and outcomes studies, and advances in applied (translational) and basic research.

Manuscripts are examined by the editorial staff and usually evaluated by expert reviewers assigned by the editors. Both clinical and basic articles will also be subject to statistical review, when appropriate. Provisional or final acceptance is based on originality, scientific content, and topical balance of the journal. Decisions are communicated by email, generally within eight weeks. All rebuttals must be submitted in writing to the editorial office.

On-line submission

Manuscript submission must be effected on line: **www.actamyologica.it** according to the following categories:

Original articles (maximum 5000 words, 8 figures or tables). A structured abstract of no more than 250 words should be included.

Reviews, Editorials (maximum 4000 words for Reviews and 1600 words for Editorials). These are usually commissioned by the Editors. Before spontaneously writing an Editorial or Review, it is advisable to contact the Editor to make sure that an article on the same or similar topic is not already in preparation.

Case Reports, Scientific Letters (maximum 1500 words, 10 references, 3 figures or tables, maximum 4 authors). A summary of 150 words may be included.

Letters to the Editor (maximum 600 words, 5 references). Letters commenting upon papers published in the journal during the previous year or concerning news in the myologic, cardio-myologic or neuro-myologic field, will be welcome. All Authors must sign the letter.

Rapid Reports (maximum 400 words, 5 references, 2 figures or tables). A letter should be included explaining why the author considers the paper justifies rapid processing.

Lectura. Invited formal discourse as a method of instruction. The structure will be suggested by the Editor.

Congress Proceedings either in the form of Selected Abstracts or Proceedings will be taken into consideration.

Information concerning new books, congresses and symposia, will be published if conforming to the policy of the Journal.

The manuscripts should be arranged as follows: 1) Title, authors, address institution, address for correspondence; 2) Repeat title, abstract, key words; 3) Text; 4) References; 5) Legends; 6) Figures or tables. Pages should be numbered (title page as page 1).

Title page. Check that it represents the content of the paper and is not misleading. Also suggest a short running title.

Key words. Supply up to three key words. Wherever possible, use terms from Index Medicus – Medical Subject Headings.

Text. Only international SI units and symbols must be used in the text. Tables and figures should be cited in numerical order as first mentioned in the text. Patients must be identified by numbers not initials.

Illustrations. Figures should be sent in .jpeg or .tiff format. Legends should be typed double-spaced and numbered with Arabic numerals corresponding to the illustrations. When symbols, arrows, numbers, or letters are used to identify parts of the illustrations, each should be explained clearly in the legend. For photomicrographs, the internal scale markers should be defined and the methods of staining should be given.

If the figure has been previously published a credit line should be included and permission in writing to reproduce should be supplied. Colour photographs can be accepted for publication, the cost to be covered by the authors.

PATIENTS IN PHOTOGRAPHS ARE NOT TO BE RECOGNISABLE

Tables. Tables should be self-explanatory, double spaced on separate sheets with the table number and title above the table and explanatory notes below. Arabic numbers should be used for tables and correspond with the order in which the table is first mentioned in the text.

References. Reference numbers in the text must be in brackets. References in the list must be numbered as they appear in the text.

Standard journal article: Figarella-Branger D, Bartoli C, Civatte M, et al. Cytokines, chemokines and cell adhesion molecules in idiopathic inflammatory myopathies. *Acta Myol* 2000;19:207-8.

Books and other monographs: Dubowitz V. Muscle disorders in childhood. London: WB Saunders Company Ltd; 1978.

Please check each item of the following checklist before mailing:

- Three index terms, short title for running head (no more than 40 letter spaces) on the title page.
Name(s) of the author(s) in full, name(s) of institution(s) in the original language, address for correspondence with telephone and fax numbers and email address on the second page.
- Summary (maximum 250 words).
- References, tables and figures cited consecutively as they appear in the text.
- Figures submitted actual size for publication (i.e., 1 column wide or 2 columns wide).
- Copyright assignment and authorship responsibility signed (with date) by all Authors.
- References prepared according to instructions.
- English style.
- Patients in photographs not recognisable.

The editor remains at the complete disposal of those with rights whom it was impossible to contact, and for any omissions.

Photocopies, for personal use, are permitted within the limits of 15% of each publication by following payment to SIAE of the charge due, article 68, paragraphs 4 and 5 of the Law April 22, 1941, No 633.

Reproductions for professional or commercial use or for any other other purpose other than personal use can be made following a written request and specific authorization in writing from AIDRO, Corso di Porta Romana, 108, 20122 Milan, Italy, E-mail: segreteria@aidro.org and web site: www.aidro.org.